Next steps in component separation for new CMB observables

Mathieu Remazeilles

Instituto de Fisica de Cantabria

"From Planck to the future of CMB"
Ferrara, Italy
May 2022, 23rd-27th

Instituto de Física de Cantabria

CSIC
Consejo Superior de Investigaciones Científicas

Foregrounds obscure the cosmological signals

Credit: ESA

M. Remazeilles

Planck: playground for component separation

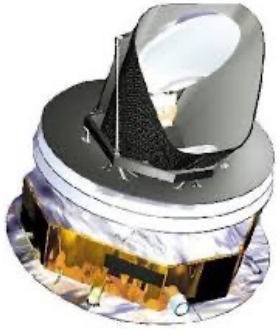

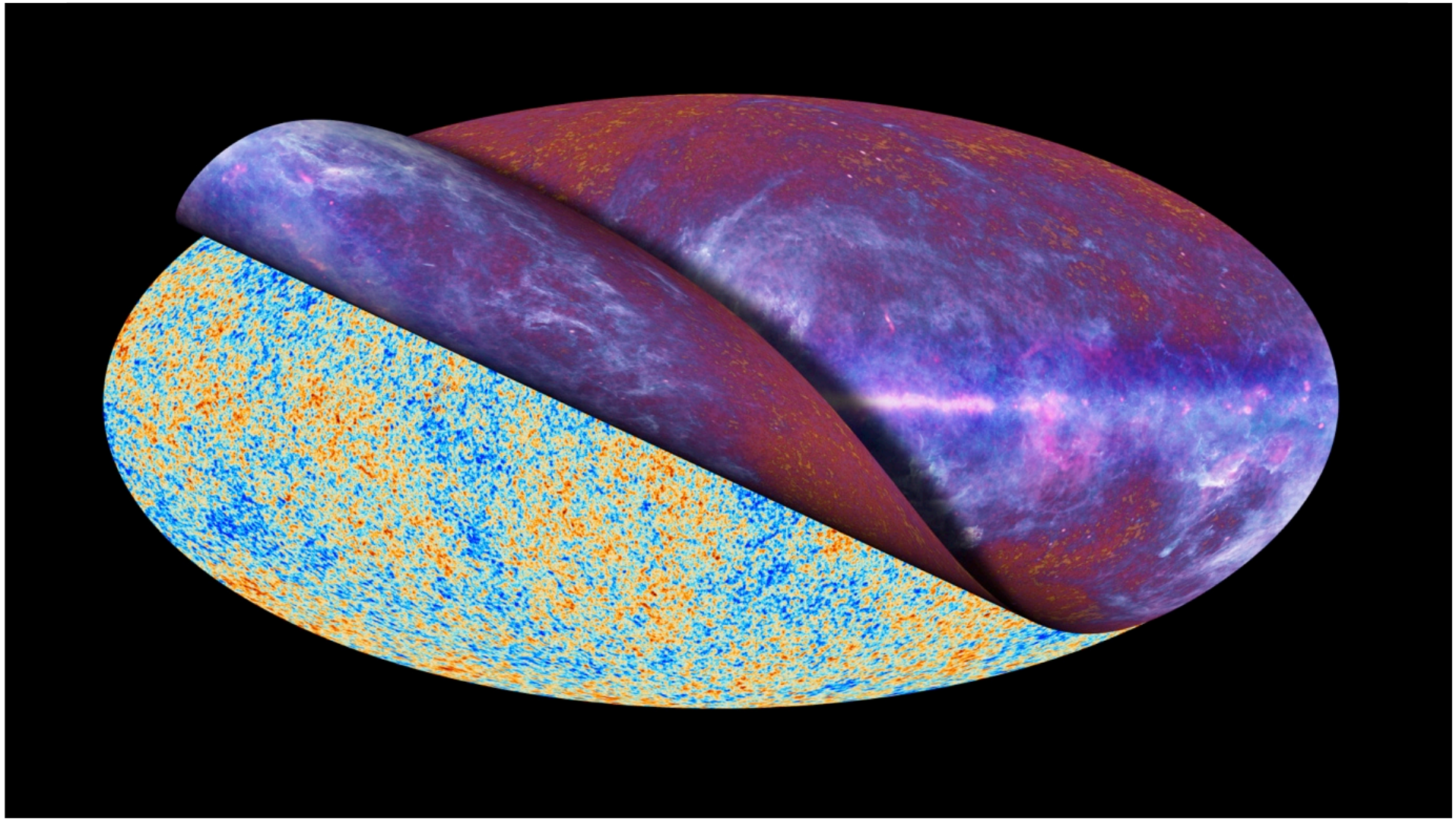

Credit: ESA

M. Remazeilles

Component separation methods

Parametric

Model-dependent

COMMANDER

Eriksen et al 2004, 2008

Blind

No assumption about foregrounds

NILC	*Delabrouille et al 2009*
SEVEM	*Fernandez-Cobos et al 2012*
SMICA	*Cardoso et al 2008* *Delabrouille et al 2003*
GNILC	*Remazeilles et al 2011b*
CILC	*Remazeilles et al 2011a*
MILCA	*Hurier et al 2013*

Component separation methods

Parametric

Model-dependent

COMMANDER

Eriksen et al 2004, 2008

fgbuster

Stompor et al 2009, 2016
Errard et al 2011, 2019

B-SeCRET

de la Hoz et al 2020

moments fitting
(not map-based)
Vacher et al 2021, 2022
Mangili et al 2021
Azzoni et al 2020

Blind

No assumption about foregrounds

NILC	*Delabrouille et al 2009*
SEVEM	*Fernandez-Cobos et al 2012*
SMICA	*Cardoso et al 2008* *Delabrouille et al 2003*
GNILC	*Remazeilles et al 2011b*
CILC	*Remazeilles et al 2011a*
MILCA	*Hurier et al 2013*
Delta-map	*Ichiki et al 2019*

Component separation methods

Parametric

Model-dependent

COMMANDER

Eriksen et al 2004, 2008

fgbuster

Stompor et al 2009, 2016
Errard et al 2011, 2019

B-SeCRET

de la Hoz et al 2020

moments fitting
(not map-based)
Vacher et al 2021, 2022
Mangili et al 2021
Azzoni et al 2020

Semi-blind

Foreground moment deprojection

cMILC

Remazeilles et al 2021

Blind

No assumption about foregrounds

NILC	*Delabrouille et al 2009*
SEVEM	*Fernandez-Cobos et al 2012*
SMICA	*Cardoso et al 2008* *Delabrouille et al 2003*
GNILC	*Remazeilles et al 2011b*
CILC	*Remazeilles et al 2011a*
MILCA	*Hurier et al 2013*
Delta-map	*Ichiki et al 2019*

M. Remazeilles

Component separation methods

Parametric

Model-dependent

COMMANDER

Eriksen et al 2004, 2008

fgbuster

Stompor et al 2009, 2016
Errard et al 2011, 2019

B-SeCRET

de la Hoz et al 2020

moments fitting
(not map-based)
Vacher et al 2021, 2022
Mangili et al 2021
Azzoni et al 2020

Semi-blind

Foreground moment deprojection

cMILC

Remazeilles et al 2021

Machine learning

moment networks

Jeffrey et al 2022

Blind

No assumption about foregrounds

NILC	*Delabrouille et al 2009*
SEVEM	*Fernandez-Cobos et al 2012*
SMICA	*Cardoso et al 2008* *Delabrouille et al 2003*
GNILC	*Remazeilles et al 2011b*
CILC	*Remazeilles et al 2011a*
MILCA	*Hurier et al 2013*
Delta-map	*Ichiki et al 2019*

M. Remazeilles

Component separation methods

Parametric

Model-dependent

COMMANDER

Eriksen et al 2004, 2008

fgbuster

Stompor et al 2009, 2016
Errard et al 2011, 2019

B-SeCRET

de la Hoz et al 2020

moments fitting
(not map-based)

Vacher et al 2021, 2022
Mangili et al 2021
Azzoni et al 2020

Semi-blind

Foreground moment deprojection

cMILC

Remazeilles et al 2021

FastMEM

Hobson et al 1998

FastICA

Baccigalupi et al 2000

Machine learning

moment networks

Jeffrey et al 2022

CCA

Bonaldi et al 2006

GMCA

Bobin et al 2008

Blind

No assumption about foregrounds

NILC — *Delabrouille et al 2009*

SEVEM — *Fernandez-Cobos et al 2012*

SMICA — *Cardoso et al 2008*, *Delabrouille et al 2003*

GNILC — *Remazeilles et al 2011b*

CILC — *Remazeilles et al 2011a*

MILCA — *Hurier et al 2013*

Delta-map — *Ichiki et al 2019*

M. Remazeilles

Component separation methods

Parametric

Model-dependent

COMMANDER

Eriksen et al 2004, 2008

fgbuster

t al 2009, 2016
et al 2011, 2019

Talk by Giuseppe Puglisi

B-SeCRET

Hoz et al 2020

Talk by Elena de la Hoz

moments fitting

(not map-based)

Vacher et al 2021, 2022
Mangili et al 2021
Azzoni et al 2020

Semi-blind

Foreground moment deprojection

cMILC

Remazeilles et al 2021

FastMEM

Hobson et al 1998

FastICA

Baccigalupi et al 2000

Machine learn

Talk by Nial Jeffrey

moment networks

Jeffrey et al 2022

CCA

Bonaldi et al 2006

GMCA

Bobin et al 2008

Blind

No assumption about foregrounds

NILC — *Delabrouille et al 2009*

SEVEM — *Fernandez-Cobos et al 2012*

SMICA — *l 2008*, *al 2003*

Talk by Benjamin Beringue

GNILC — *Remazeilles et al 2011b*

CILC — *Remazeilles et al 2011a*

MILCA — *Hurier et al 2013*

Delta-map — *Ichiki et al 2019*

M. Remazeilles

New CMB observables

CMB B-mode polarization

- *Footprint of primordial gravitational waves of quantum origin*
- *Direct evidence for inflation epoch in the early Universe*
- *Informs on the energy scale of inflation (tensor-to-scalar ratio)*

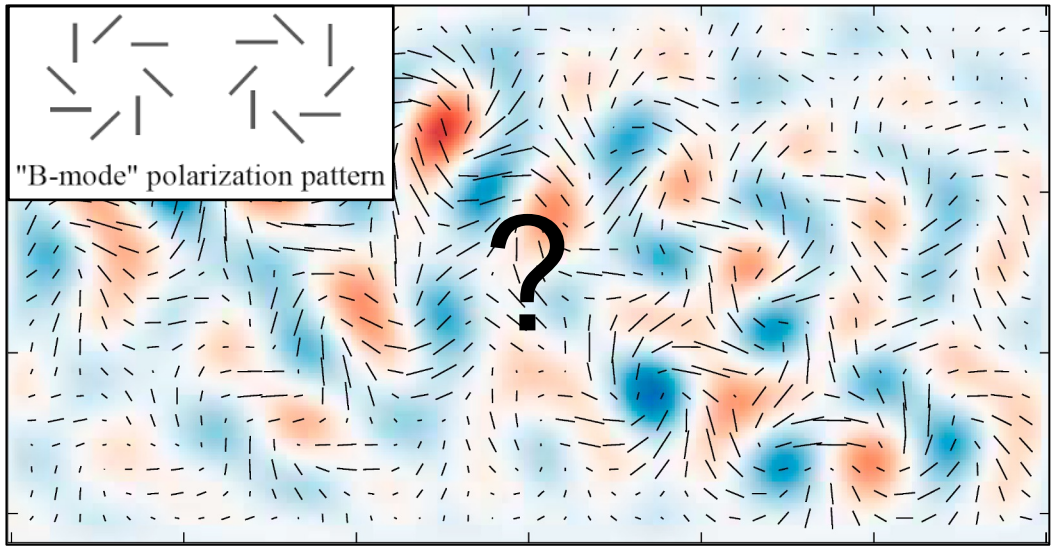

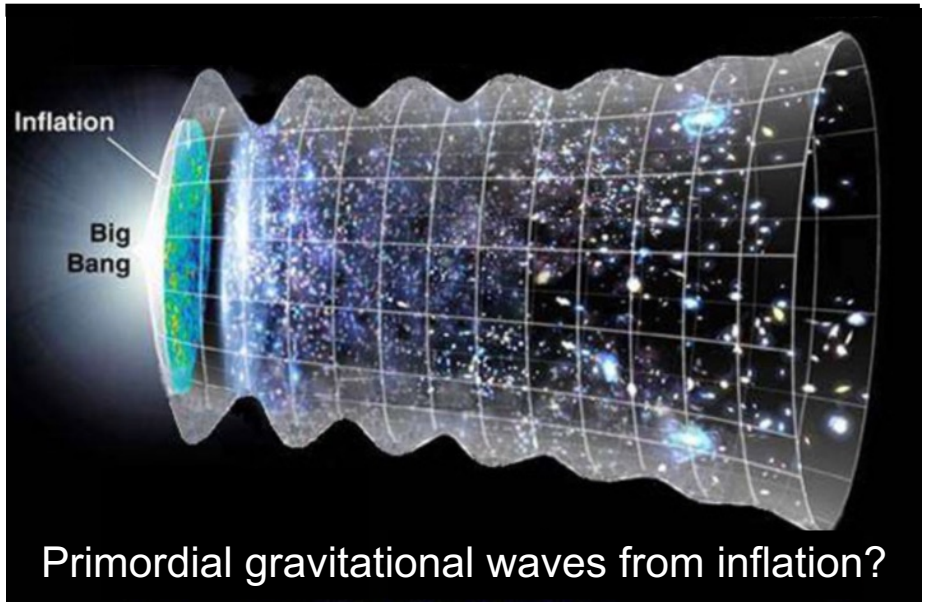

M. Remazeilles

New CMB observables

CMB backlight (secondary spectral / spatial distortions)

- *Spectral and spatial distortions imprinted on the CMB by the cosmic web*
- *Scattering by free electrons, atoms and molecules / gravitational lensing by LSS*
- *CMB "backlight" to probe baryonic and dark matter across the Universe*

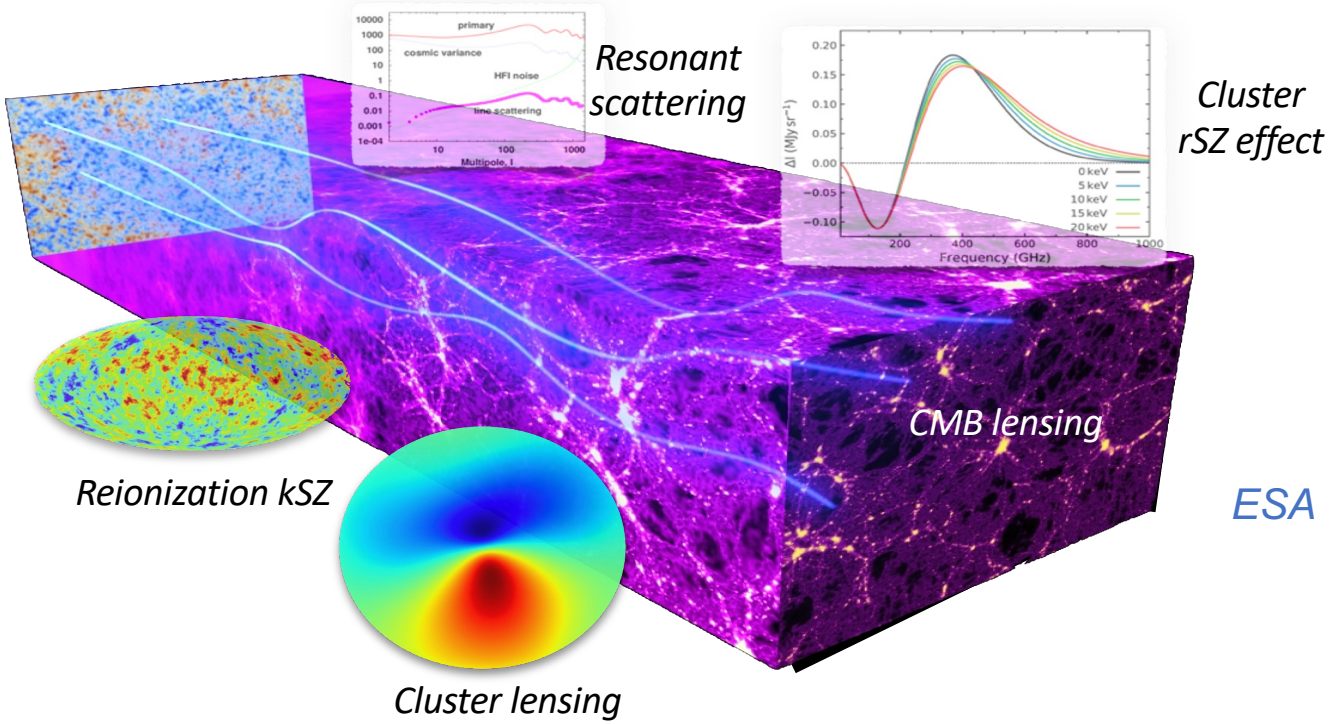

ESA Voyage 2050 White Paper
arXiv:1909.01592

M. Remazeilles

New era of faint signal regimes

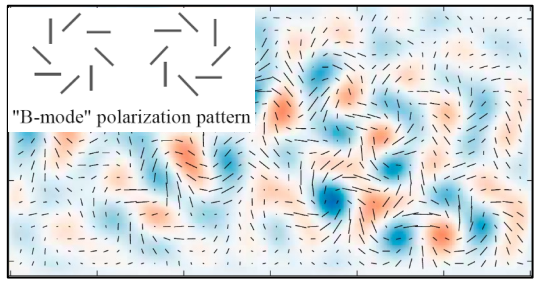

Primary B-mode ~ 10 *nK* $\ll$ *Galactic foreground B-mode* $\sim 10^7$ *nK*

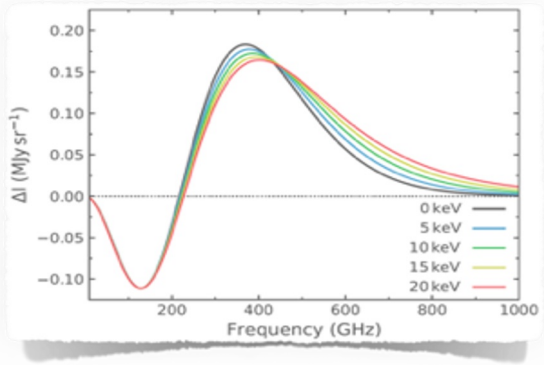

Relativistic SZ $\sim \frac{1}{10}$ *thermal SZ* $\ll$ *(Extra)galactic foregrounds*

Tiny modelling errors on foregrounds = Large error / bias on the signal!

M. Remazeilles

New sensitivities

SIMONS OBSERVATORY

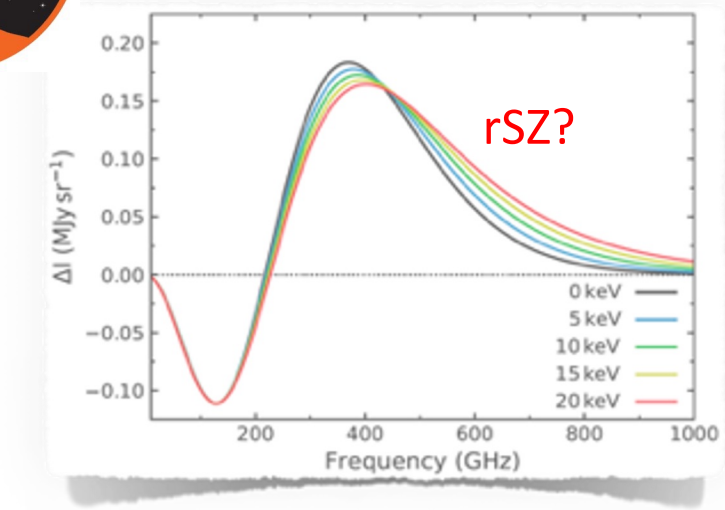

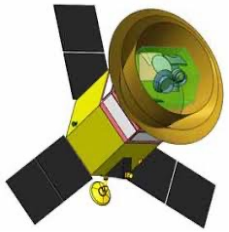

LiteBIRD

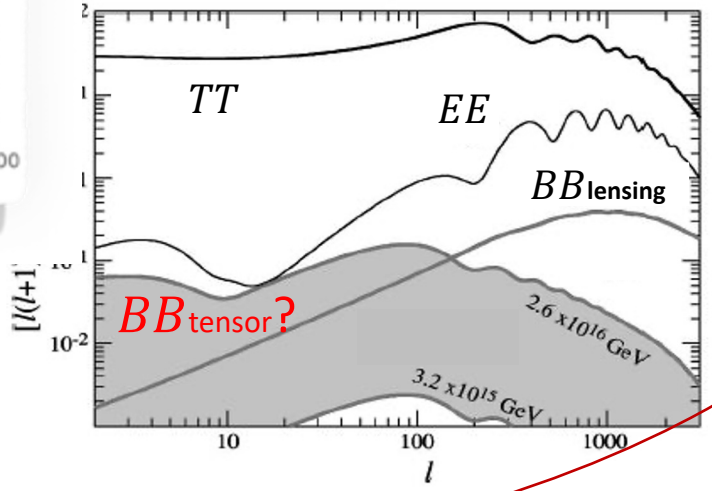

PICO

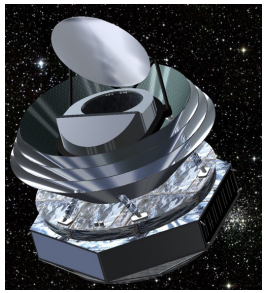

CMB-S4

Much more sensitive to imperfect foreground modelling!
Can we mitigate biases due to foregrounds down to below the noise?

M. Remazeilles

New layers of foregrounds complexity

- **Lack of spectral information:** foregrounds are poorly known at the sensitivity levels required for these signals
- **Spectral distortions of the foregrounds**
- **Spectral degeneracies**
- **Foregrounds correlated with the signal of interest**

M. Remazeilles

Four consistent Planck CMB maps

NILC

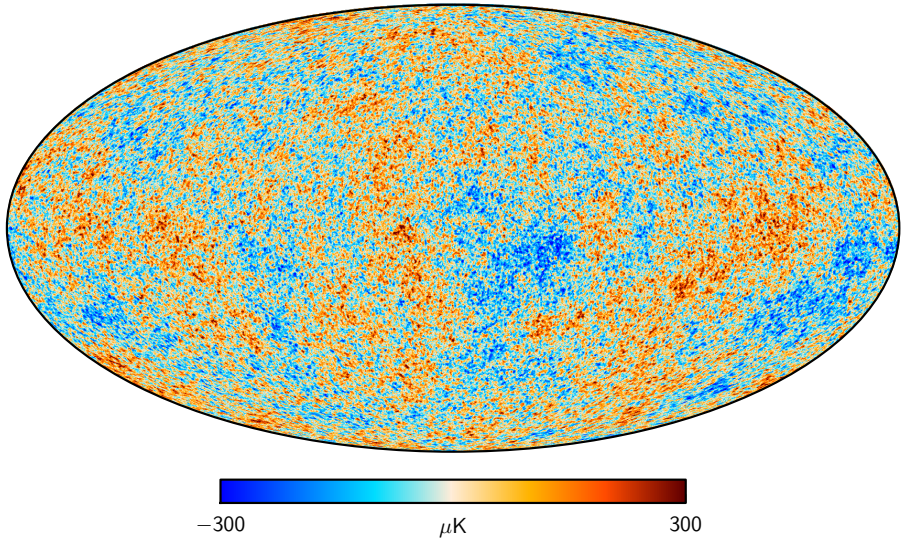

SMICA

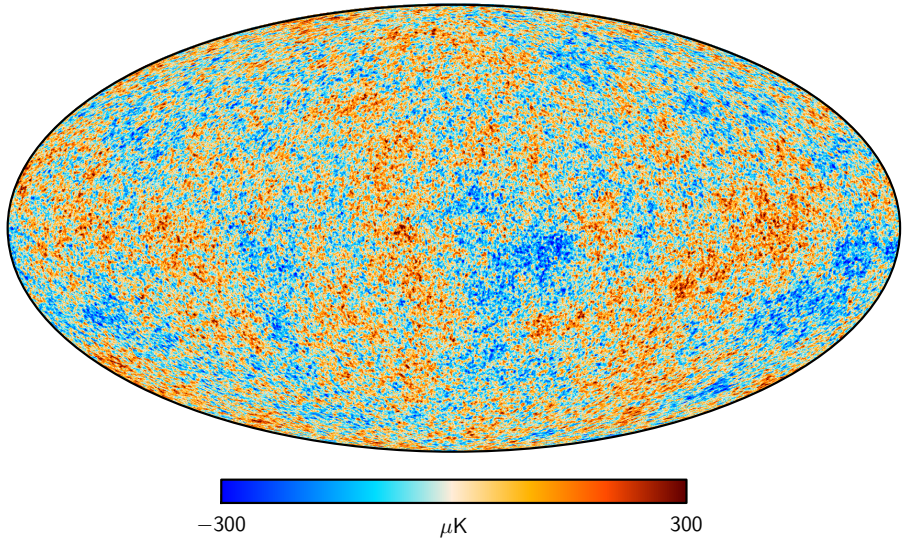

SEVEM

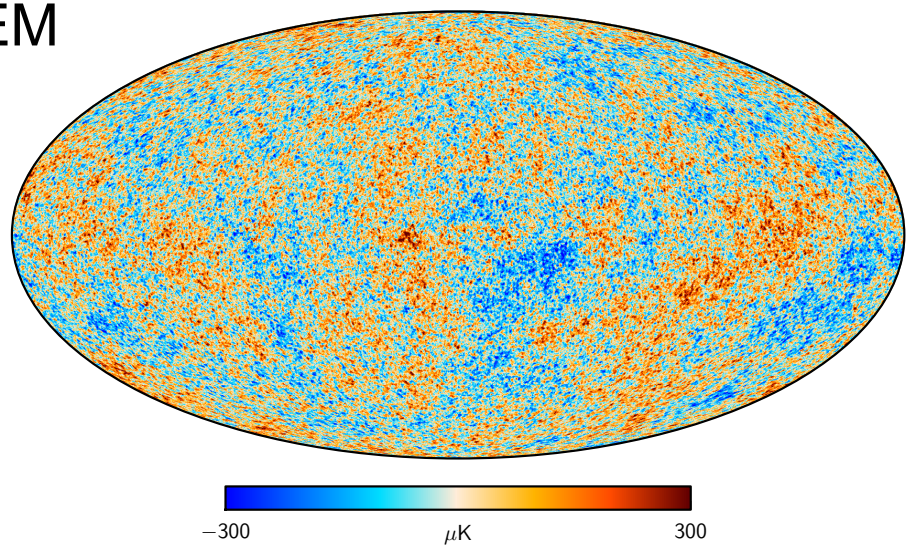

COMMANDER

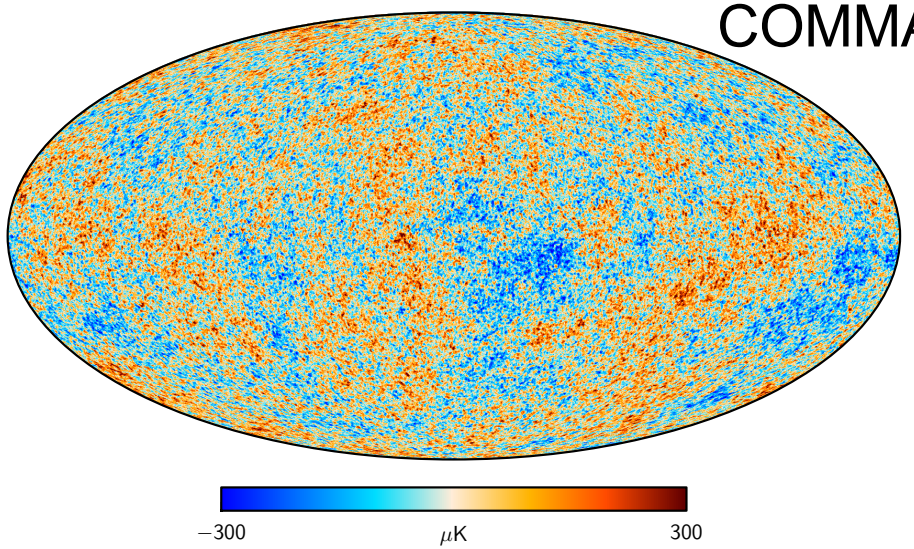

M. Remazeilles

Four consistent Planck CMB maps stacked on galaxy cluster locations

Chen, Remazeilles, Dickinson
MNRAS 2018

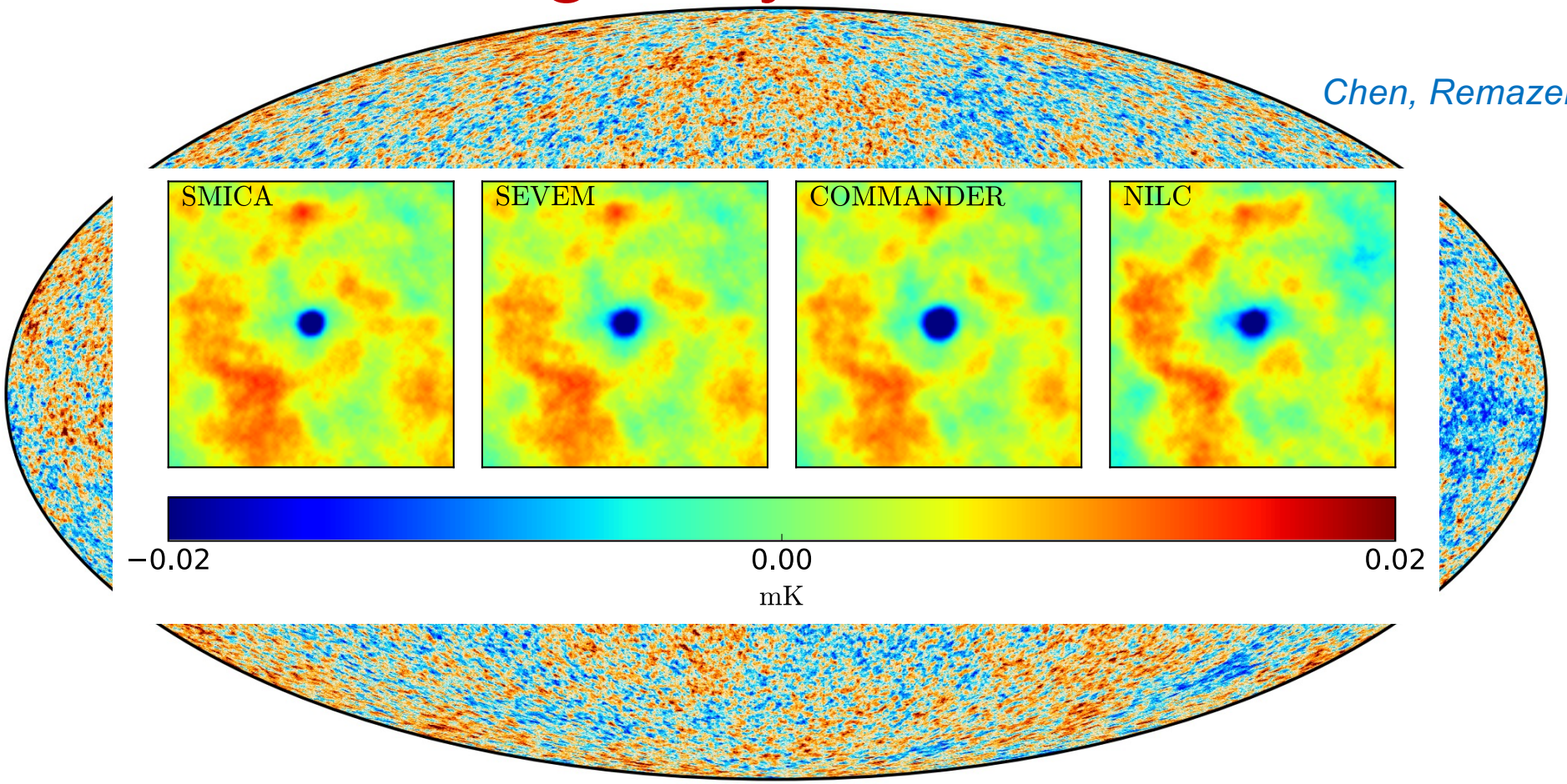

Thermal SZ cluster residuals in all Planck CMB maps!

Major issue for kinetic SZ, CMB lensing, non-Gaussianity, cross-correlations with LSS

M. Remazeilles

Planck residual SZ-induced lensing field

Increment of lensing convergence in the central part of the clusters

Decrement of lensing convergence in the outskirts of the clusters

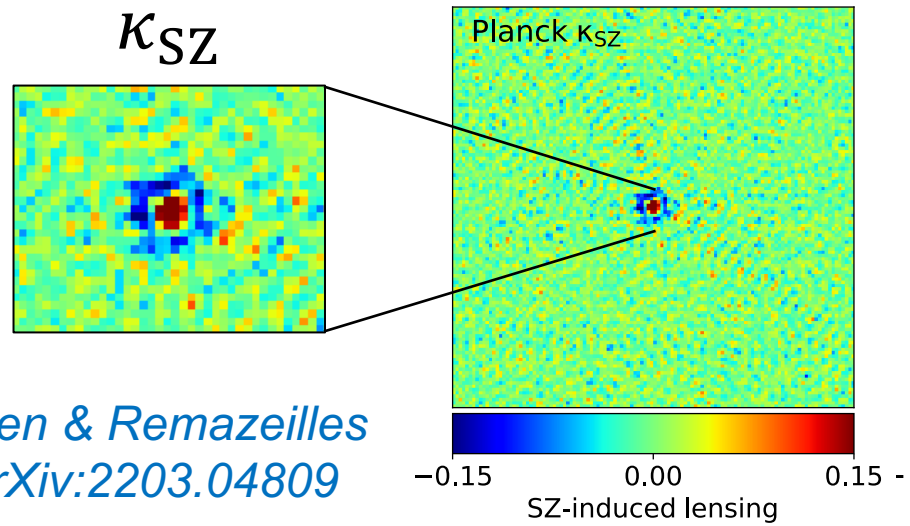

Chen & Remazeilles arXiv:2203.04809

Planck residual SZ-induced lensing field

Increment of lensing convergence in the central part of the clusters

Decrement of lensing convergence in the outskirts of the clusters

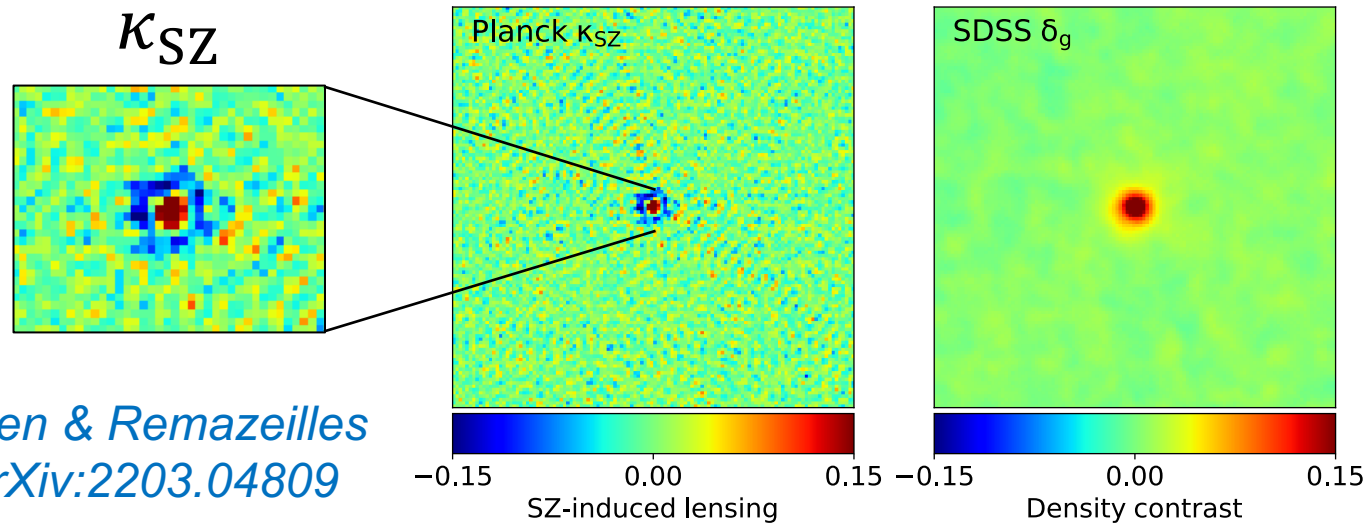

Chen & Remazeilles arXiv:2203.04809

- correlated with LSS at small scale
- anticorrelated with LSS at large scale

Planck residual SZ-induced lensing field

Increment of lensing convergence in the central part of the clusters

Decrement of lensing convergence in the outskirts of the clusters

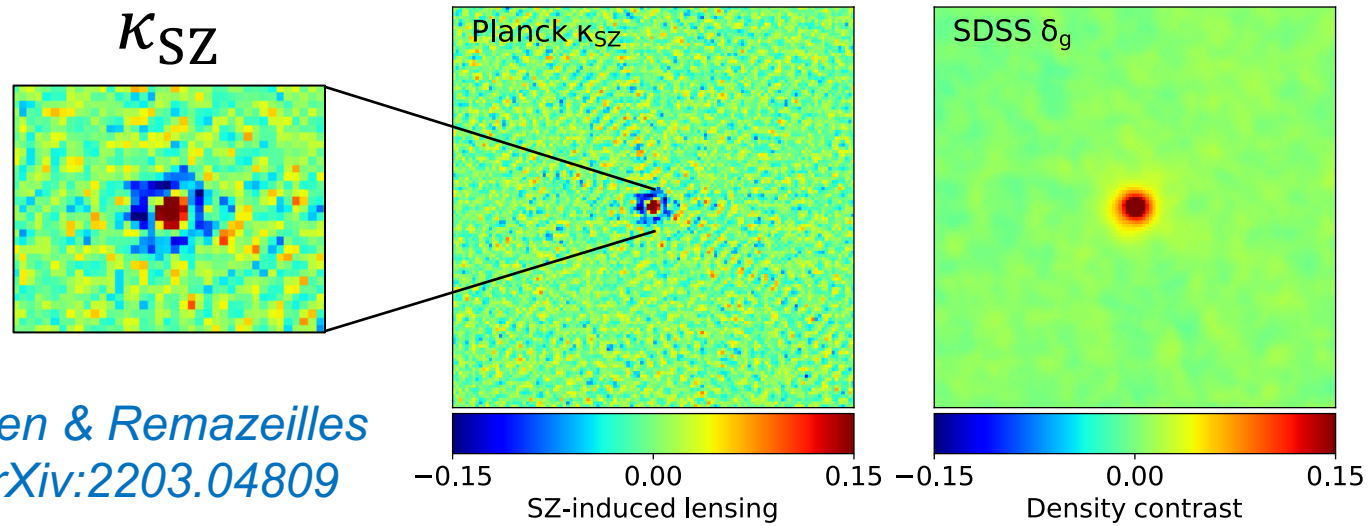

Chen & Remazeilles arXiv:2203.04809

- correlated with LSS at small scale
- anticorrelated with LSS at large scale

scale-dependent bias on CMB lensing × LSS cross-correlations

Planck residual SZ-induced lensing field

Increment of lensing convergence in the central part of the clusters

Decrement of lensing convergence in the outskirts of the clusters

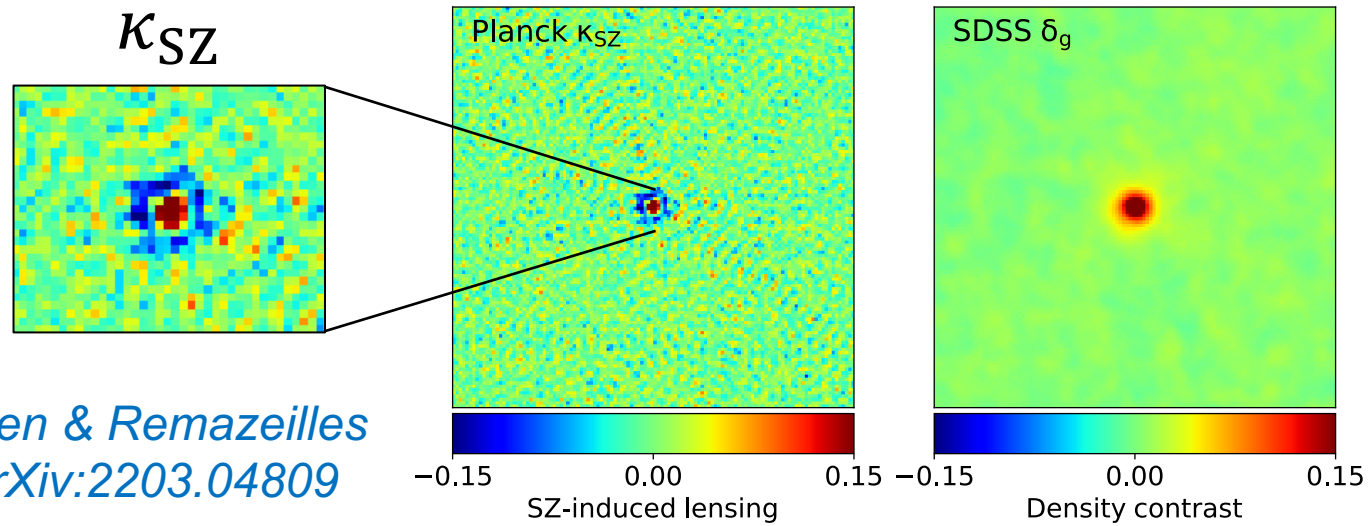

Chen & Remazeilles arXiv:2203.04809

- correlated with LSS at small scale
- anticorrelated with LSS at large scale

scale-dependent bias on CMB lensing × LSS cross-correlations

consistent with earlier theoretical predictions

van Engelen et al, ApJ (2014)

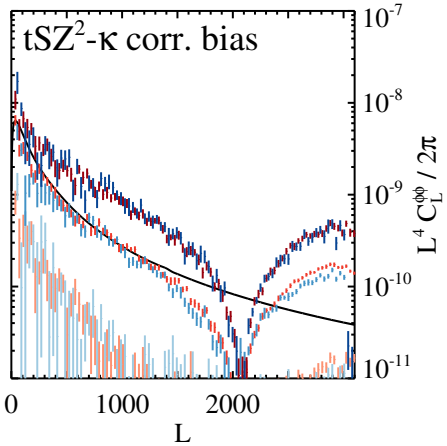

Madhavacheril & Hill PRD (2018)

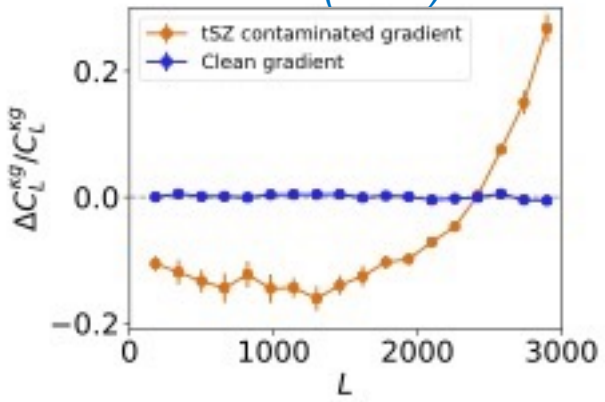

Foreground correlated with the signal

(e.g. SZ in CMB lensing × LSS)

Component separation: standard NILC

input thermal SZ

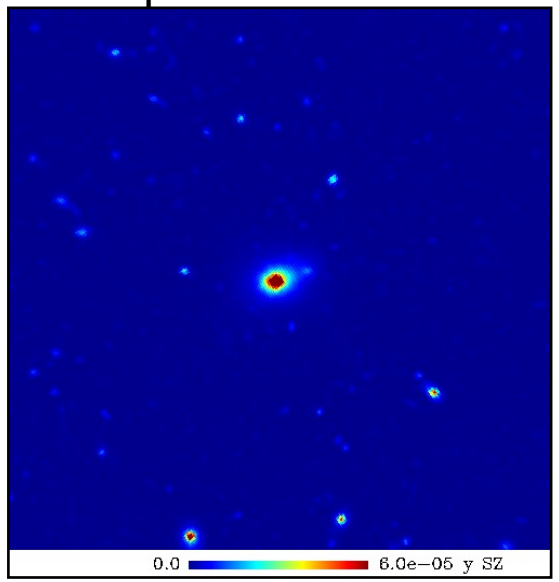

input kinetic SZ

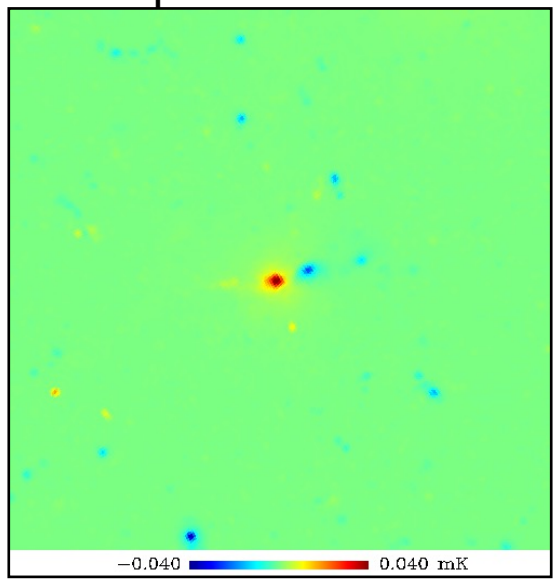

input CMB

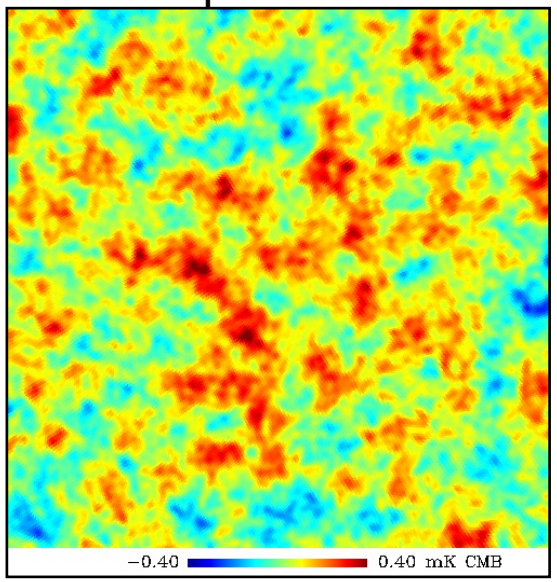

ILC

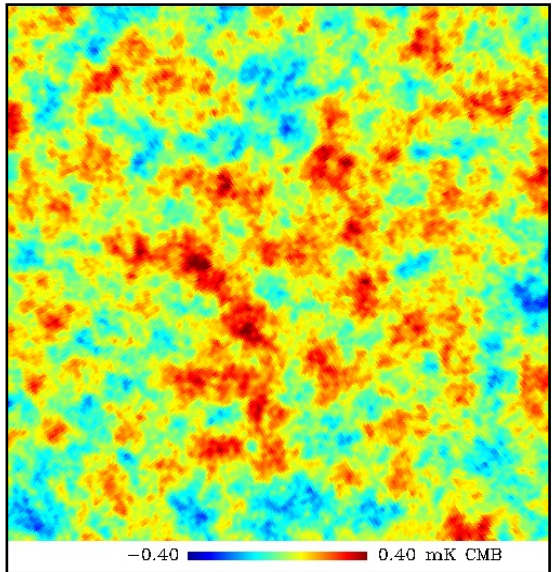

$$\boldsymbol{w} = \frac{\boldsymbol{a}^{\mathrm{T}}\mathbf{C}^{-1}}{\boldsymbol{a}^{\mathrm{T}}\mathbf{C}^{-1}\boldsymbol{a}}$$

Bennett et al 2003, Tegmark et al 2003
Eriksen et al 2004, Delabrouille et al 2009

Minimum-variance solution not adequate for certain scientific purposes!

M. Remazeilles

Component separation: standard NILC

input thermal SZ

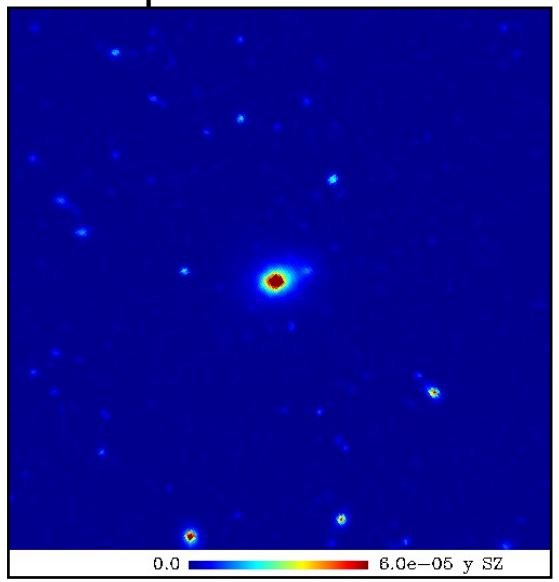

input kinetic SZ

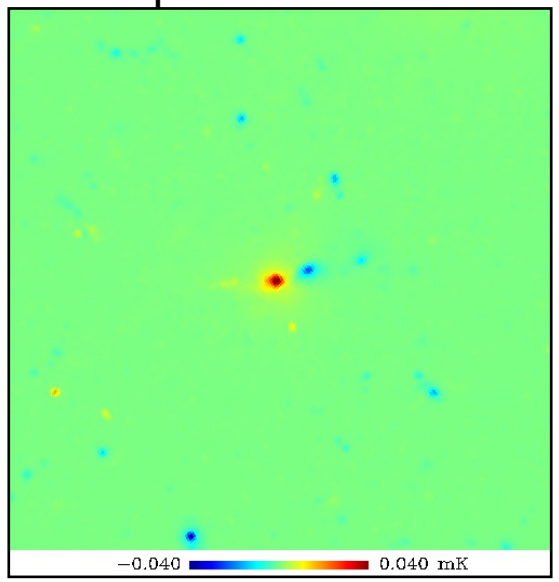

input CMB

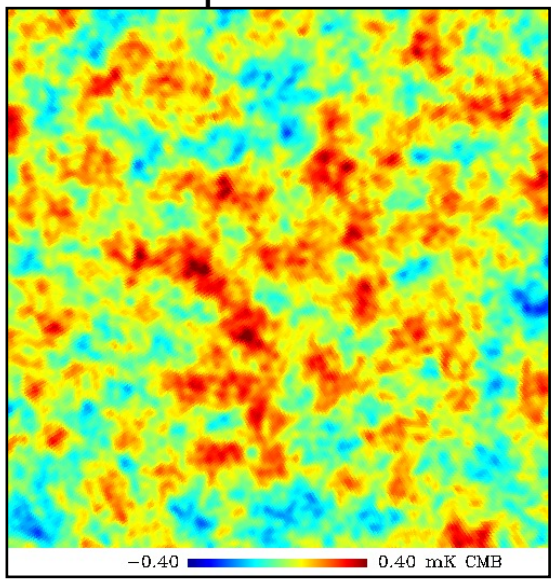

Error: ILC – CMB

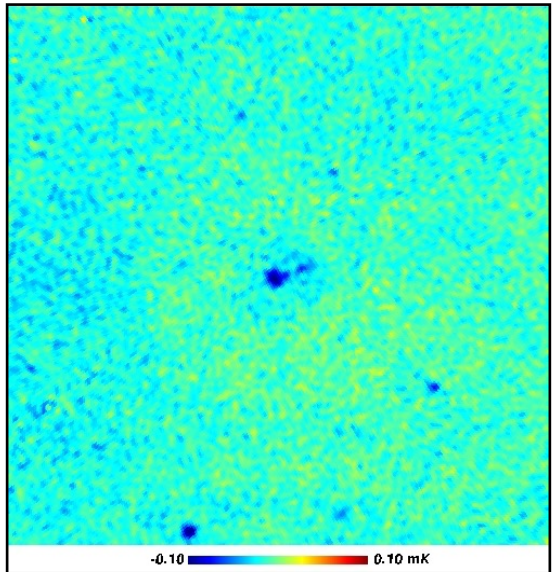

$$\boldsymbol{w} = \frac{\boldsymbol{a}^{\mathrm{T}}\mathbf{C}^{-1}}{\boldsymbol{a}^{\mathrm{T}}\mathbf{C}^{-1}\boldsymbol{a}}$$

Bennett et al 2003, Tegmark et al 2003
Eriksen et al 2004, Delabrouille et al 2009

Minimum-variance solution not adequate for certain scientific purposes!

Component separation: standard NILC

input thermal SZ

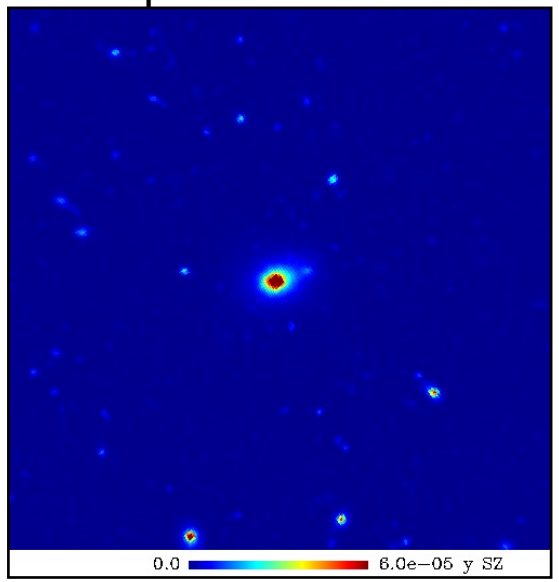

input kinetic SZ

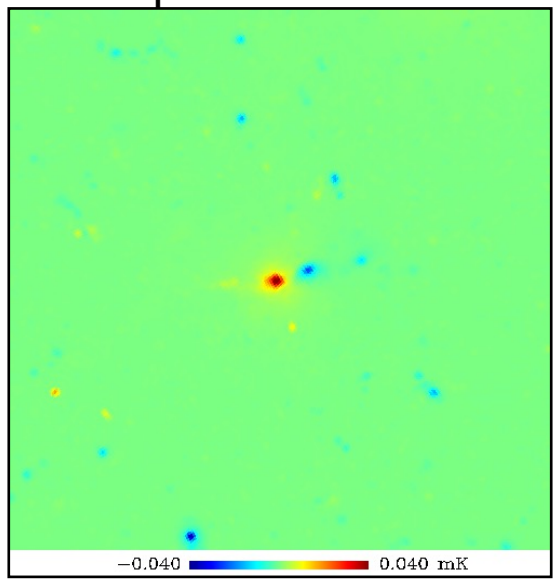

input CMB

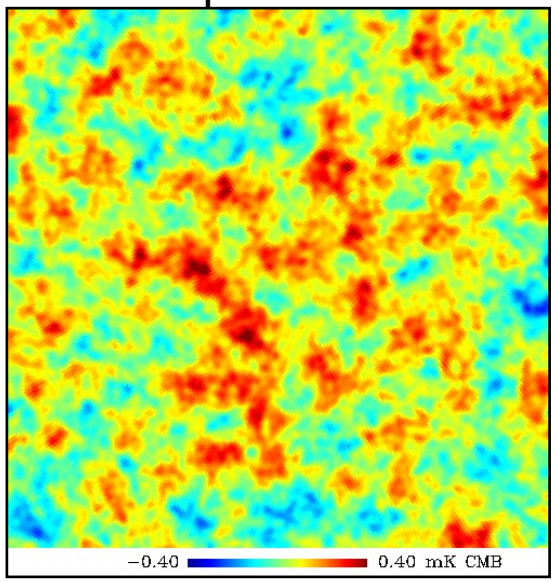

Error: ILC – CMB

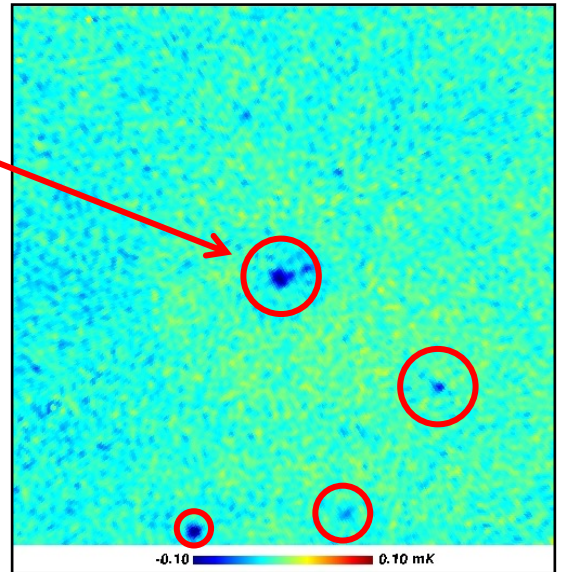

Thermal SZ residuals!

(galaxy clusters in the CMB)

$$\boldsymbol{w} = \frac{\boldsymbol{a}^{\mathrm{T}}\mathbf{C}^{-1}}{\boldsymbol{a}^{\mathrm{T}}\mathbf{C}^{-1}\boldsymbol{a}}$$

Minimum-variance solution not adequate for certain scientific purposes!

Bennett et al 2003, Tegmark et al 2003
Eriksen et al 2004, Delabrouille et al 2009

Component separation: “Constrained ILC” (CILC)

input thermal SZ

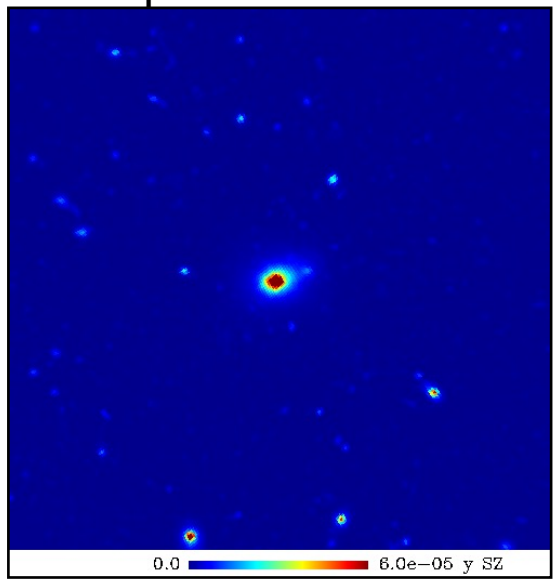

input kinetic SZ

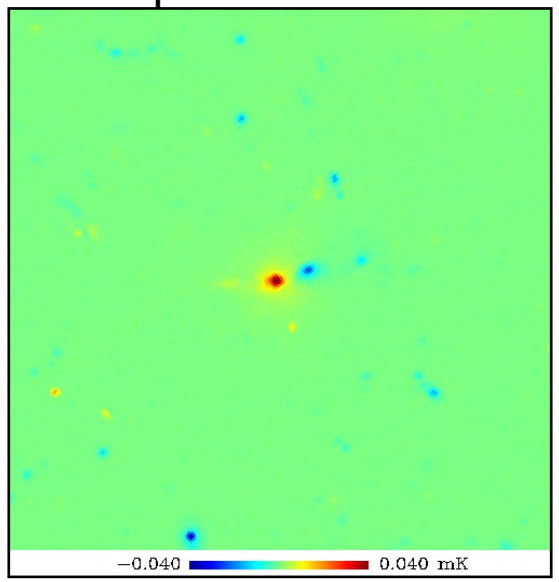

input CMB

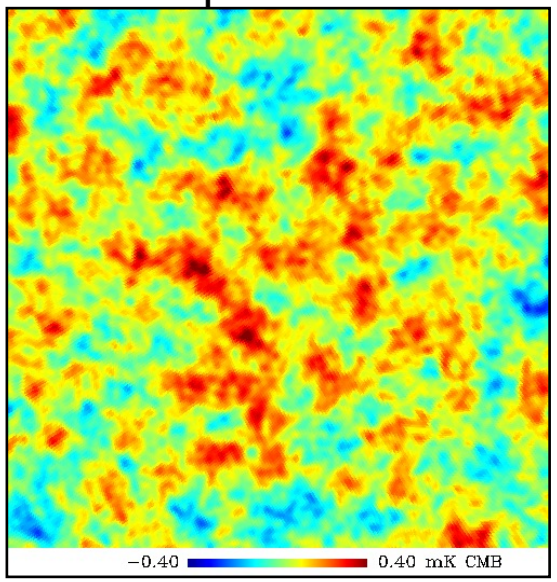

Error: CILC – CMB

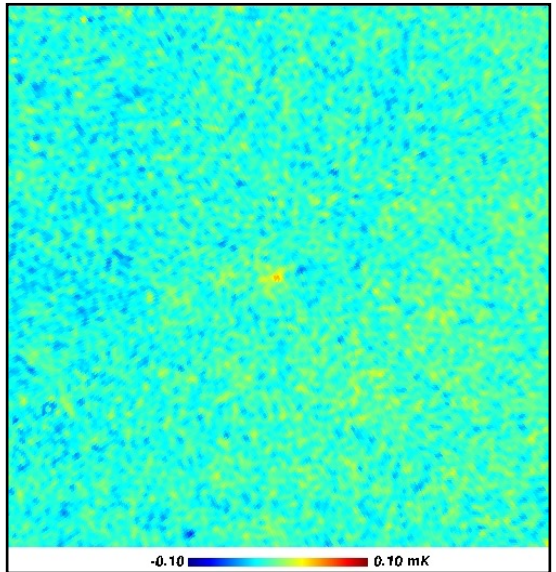

$$\boldsymbol{w} = \frac{(\boldsymbol{b}^{\mathrm{T}}\mathbf{C}^{-1}\boldsymbol{b})\boldsymbol{a}^{\mathrm{T}}\mathbf{C}^{-1} - (\boldsymbol{a}^{\mathrm{T}}\mathbf{C}^{-1}\boldsymbol{b})\boldsymbol{b}^{\mathrm{T}}\mathbf{C}^{-1}}{(\boldsymbol{a}^{\mathrm{T}}\mathbf{C}^{-1}\boldsymbol{a})(\boldsymbol{b}^{\mathrm{T}}\mathbf{C}^{-1}\boldsymbol{b}) - (\boldsymbol{a}^{\mathrm{T}}\mathbf{C}^{-1}\boldsymbol{b})^2}$$

Remazeilles, Delabrouille, Cardoso, MNRAS 2011a

Four consistent Planck CMB maps stacked on galaxy cluster locations

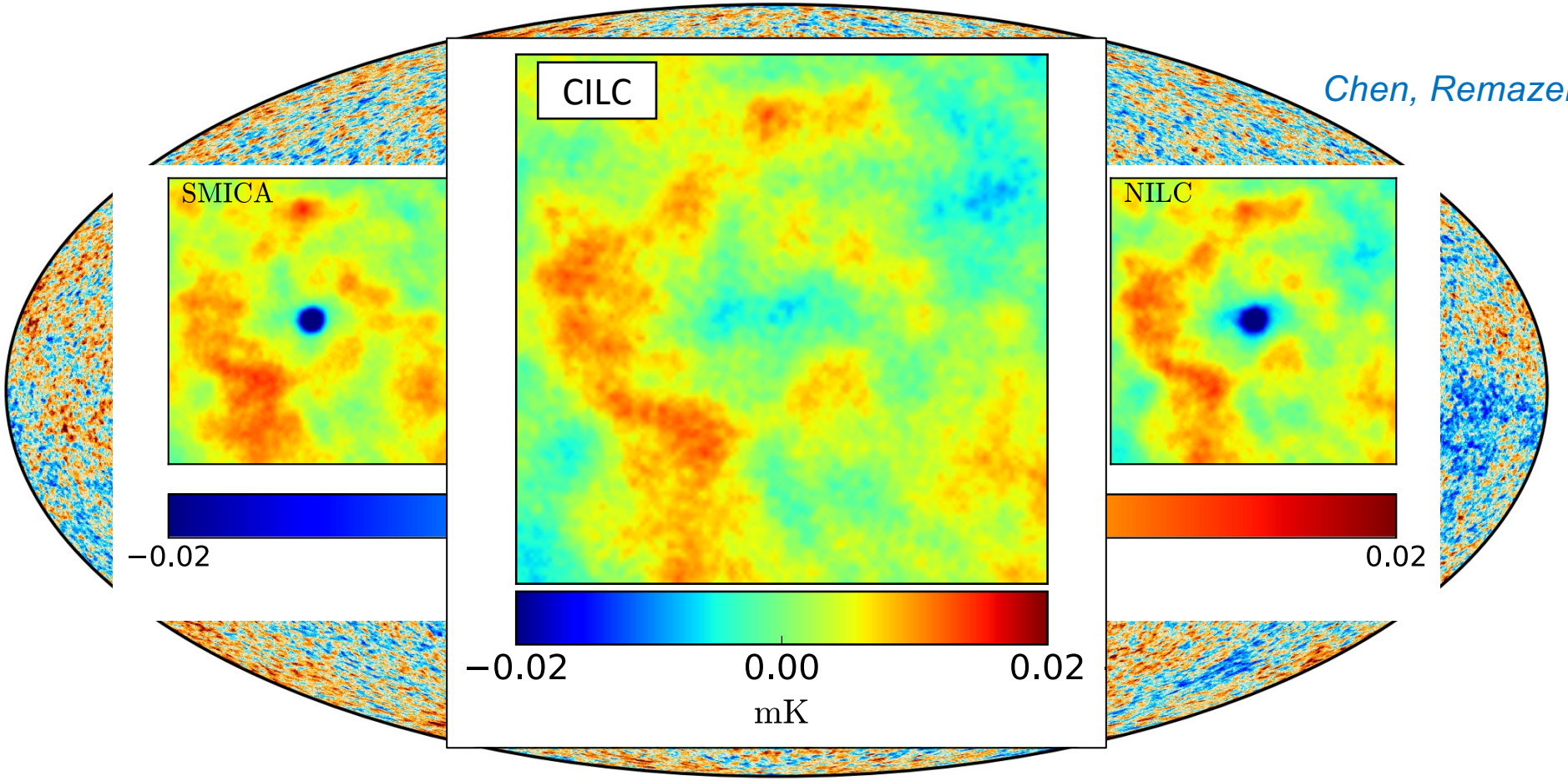

Chen, Remazeilles, Dickinson
MNRAS 2018

CILC erases SZ clusters in primary CMB maps (at the cost of larger noise)

M. Remazeilles

Foreground correlated with the signal

(e.g. relativistic SZ)

Relativistic SZ effect

$$I_\nu^{\mathrm{SZ}} = f(\nu, T_{\mathrm{e}}(\vec{n}))\, y(\vec{n})$$

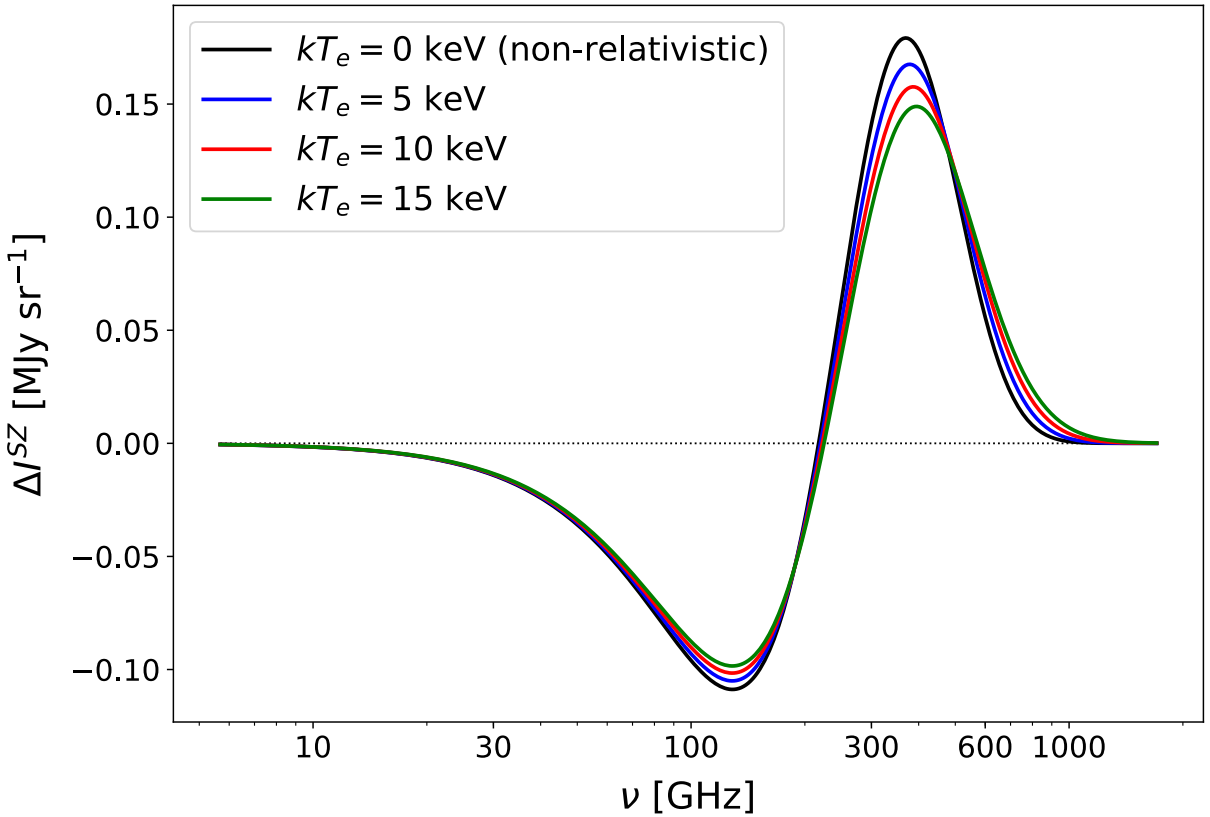

Relativistic electron temperatures distort the shape of the SZ spectrum

Two complementary observables

$$y(\vec{n})\ ,\ T_{\mathrm{e}}(\vec{n})$$

whose statistics have different dependencies on cosmological parameters

“First SZ revolution”:
The *Planck* Compton y-map

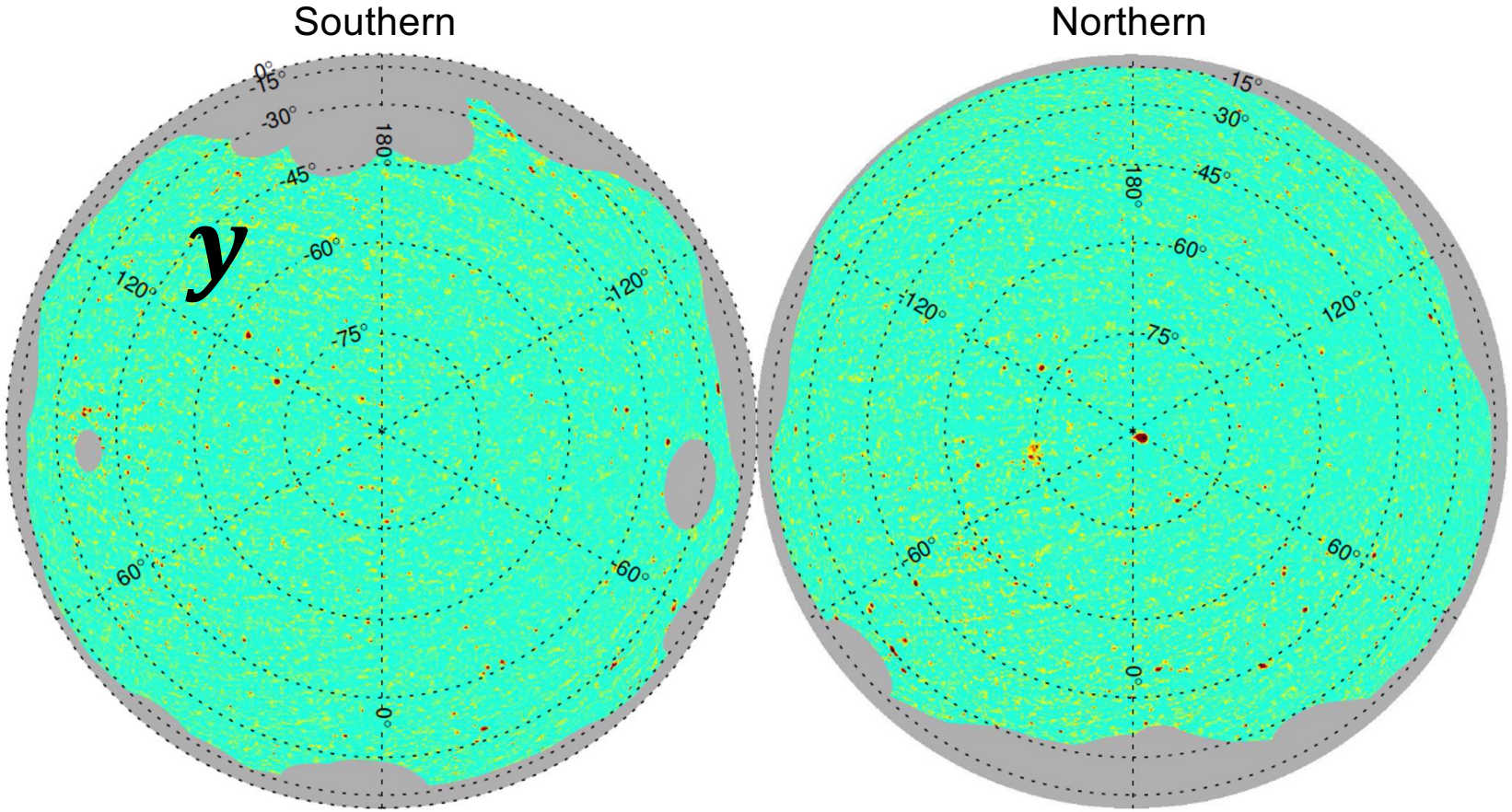

Planck 2015 results XXII, A&A (2016)

“Second SZ revolution”:
The electron temperature T_e-map?

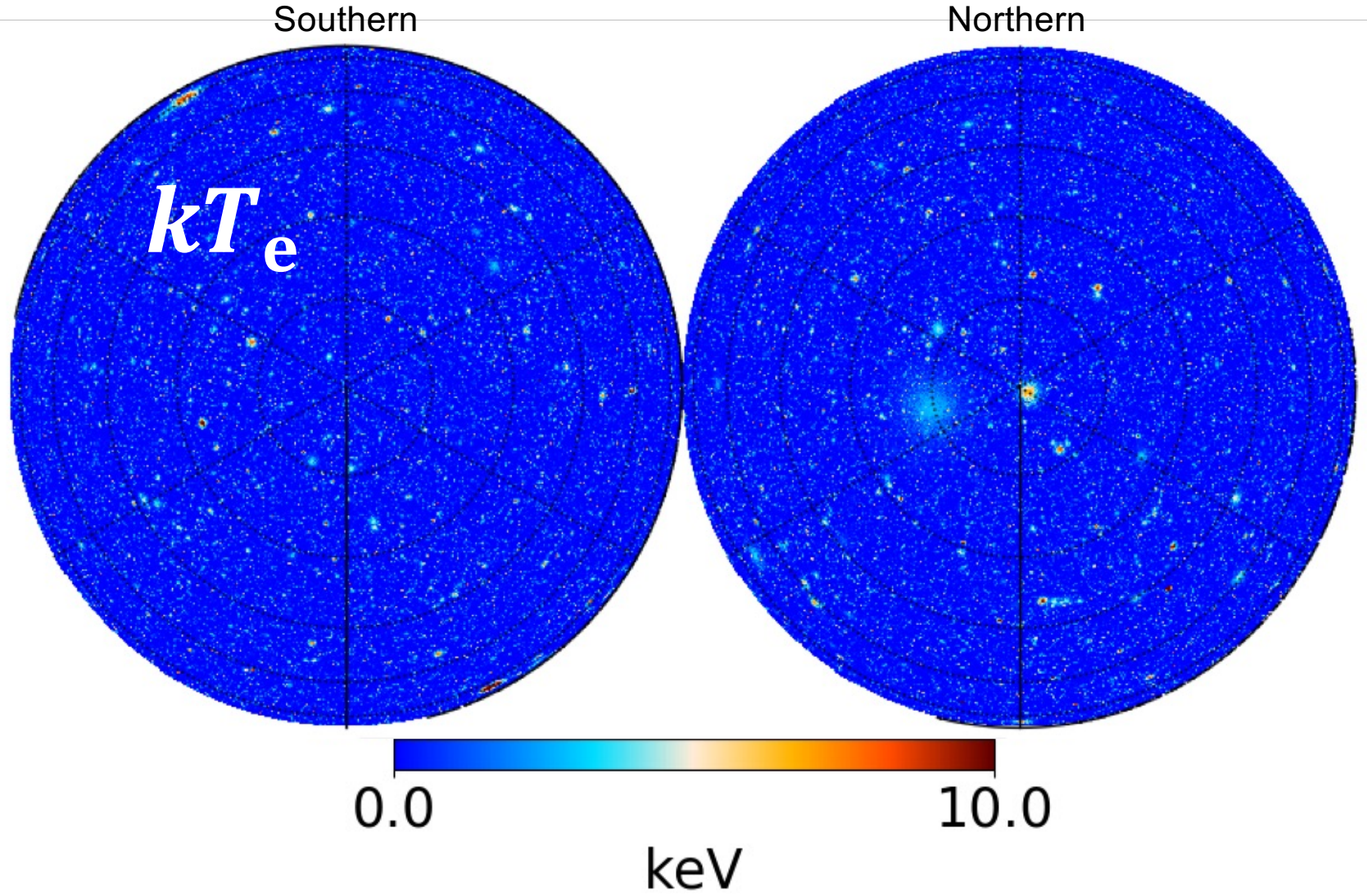

Relativistic SZ temperature corrections

$$I_\nu^{\mathrm{SZ}} = f(\nu, T_{\mathrm{e}}(\vec{n}))\, y(\vec{n})$$

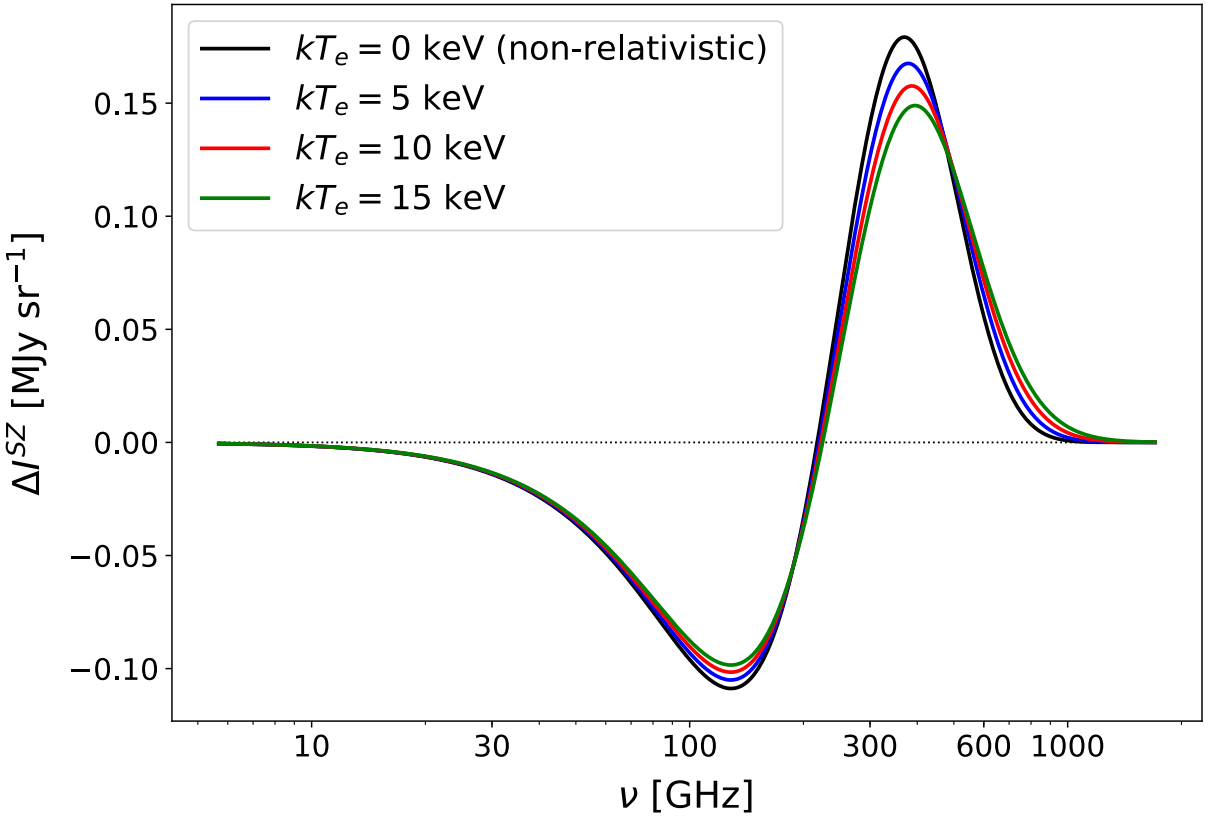

The spectral signature of SZ emission from galaxy clusters changes with the local electron gas temperature

Relativistic SZ temperature corrections

$$I_\nu^{\mathrm{SZ}} = f(\nu, T_{\mathrm{e}}(\vec{n}))\, y(\vec{n})$$

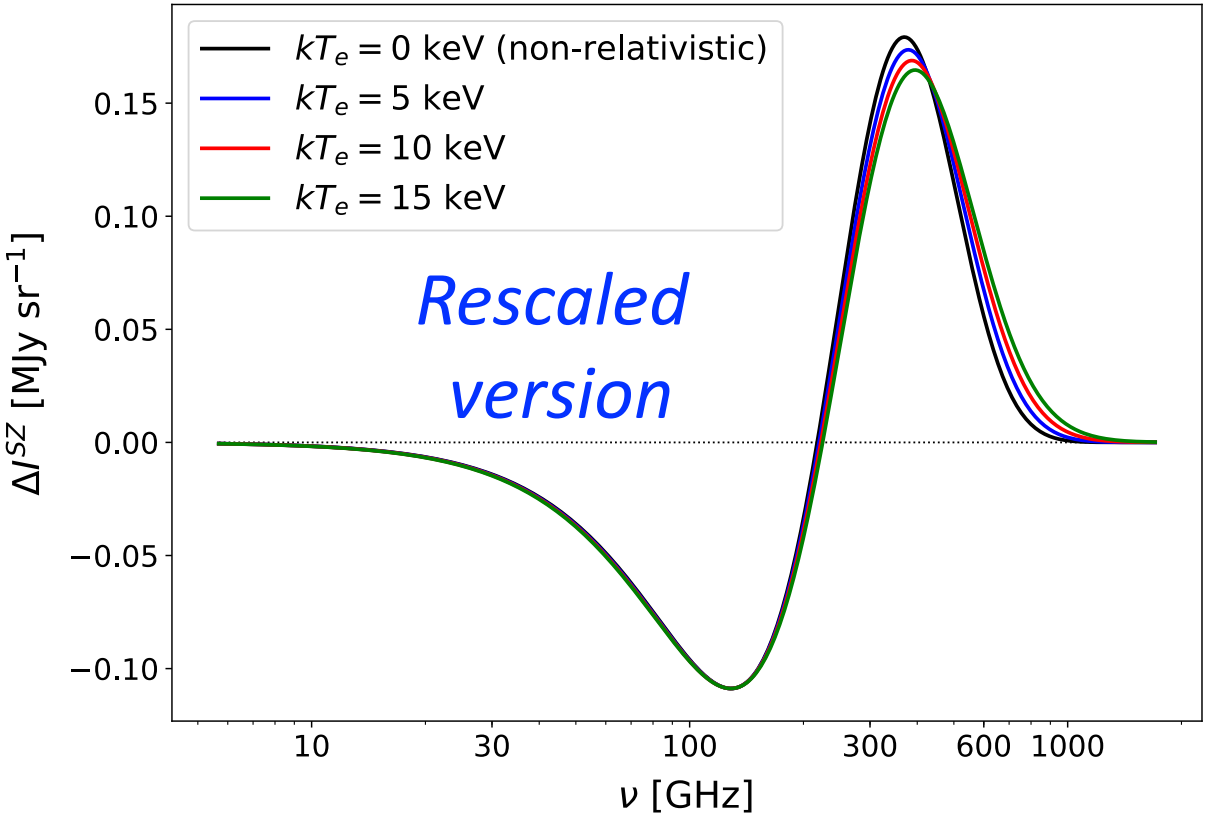

The spectral signature of SZ emission from galaxy clusters changes with the local electron gas temperature

The y-T_e degeneracy at low frequency

$$I_\nu^{SZ} = f(\nu, T_e(\vec{n}))\, y(\vec{n})$$

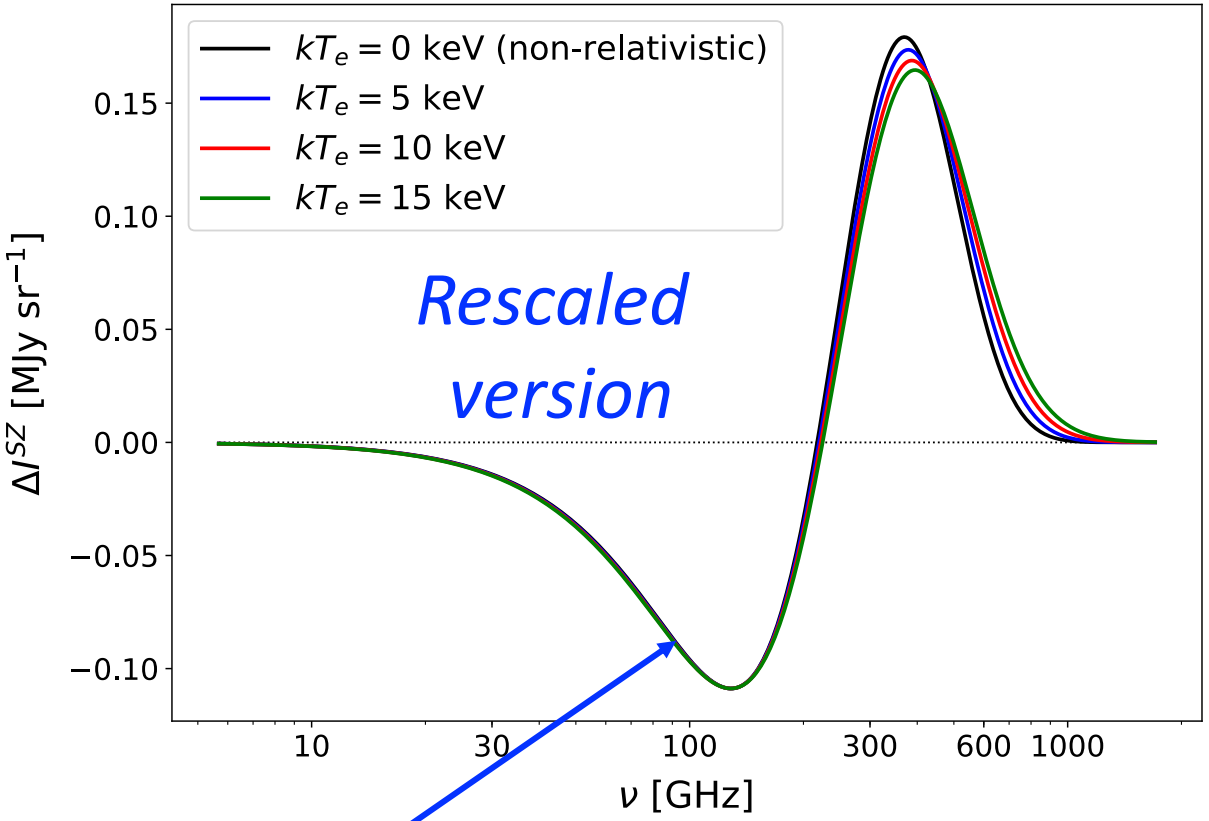

Spectral shapes are degenerate at low frequencies

(impossible to disentangle y and T_e)

The y-T_e degeneracy at low frequency

$$I_\nu^{SZ} = f(\nu, T_e(\vec{n}))\, y(\vec{n})$$

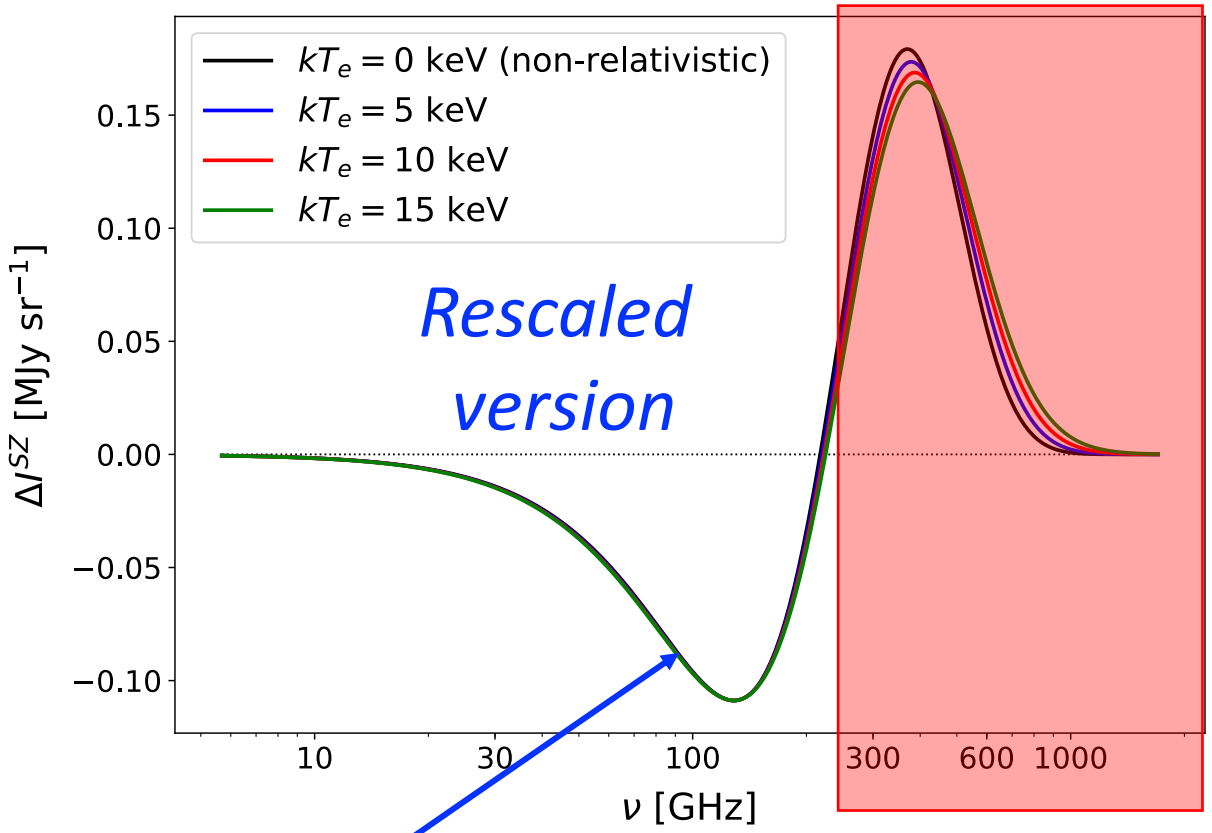

High frequencies are essential to extract rSZ

Spectral shapes are degenerate at low frequencies

(impossible to disentangle y and T_e)

rSZ component separation

How to disentangle the y and T_{e} observables of the rSZ effect in sky observations?

SZ temperature moment expansion

$$I_{\nu}^{SZ}(\vec{n}) = f(\nu, T_e(\vec{n}))\, y(\vec{n})$$

Remazeilles & Chluba, MNRAS (2020)

SZ temperature moment expansion

$$I_\nu^{SZ}(\vec{n}) = f(\nu, T_e(\vec{n}))\, y(\vec{n})$$

Taylor expansion around some pivot temperature $\bar{T}_e$

$$I_\nu^{SZ}(\vec{n}) = f(\nu, \bar{T}_e)\ \ y(\vec{n}) + \frac{\partial f(\nu, \bar{T}_e)}{\partial T_e}\ (T_e(\vec{n}) - \bar{T}_e) y(\vec{n}) + \mathcal{O}(T_e^2)$$

Remazeilles & Chluba, MNRAS (2020)

SZ temperature moment expansion

$$I_\nu^{SZ}(\vec{n}) = f(\nu, T_e(\vec{n}))\, y(\vec{n})$$

Taylor expansion around some pivot temperature $\bar{T}_e$

$$I_\nu^{SZ}(\vec{n}) = \underbrace{f(\nu, \bar{T}_e)}_{\text{spectrum of } y} \underbrace{y(\vec{n})}_{y \text{ component}} + \underbrace{\frac{\partial f(\nu, \bar{T}_e)}{\partial T_e}}_{\text{spectrum of } yT_e} \underbrace{(T_e(\vec{n}) - \bar{T}_e) y(\vec{n})}_{y\Delta T_e \text{ component}} + \mathcal{O}(T_e^2)$$

Remazeilles & Chluba, MNRAS (2020)

SZ temperature moment expansion

$$I_\nu^{SZ}(\vec{n}) = f(\nu, T_e(\vec{n}))\, y(\vec{n})$$

Taylor expansion around some pivot temperature $\bar{T}_e$

$$I_\nu^{SZ}(\vec{n}) = \underbrace{f(\nu, \bar{T}_e)}_{\text{spectrum of } y}\ \underbrace{y(\vec{n})}_{y \text{ component}} + \underbrace{\frac{\partial f(\nu, \bar{T}_e)}{\partial T_e}}_{\text{spectrum of } yT_e}\ \underbrace{(T_e(\vec{n}) - \bar{T}_e) y(\vec{n})}_{y\Delta T_e \text{ component}} + \mathcal{O}(T_e^2)$$

Two distinct components of emission, y and $y\Delta T_e$,
with different spectral signatures

Remazeilles & Chluba, MNRAS (2020)

rSZ component separation

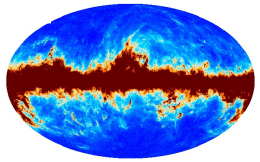

$$d(\nu,\vec{n}) = \underbrace{f(\nu,\overline{T}_{\mathrm{e}})}_{\text{spectrum of } y(\vec{n})} \underbrace{y(\vec{n})}_{y(\vec{n})} + \underbrace{\frac{\partial f(\nu,\overline{T}_{\mathrm{e}})}{\partial T_{\mathrm{e}}}}_{\text{spectrum of } y\Delta T_{\mathrm{e}}(\vec{n})} \underbrace{(T_{\mathrm{e}}(\vec{n}) - \overline{T}_{\mathrm{e}})y(\vec{n})}_{y\Delta T_{\mathrm{e}}(\vec{n})} + \underbrace{N(\nu,\vec{n})}_{\text{foregrounds + noise}}$$

Remazeilles & Chluba, MNRAS (2020)

rSZ component separation

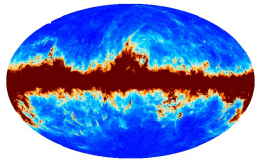

$$d(\nu,\vec{n}) = \underbrace{f(\nu,\overline{T}_e)}_{\text{spectrum of } y(\vec{n})} \underbrace{y(\vec{n})}_{y(\vec{n})} + \underbrace{\frac{\partial f(\nu,\overline{T}_e)}{\partial T_e}}_{\text{spectrum of } y\Delta T_e(\vec{n})} \underbrace{(T_e(\vec{n}) - \overline{T}_e)y(\vec{n})}_{y\Delta T_e(\vec{n})} + \underbrace{N(\nu,\vec{n})}_{\text{foregrounds + noise}}$$

signal of interest (rSZ)

Remazeilles & Chluba, MNRAS (2020)

rSZ component separation

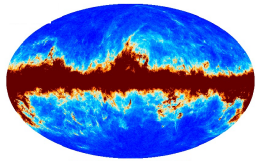

$$d(\nu,\vec{n}) = \underbrace{f(\nu,\bar{T}_e)}_{\text{spectrum of } y(\vec{n})} \underbrace{y(\vec{n})}_{y(\vec{n})} + \underbrace{\frac{\partial f(\nu,\bar{T}_e)}{\partial T_e}}_{\text{spectrum of } y\Delta T_e(\vec{n})} \underbrace{(T_e(\vec{n}) - \bar{T}_e)y(\vec{n})}_{y\Delta T_e(\vec{n})} + \underbrace{N(\nu,\vec{n})}_{\text{foregrounds + noise}}$$

foreground correlated with the signal!

signal of interest (rSZ)

Remazeilles & Chluba, MNRAS (2020)

rSZ component separation

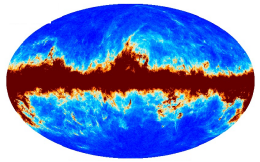

$$d(\nu,\vec{n}) = \underbrace{f(\nu,\bar{T}_e)}_{\text{spectrum of } y(\vec{n})} \underbrace{y(\vec{n})}_{y(\vec{n})} + \underbrace{\frac{\partial f(\nu,\bar{T}_e)}{\partial T_e}}_{\text{spectrum of } y\Delta T_e(\vec{n})} \underbrace{(T_e(\vec{n}) - \bar{T}_e)y(\vec{n})}_{y\Delta T_e(\vec{n})} + \underbrace{N(\nu,\vec{n})}_{\text{foregrounds + noise}}$$

Component separation with the CILC method (*Remazeilles et al MNRAS 2011a*)

$$\widehat{y\Delta T_e}(\vec{n}) = \sum_\nu w(\nu)\, d(\nu,\vec{n}) \quad \text{such that} \quad \begin{cases} \left\langle \left(\widehat{y\Delta T_e}\right)^2 \right\rangle \text{ of minimum variance} \\ \sum_\nu w(\nu) \dfrac{\partial f(\nu,\bar{T}_e)}{\partial T_e} = 1 \\ \sum_\nu w(\nu)\, f(\nu,\bar{T}_e) = 0 \end{cases}$$

Remazeilles & Chluba, MNRAS (2020)

rSZ component separation

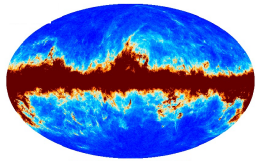

$$d(\nu,\vec{n}) = \underbrace{f(\nu,\bar{T}_e)}_{\text{spectrum of } y(\vec{n})} \underbrace{y(\vec{n})}_{y(\vec{n})} + \underbrace{\frac{\partial f(\nu,\bar{T}_e)}{\partial T_e}}_{\text{spectrum of } y\Delta T_e(\vec{n})} \underbrace{(T_e(\vec{n}) - \bar{T}_e)y(\vec{n})}_{y\Delta T_e(\vec{n})} + \underbrace{N(\nu,\vec{n})}_{\text{foregrounds + noise}}$$

Component separation with the CILC method (*Remazeilles et al MNRAS 2011a*)

$$\widehat{y\Delta T_e}(\vec{n}) = \sum_\nu w(\nu)\, d(\nu,\vec{n}) \quad \text{such that} \quad \begin{cases} \left\langle \left(\widehat{y\Delta T_e}\right)^2 \right\rangle \text{ of minimum variance} \\ \boxed{\sum_\nu w(\nu) \frac{\partial f(\nu,\bar{T}_e)}{\partial T_e} = 1} \\ \sum_\nu w(\nu)\, f(\nu,\bar{T}_e) = 0 \end{cases}$$

Guarantees the conservation of the signal of interest $y\Delta T_e$

Remazeilles & Chluba, MNRAS (2020)

rSZ component separation

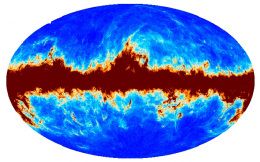

$$d(\nu,\vec{n}) = \underbrace{f(\nu,\bar{T}_e)}_{\text{spectrum of } y(\vec{n})} \underbrace{y(\vec{n})}_{y(\vec{n})} + \underbrace{\frac{\partial f(\nu,\bar{T}_e)}{\partial T_e}}_{\text{spectrum of } y\Delta T_e(\vec{n})} \underbrace{(T_e(\vec{n}) - \bar{T}_e)y(\vec{n})}_{y\Delta T_e(\vec{n})} + \underbrace{N(\nu,\vec{n})}_{\text{foregrounds + noise}}$$

Component separation with the CILC method (*Remazeilles et al MNRAS 2011a*)

$$\widehat{y\Delta T_e}(\vec{n}) = \sum_\nu w(\nu)\, d(\nu,\vec{n}) \quad \text{such that} \quad \begin{cases} \left\langle \left(\widehat{y\Delta T_e}\right)^2 \right\rangle \text{ of minimum variance} \\ \sum_\nu w(\nu) \dfrac{\partial f(\nu,\bar{T}_e)}{\partial T_e} = 1 \\ \boxed{\sum_\nu w(\nu)\, f(\nu,\bar{T}_e) = 0} \end{cases}$$

Guarantees the cancellation of y residuals in the $y\Delta T_e$ map

Remazeilles & Chluba, MNRAS (2020)

rSZ component separation

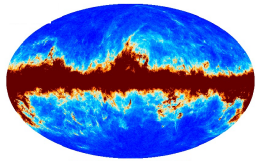

$$d(\nu,\vec{n}) = \underbrace{f(\nu,\bar{T}_e)}_{\text{spectrum of } y(\vec{n})} \underbrace{y(\vec{n})}_{y(\vec{n})} + \underbrace{\frac{\partial f(\nu,\bar{T}_e)}{\partial T_e}}_{\text{spectrum of } y\Delta T_e(\vec{n})} \underbrace{(T_e(\vec{n}) - \bar{T}_e)y(\vec{n})}_{y\Delta T_e(\vec{n})} + \underbrace{N(\nu,\vec{n})}_{\text{foregrounds + noise}}$$

Component separation with the CILC method (*Remazeilles et al MNRAS 2011a*)

$$\widehat{y\Delta T_e}(\vec{n}) = \sum_\nu w(\nu)\, d(\nu,\vec{n}) \quad \text{such that} \quad \begin{cases} \boxed{\left\langle \left(\widehat{y\Delta T_e}\right)^2 \right\rangle \text{ of minimum variance}} \\ \sum_\nu w(\nu) \dfrac{\partial f(\nu,\bar{T}_e)}{\partial T_e} = 1 \\ \sum_\nu w(\nu)\, f(\nu,\bar{T}_e) = 0 \end{cases}$$

Guarantees the mitigation of foregrounds and noise

Remazeilles & Chluba, MNRAS (2020)

rSZ component separation

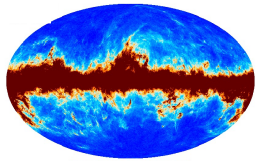

$$d(\nu,\vec{n}) = \underbrace{f(\nu,\bar{T}_e)}_{\text{spectrum of } y(\vec{n})}\ \underbrace{y(\vec{n})}_{y(\vec{n})} + \underbrace{\frac{\partial f(\nu,\bar{T}_e)}{\partial T_e}}_{\text{spectrum of } y\Delta T_e(\vec{n})}\ \underbrace{(T_e(\vec{n}) - \bar{T}_e)y(\vec{n})}_{y\Delta T_e(\vec{n})} + \underbrace{N(\nu,\vec{n})}_{\text{foregrounds + noise}}$$

Component separation with the CILC method (*Remazeilles et al MNRAS 2011a*)

$$\widehat{y\Delta T_e}(\vec{n}) = \sum_\nu w(\nu)\, d(\nu,\vec{n}) \quad \text{such that} \quad \begin{cases} \left\langle \left(\widehat{y\Delta T_e}\right)^2 \right\rangle \text{ of minimum variance} \\ \sum_\nu w(\nu) \dfrac{\partial f(\nu,\bar{T}_e)}{\partial T_e} = 1 \\ \sum_\nu w(\nu)\, f(\nu,\bar{T}_e) = 0 \end{cases}$$

$$\Rightarrow \widehat{y\Delta T_e}(\vec{n}) = \underbrace{(w\cdot f)}_{=0} y(\vec{n}) + \underbrace{(w\cdot \partial_{T_e} f)}_{=1}(T_e(\vec{n}) - \bar{T}_e)\, y(n) + \underbrace{w\cdot N}_{\text{minimized}}$$

Remazeilles & Chluba, MNRAS (2020)

rSZ component separation

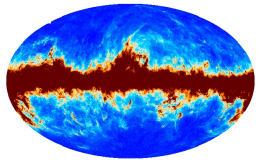

$$d(\nu,\vec{n}) = \underbrace{f(\nu,\bar{T}_e)}_{\text{spectrum of } y(\vec{n})} \underbrace{y(\vec{n})}_{y(\vec{n})} + \underbrace{\frac{\partial f(\nu,\bar{T}_e)}{\partial T_e}}_{\text{spectrum of } y\Delta T_e(\vec{n})} \underbrace{(T_e(\vec{n}) - \bar{T}_e)y(\vec{n})}_{y\Delta T_e(\vec{n})} + \underbrace{N(\nu,\vec{n})}_{\text{foregrounds + noise}}$$

Component separation with the CILC method (*Remazeilles et al MNRAS 2011a*)

$$\widehat{y\Delta T_e}(\vec{n}) = \sum_\nu w(\nu)\, d(\nu,\vec{n}) \quad \text{such that} \quad \begin{cases} \left\langle \left(\widehat{y\Delta T_e}\right)^2 \right\rangle \text{ of minimum variance} \\ \sum_\nu w(\nu) \dfrac{\partial f(\nu,\bar{T}_e)}{\partial T_e} = 1 \\ \sum_\nu w(\nu)\, f(\nu,\bar{T}_e) = 0 \end{cases}$$

$$\Rightarrow \widehat{y\Delta T_e}(\vec{n}) = \underline{(T_e(\vec{n}) - \bar{T}_e)\, y(n)} + w \cdot N$$

T_e-modulated y-map!

Remazeilles & Chluba, MNRAS (2020)

Why is this new SZ observable so interesting?

$$y\Delta T_{\mathrm{e}}(\vec{n}) \equiv y(\vec{n})(T_{\mathrm{e}}(\vec{n}) - \overline{T}_{\mathrm{e}})$$

Varying the pivot temperature $\overline{T}_{\mathrm{e}}$ in the analysis allows us to perform a real **temperature spectroscopy** of the cluster:

- <u>Decrement</u> if actual temperature $T_{\mathrm{e}}(\vec{n}) < \overline{T}_{\mathrm{e}}$
- <u>Increment</u> if actual temperature $T_{\mathrm{e}}(\vec{n}) > \overline{T}_{\mathrm{e}}$
- <u>Null</u> if actual temperature $T_{\mathrm{e}}(\vec{n}) \simeq \overline{T}_{\mathrm{e}}$

Remazeilles & Chluba, MNRAS 2020

Cluster spectroscopy across temperature

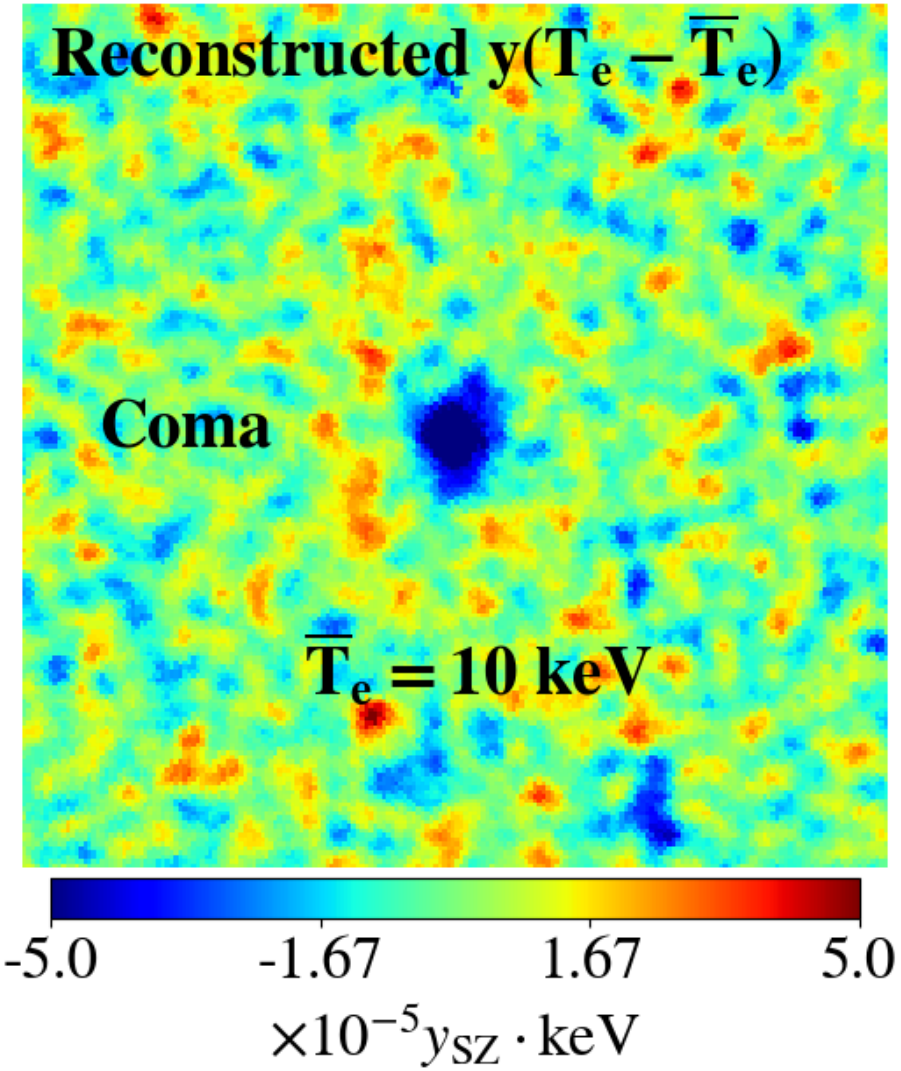

$\bar{T}_e = 10$ keV

Remazeilles & Chluba, MNRAS (2020)

Cluster spectroscopy across temperature

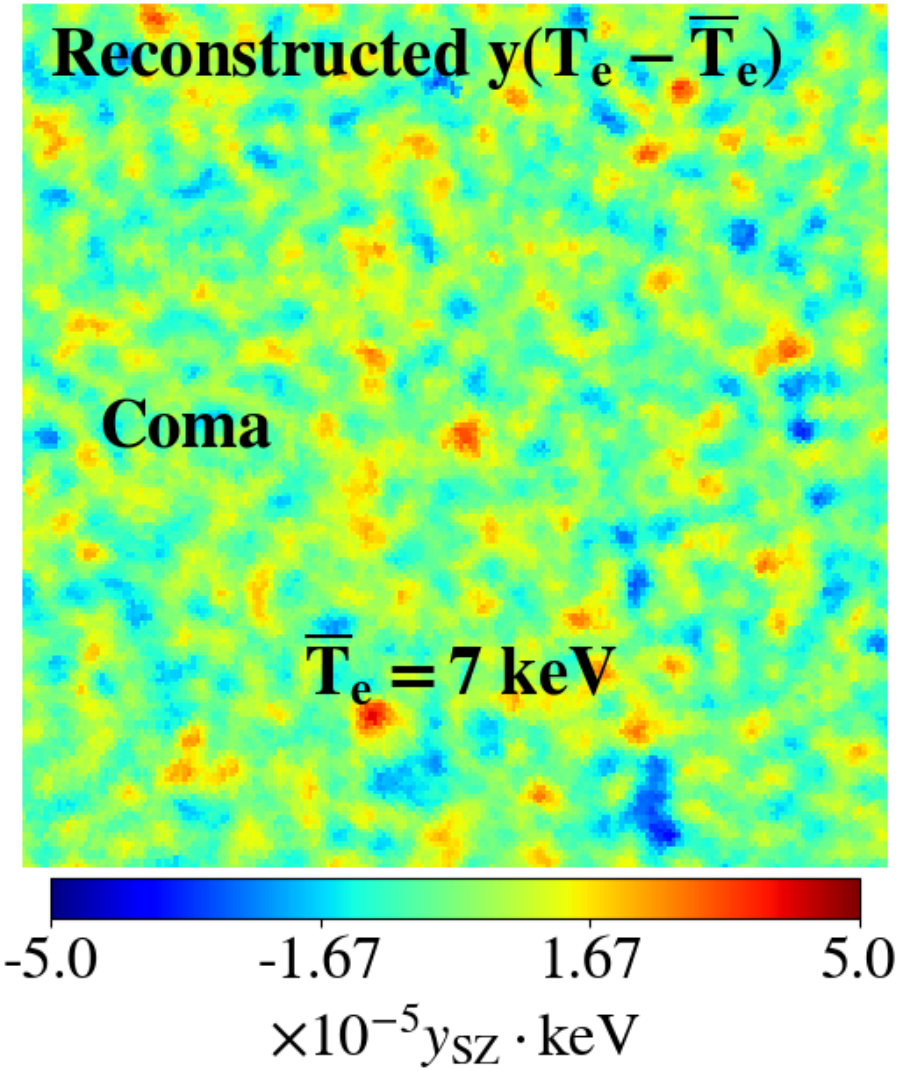

$\bar{T}_e = 7$ keV

Remazeilles & Chluba, MNRAS (2020)

Cluster spectroscopy across temperature

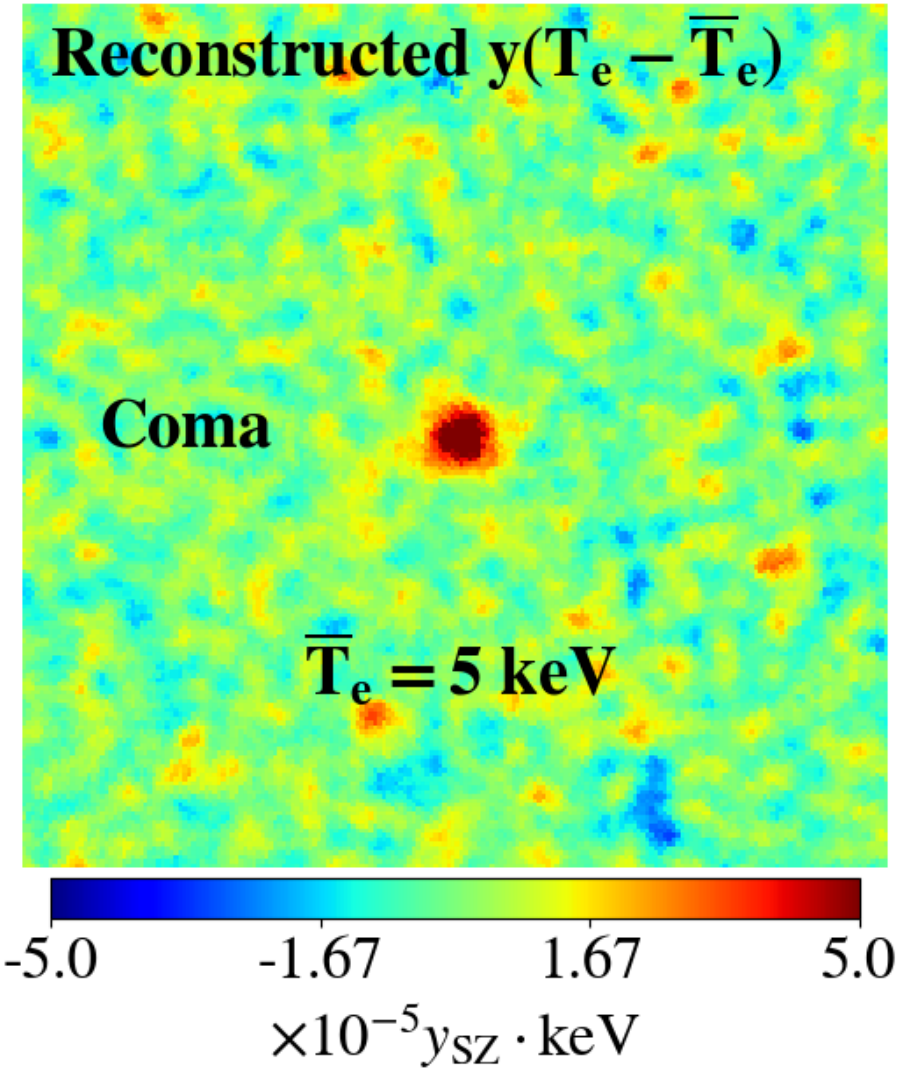

$\bar{T}_e = 5$ keV

Remazeilles & Chluba, MNRAS (2020)

“First SZ revolution”:
cluster spectroscopy across frequencies

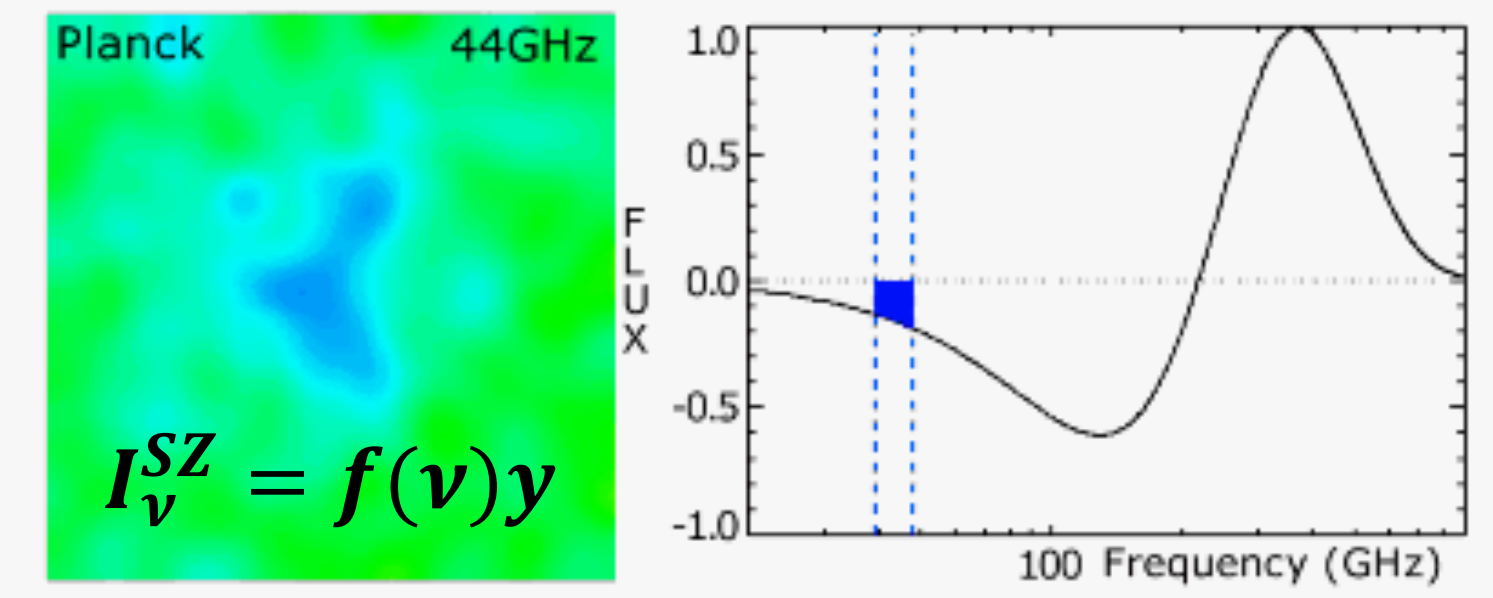

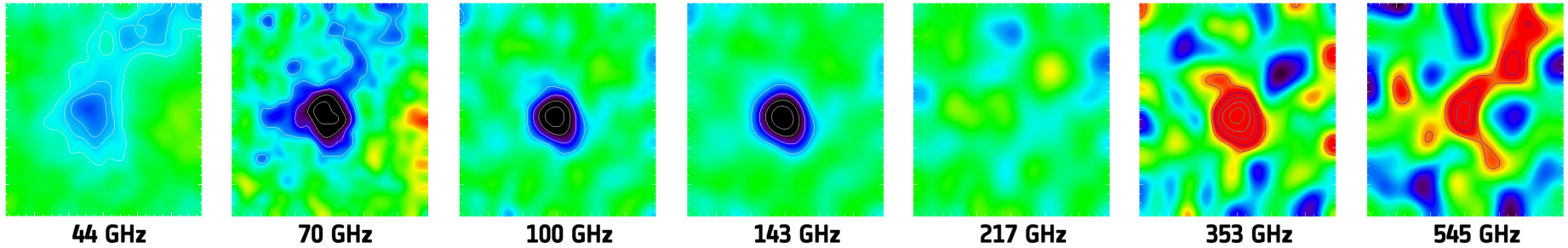

Credit: ESA/Planck Collaboration

“Second SZ revolution”: cluster spectroscopy across temperatures

Recovered $y(T_e - \bar{T}_e)$-map for different pivots

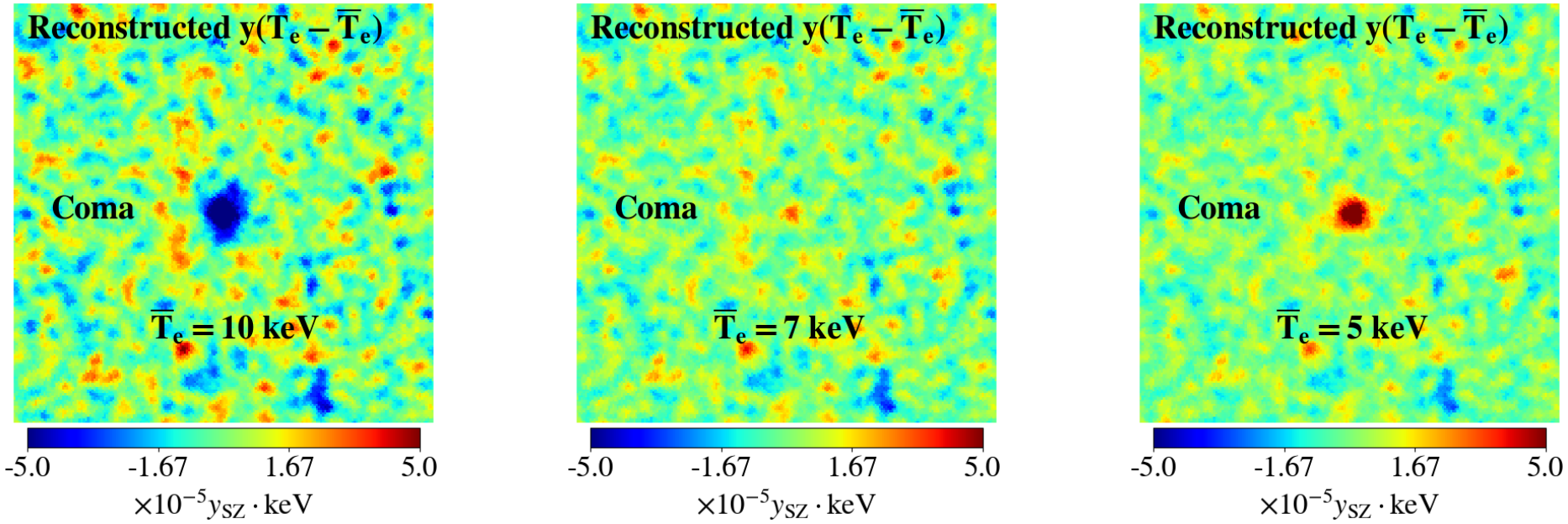

colder than 10 keV (decrement)

closer to 7 keV (null)

hotter than 5 keV (increment)

Remazeilles & Chluba, MNRAS (2020)

Spectral degeneracies

(e.g. dust and CIB)

Planck 2013 map of Galactic dust

Planck 2013 results XI, A&A 2014

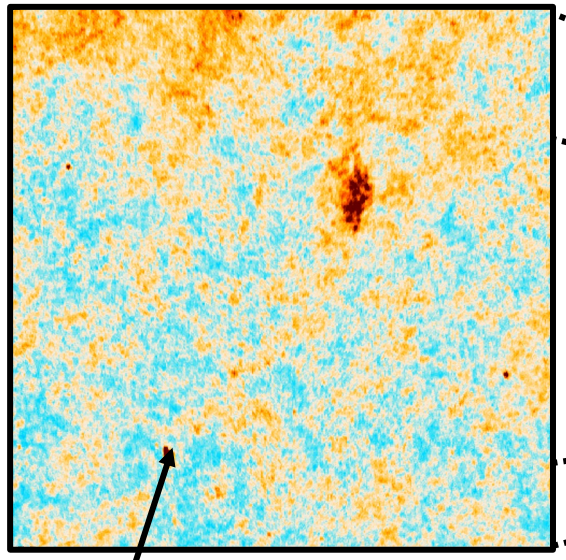

CIB contamination
at small scales!

(background galaxies)

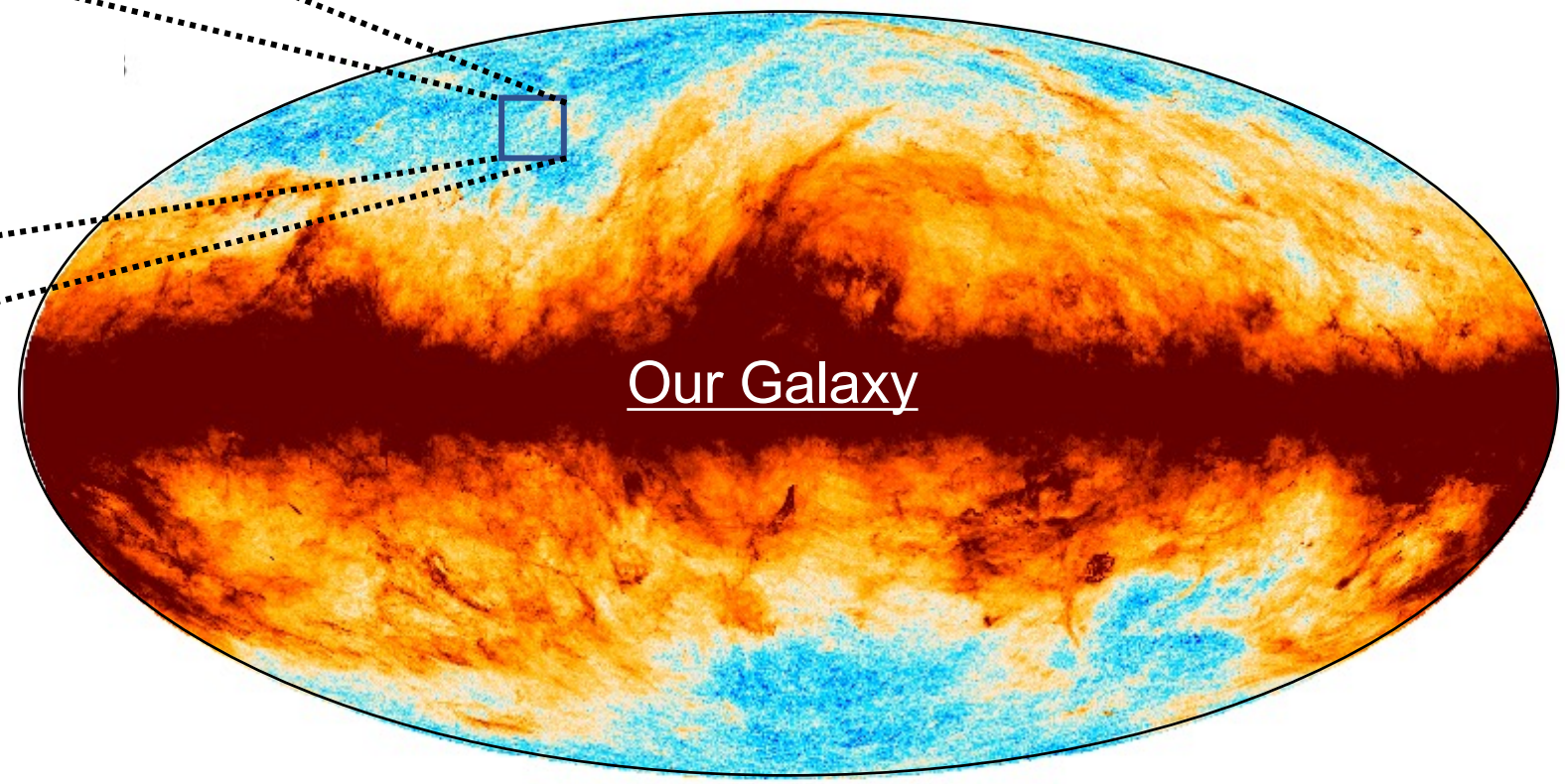

M. Remazeilles

Dust-CIB spectral degeneracy

CIB and thermal dust have similar spectral signatures (modified blackbody)

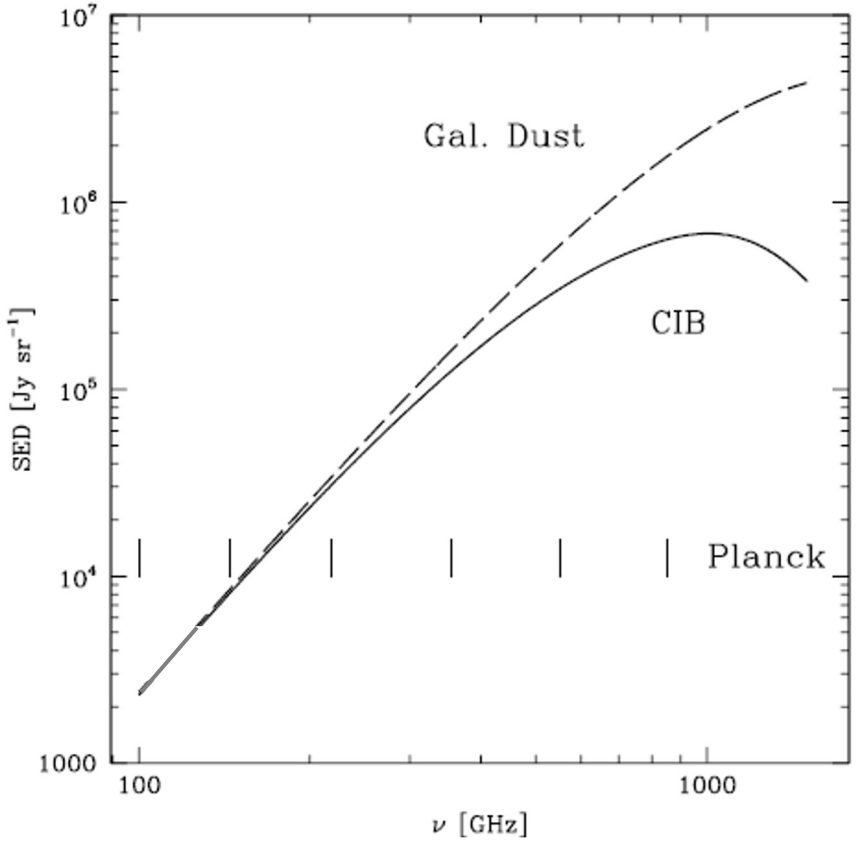

- Fitting a modified blackbody to *Planck* multi-frequency data cannot help disentangling thermal dust and CIB emissions
- Need to think beyond spectral modelling for component separation
- Instead of relying solely on spectral information, we can use statistical information to discriminate between dust and CIB

Breaking the dust-CIB spectral degeneracy

Thermal dust and CIB have similar spectral signatures (modified blackbody)

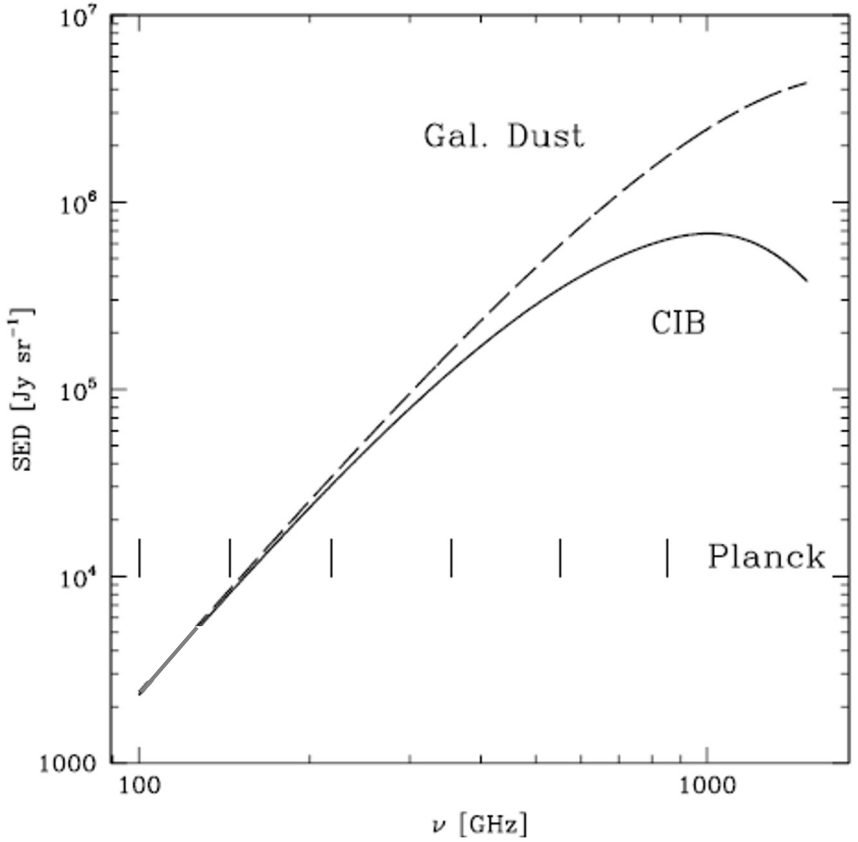

Thermal dust and CIB have different angular power spectra!

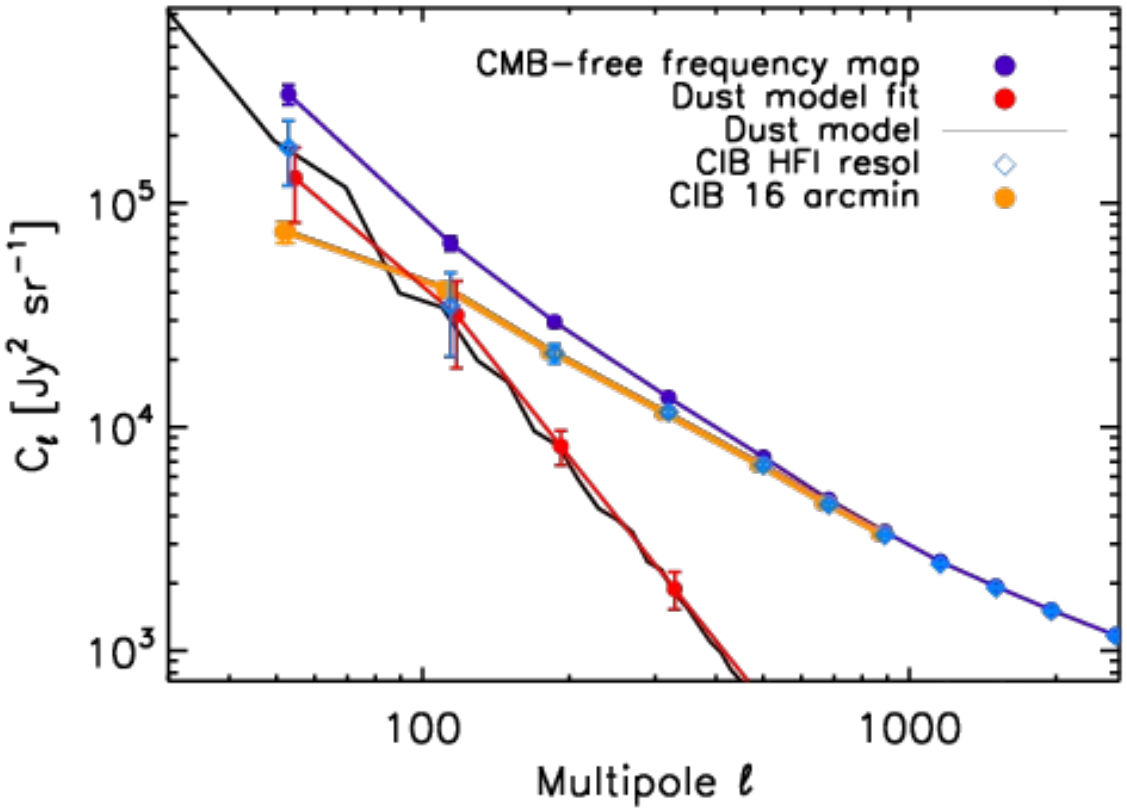

M. Remazeilles

GNILC

Remazeilles, Delabrouille, Cardoso, MNRAS 2011b

- **Use statistical / spatial information** (power spectrum) to break spectral degeneracies

- **Blind,** i.e. no assumption about astrophysical foregrounds

  sole prior assumption: power spectrum of the cosmological signal

- **Wavelet-based**

  Allow us to optimize component separation depending on the local variations of the foregrounds across the sky and across angular scales

Planck 2013 map of Galactic dust

Planck 2013 results XI, A&A 2014

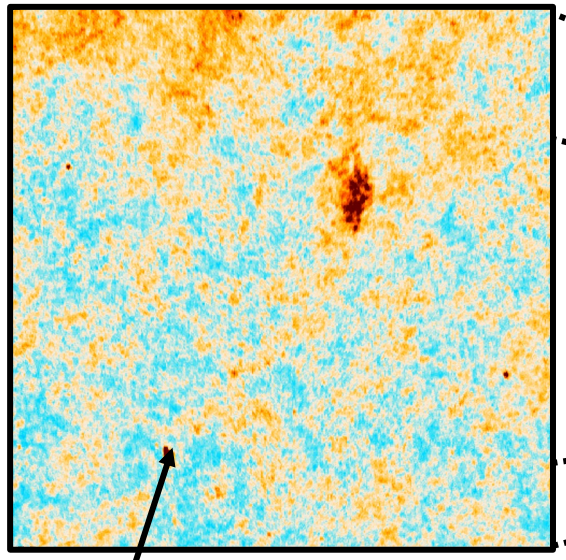

CIB contamination
at small scales!

(background galaxies)

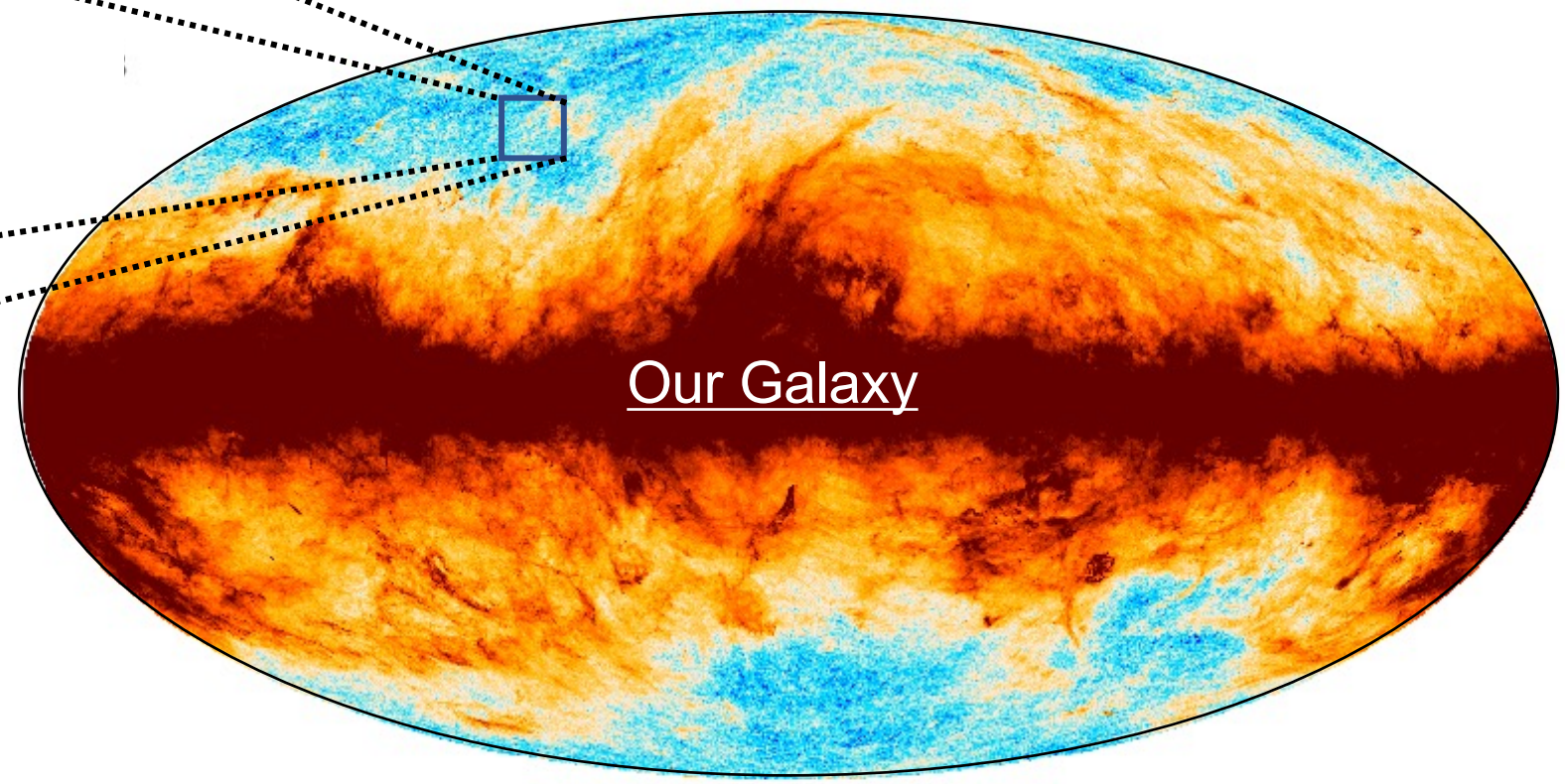

M. Remazeilles

Planck GNILC map of Galactic dust

Planck intermediate results XLVIII, A&A 2016

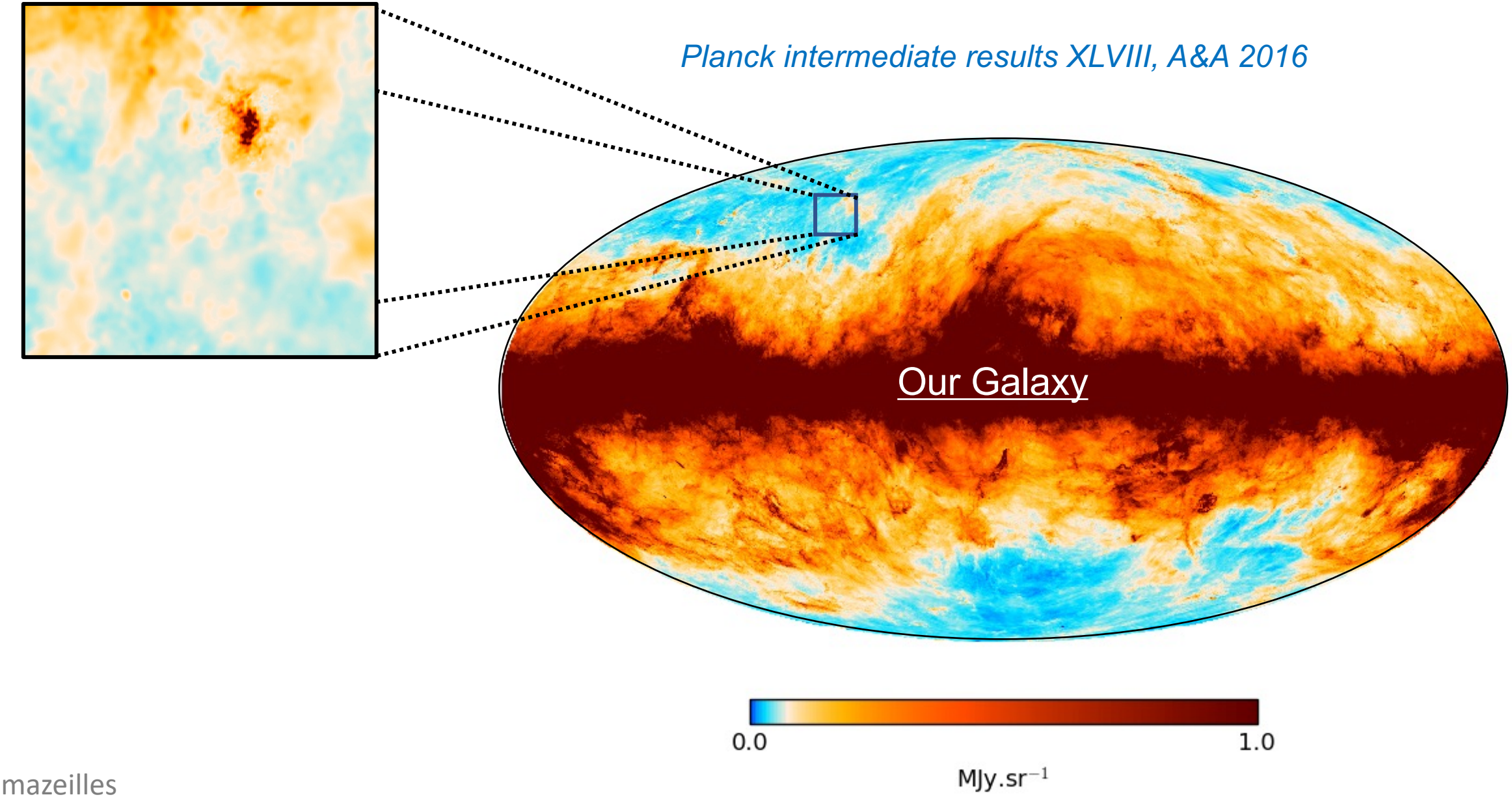

M. Remazeilles

Planck GNILC map of CIB fluctuations

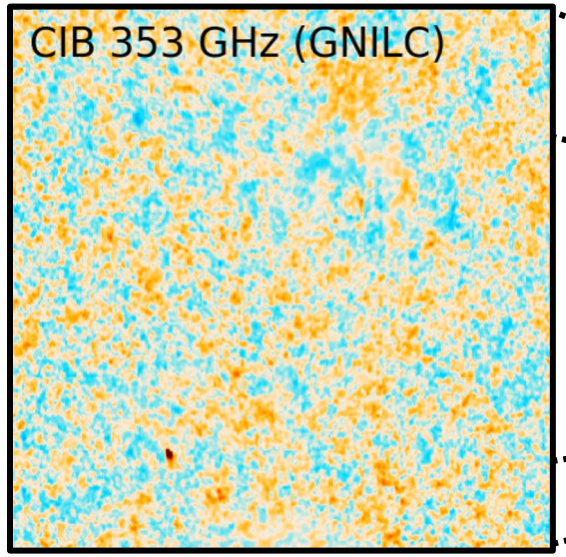

Planck intermediate results XLVIII, A&A 2016

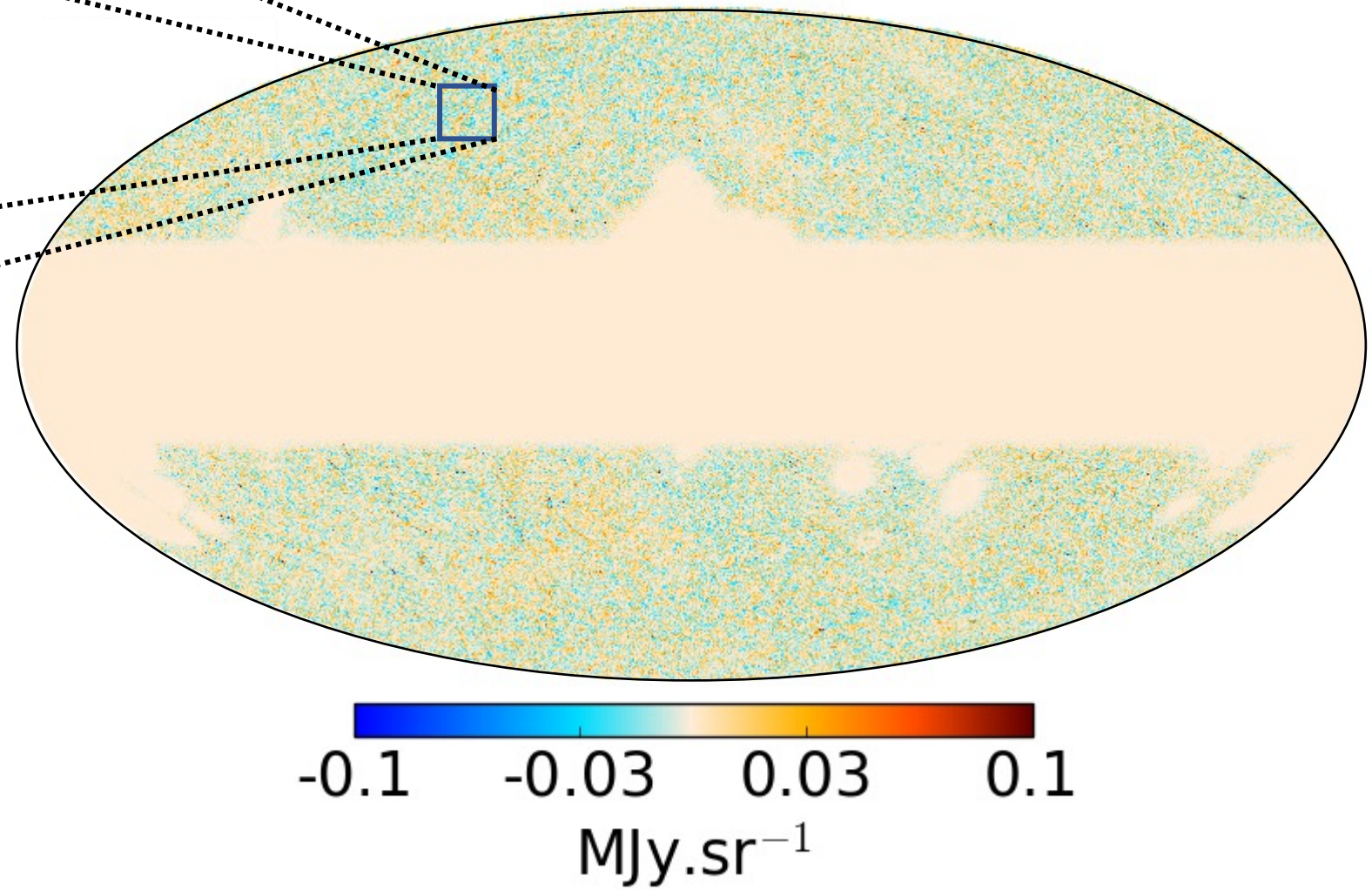

”Cosmological dust”

Best template to date for CMB delensing

(see A. Challinor’s talk)

M. Remazeilles

GNILC disentangles Galactic dust and CIB

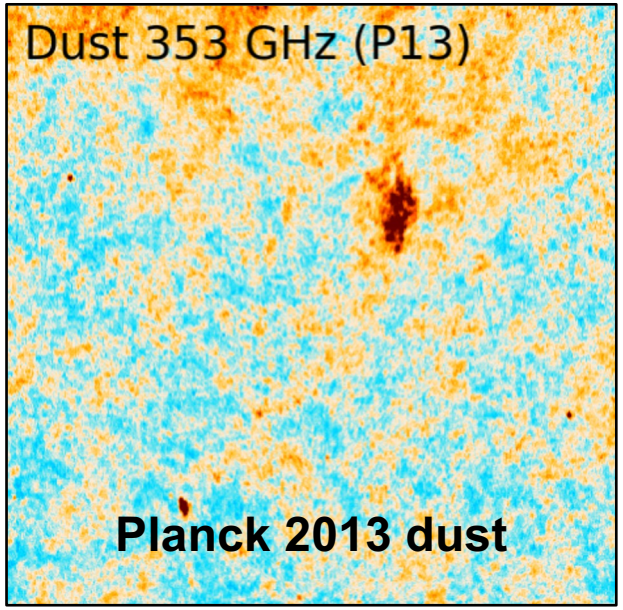

GNILC

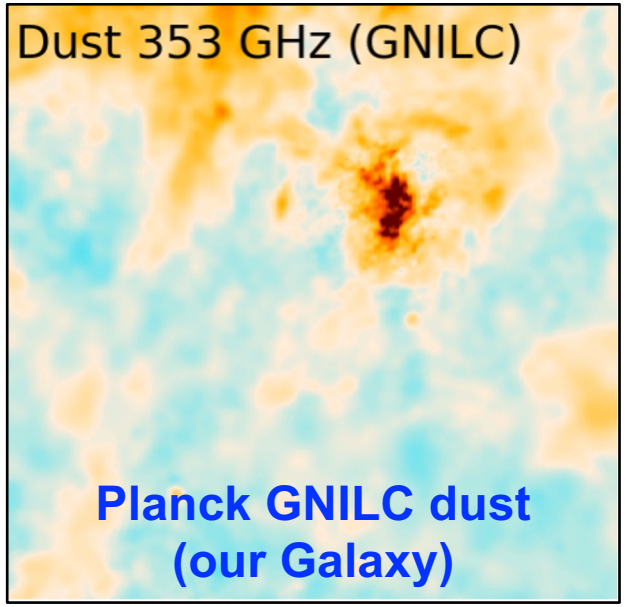

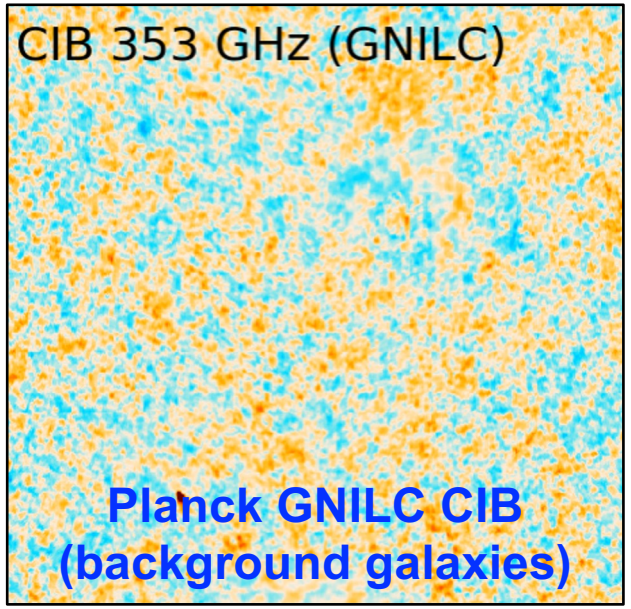

Planck intermediate results XLVIII, A&A (2016)

Remazeilles, Delabrouille, Cardoso, MNRAS (2011b)

M. Remazeilles

Search for primordial B-modes

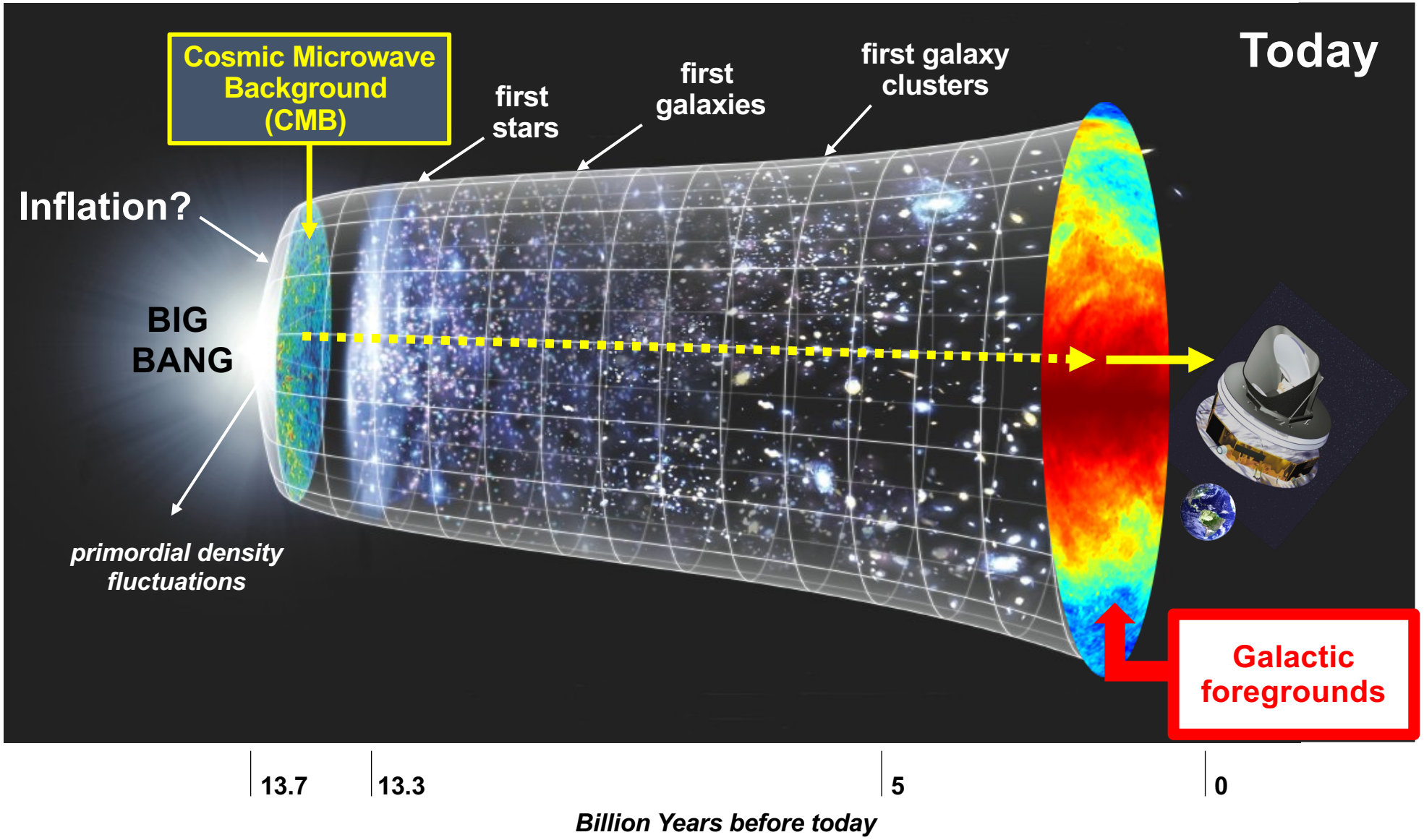

M. Remazeilles

Search for primordial B-modes

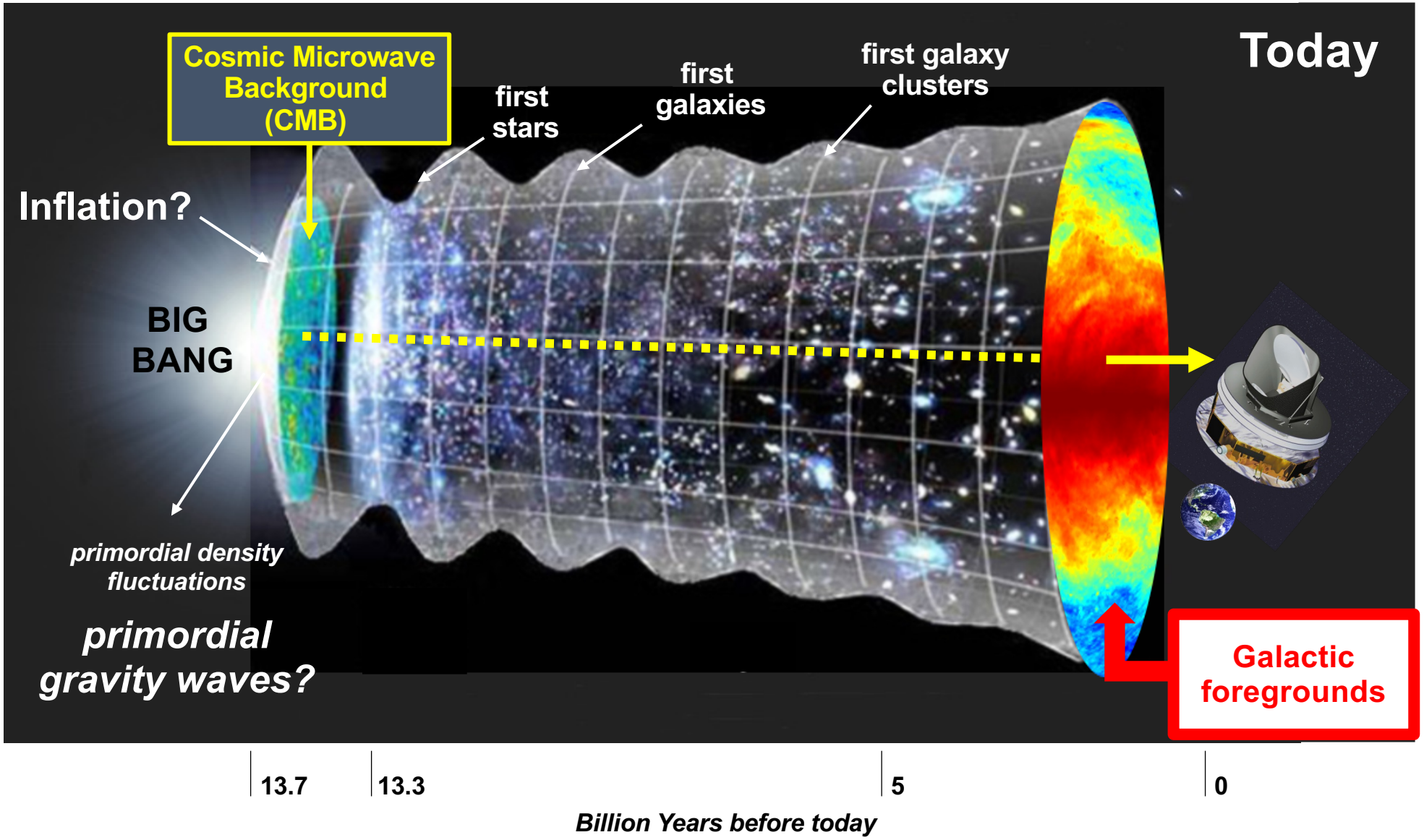

M. Remazeilles

Future CMB experiments aim at detecting $r \lesssim 0.001$

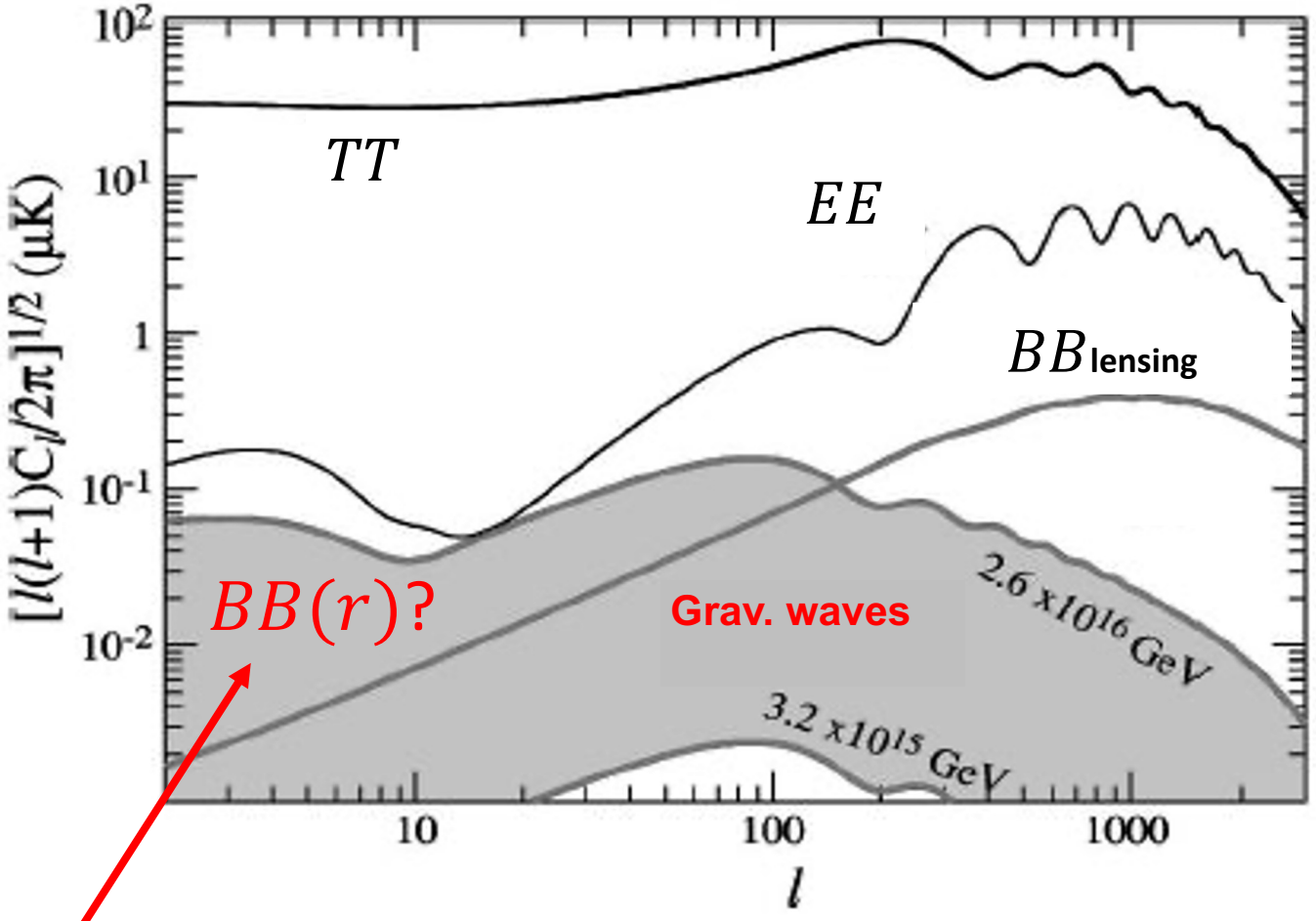

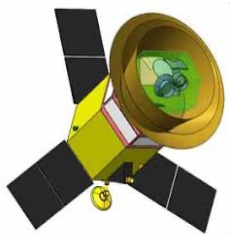

TT

PICO

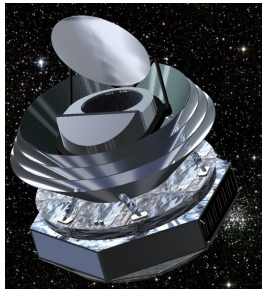

footprint of
primordial gravitational waves
predicted by inflation

$$E_{inf} \simeq (r/0.01)^{1/4} \times 10^{16}\ \text{GeV}$$

M. Remazeilles

Poor knowledge of the foregrounds at sensitivity levels of r~0.001

A variety of plausible foreground skies compatible with current polarization data

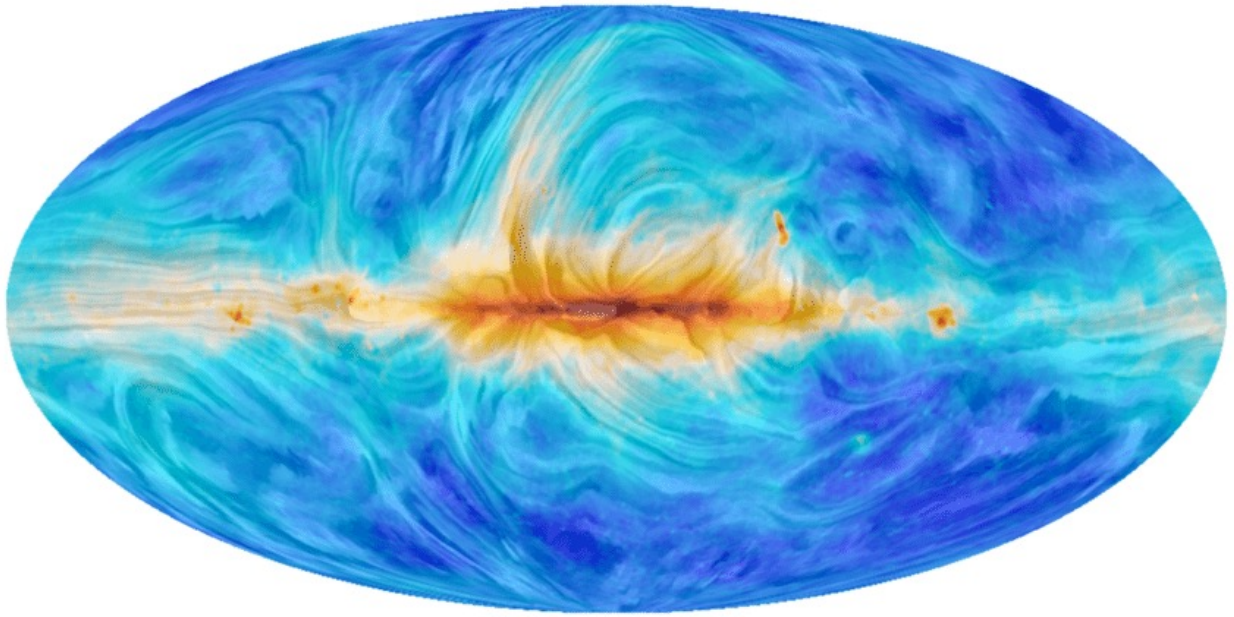

Synchrotron

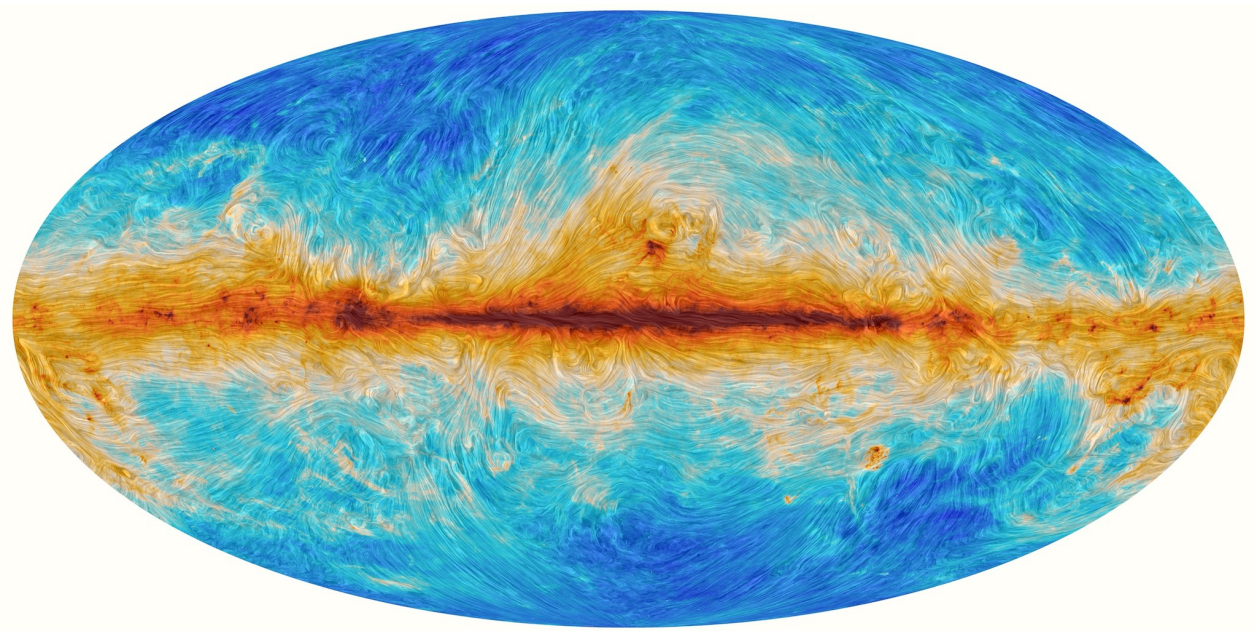

Thermal dust

Planck 2015 results I, A&A 2016

M. Remazeilles

A variety of plausible foreground skies

- **Model 91 (d1s1):** *Planck* dust MBB with β, T variations, synchrotron power-law with β variations

  Planck Collaboration X (2016)

- **Model 92 (d4s3a2):** Two dust MBBs with T_1, T_2 variations, synchrotron curvature, AME 2% polarization

  Meissner & Finkbeiner (2015)

- **Model 93 (d7s3a2):** Physical dust model (not MBB), synchrotron curvature, AME 2% polarization

  Hensley (2015)

- **Model 96 (MHD):** dust and synchrotron derived from MHD, multiple MBBs along the line-of-sight

  Kim et al (2019)

- **Model 98 (MKD):** Multi-layer 3D dust model (decorrelation), MBB layers along the line-of-sight

  Martínez-Solaeche et al (2018)

M. Remazeilles

Some foreground skies are more challenging

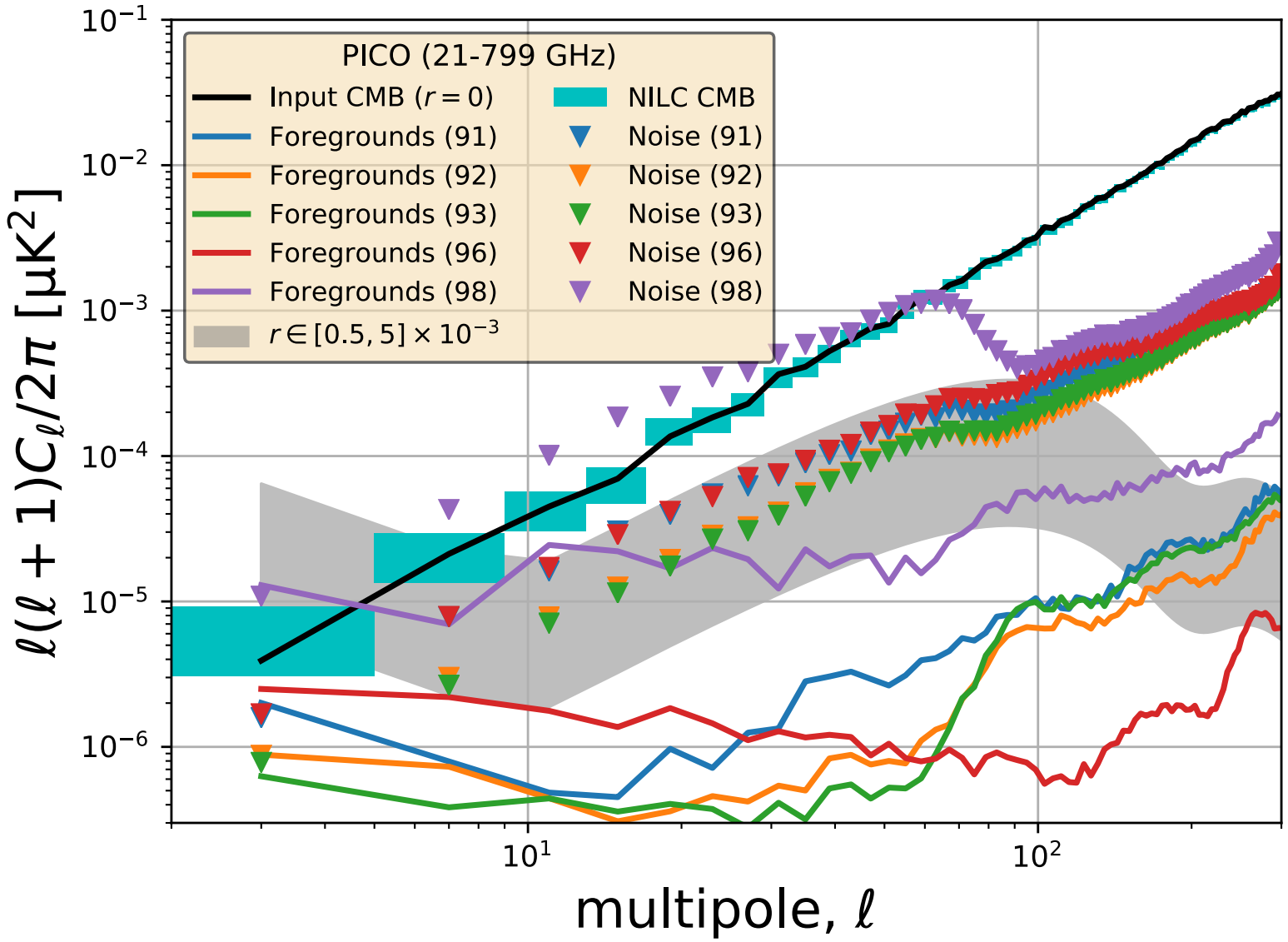

Aurlien, Belkner, Carron, Delabrouille, Eriksen, Fuskeland, Galloway, Górski, Hanany, Hensley, Lawrence, Pryke, Remazeilles, and Wehus (in preparation)

PICO

M. Remazeilles

CMB B-mode versus foregrounds

Remazeilles et al, JCAP 2018

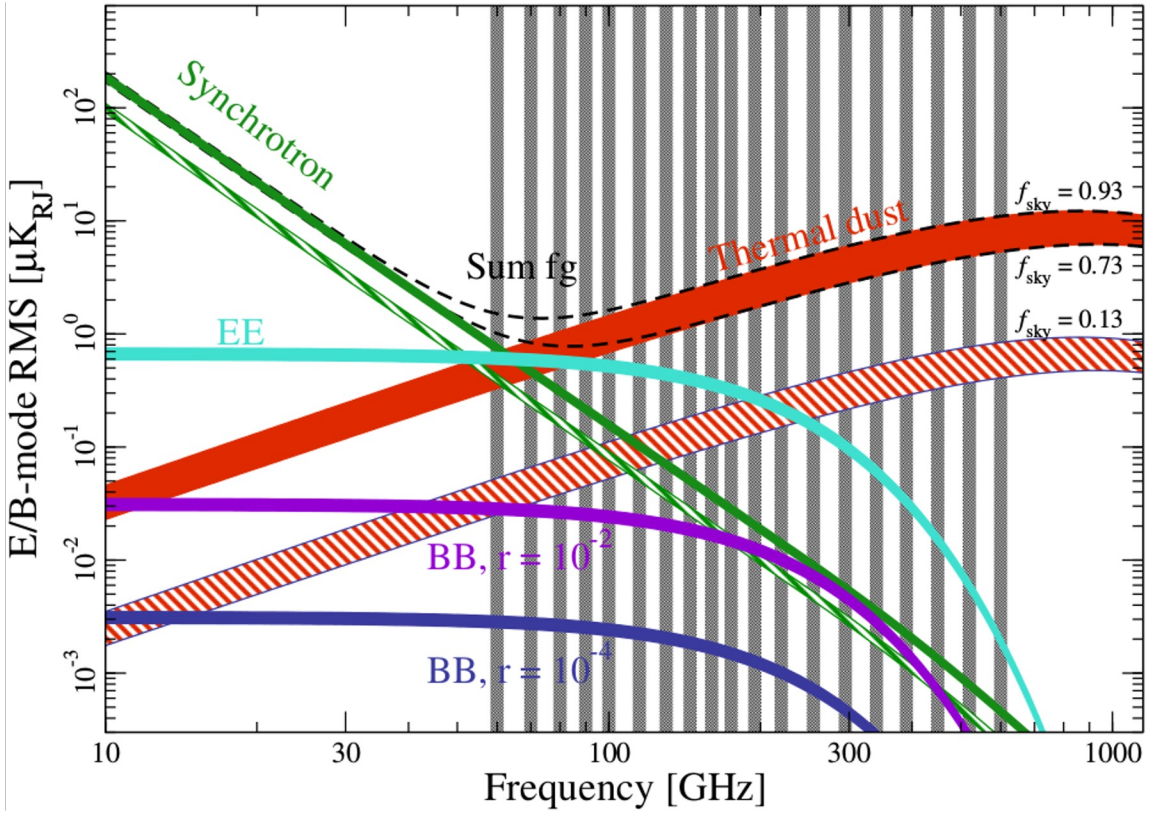

- **Polarization less complex than intensity (fewer foregrounds) but more challenging (weaker signal)**

  → *Huge dynamic range in amplitude between CMB B-modes and foregrounds*

  → *Component separation much more sensitive to any slight mismodeling of the foregrounds*

- **Foregrounds cannot be avoided by narrowing the frequency range of observations**

  → *At ~300 GHz, synchrotron and CMB B-modes with $r = 0.01$ have similar amplitude and color!*

  → *A broad frequency coverage of the instrument is essential to break degeneracies*

M. Remazeilles

Impact on r of foreground mismodeling

Mismatch between the foreground model and the data

Model

$$\mathrm{Model}(\nu,\hat{n}) = a(\nu)s_{\mathrm{CMB}}(\hat{n}) + \nu^{\beta_s} s_{\mathrm{sync}}(\hat{n}) + \nu^{\beta_d} B_\nu(T_d) s_{\mathrm{dust}}(\hat{n}) + n(\nu,\hat{n})$$

Data

$$\mathrm{Data}(\nu,\hat{n}) = a(\nu)s_{\mathrm{CMB}}(\hat{n}) + \nu^{(\beta_s + \boxed{C \ln \nu})} s_{\mathrm{sync}}(\hat{n}) + \left(f_1 \nu^{\beta_1} B_\nu(T_1) + \boxed{f_2 \nu^{\beta_2} B_\nu(T_2)}\right) s_{\mathrm{dust}}(\hat{n}) \boxed{+ \varepsilon(\nu) s_{\mathrm{AME}}(\hat{n})} + n(\nu,\hat{n})$$

Synchrotron curvature

Extra dust MBB

AME polarization

Remazeilles, Dickinson, Eriksen, Wehus, MNRAS (2016)

M. Remazeilles

Impact on r of foreground mismodeling

Omitting synchrotron curvature

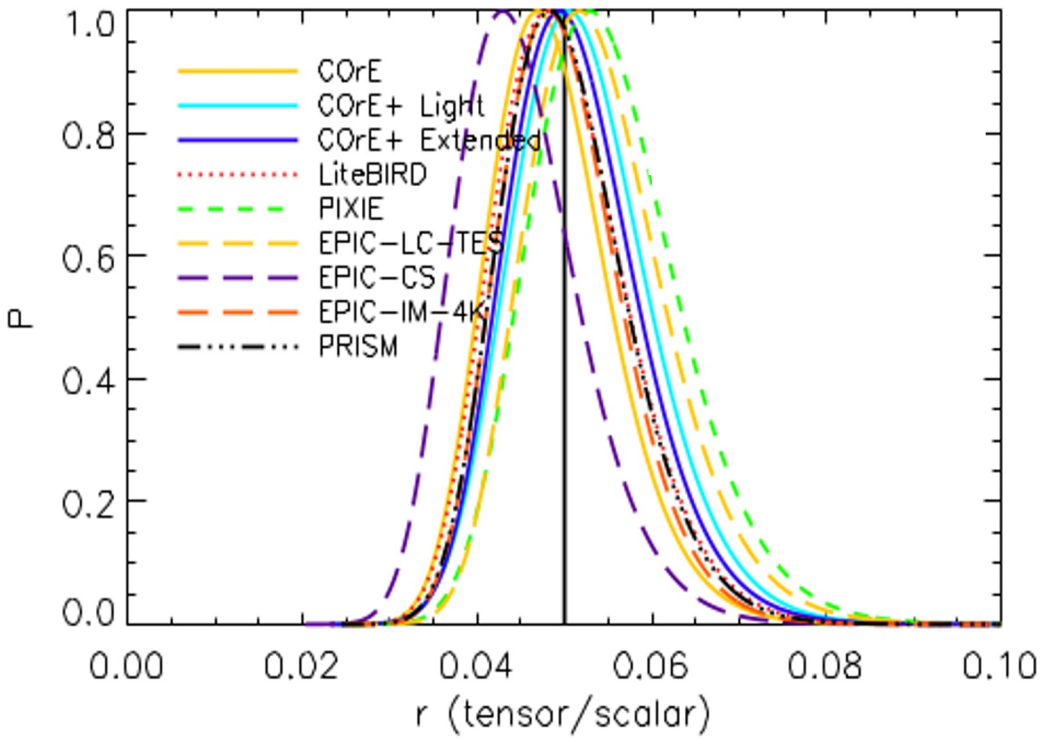

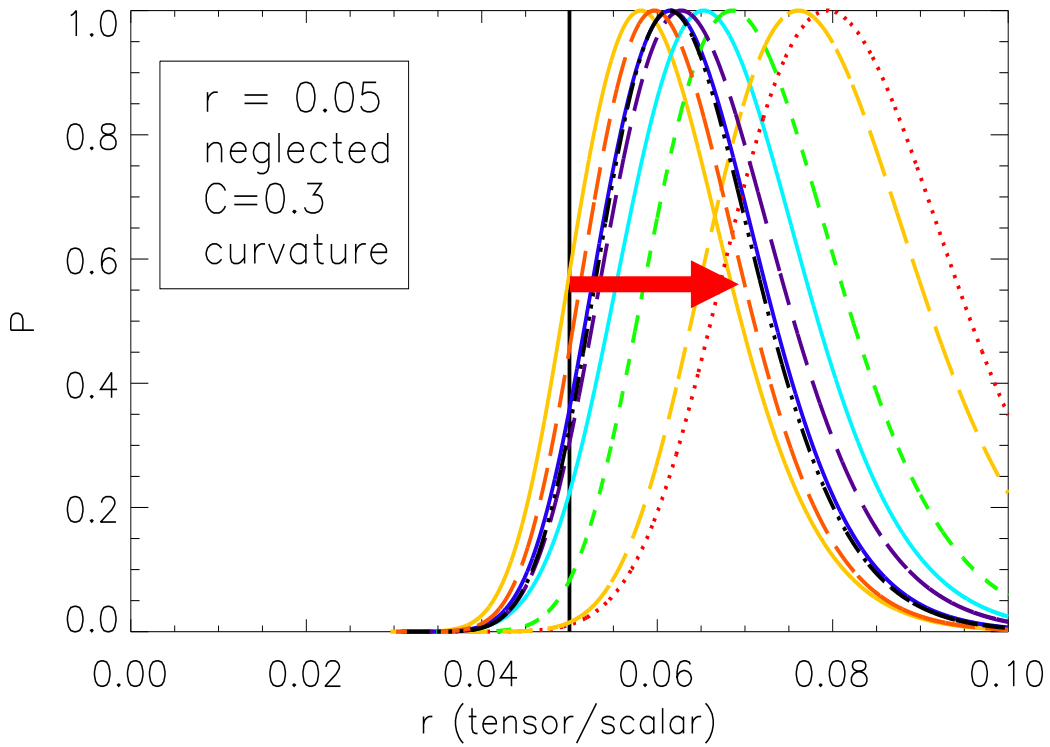

Remazeilles, Dickinson, Eriksen, Wehus, MNRAS (2016)

Impact on r of foreground mismodeling

Neglecting AME polarization

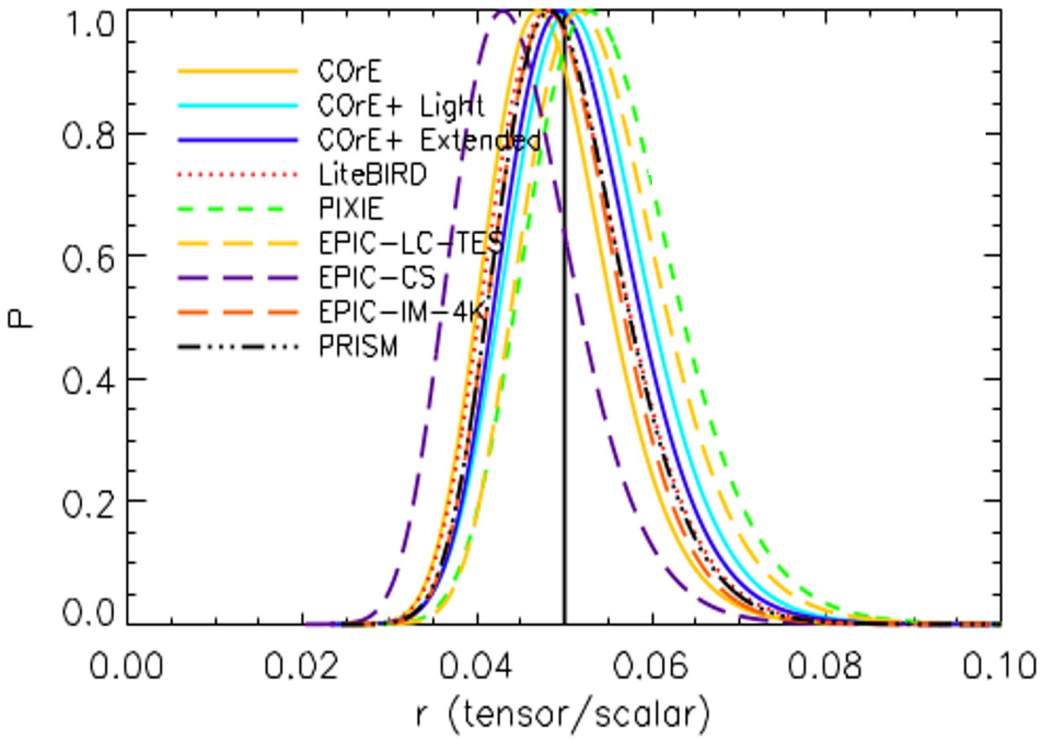

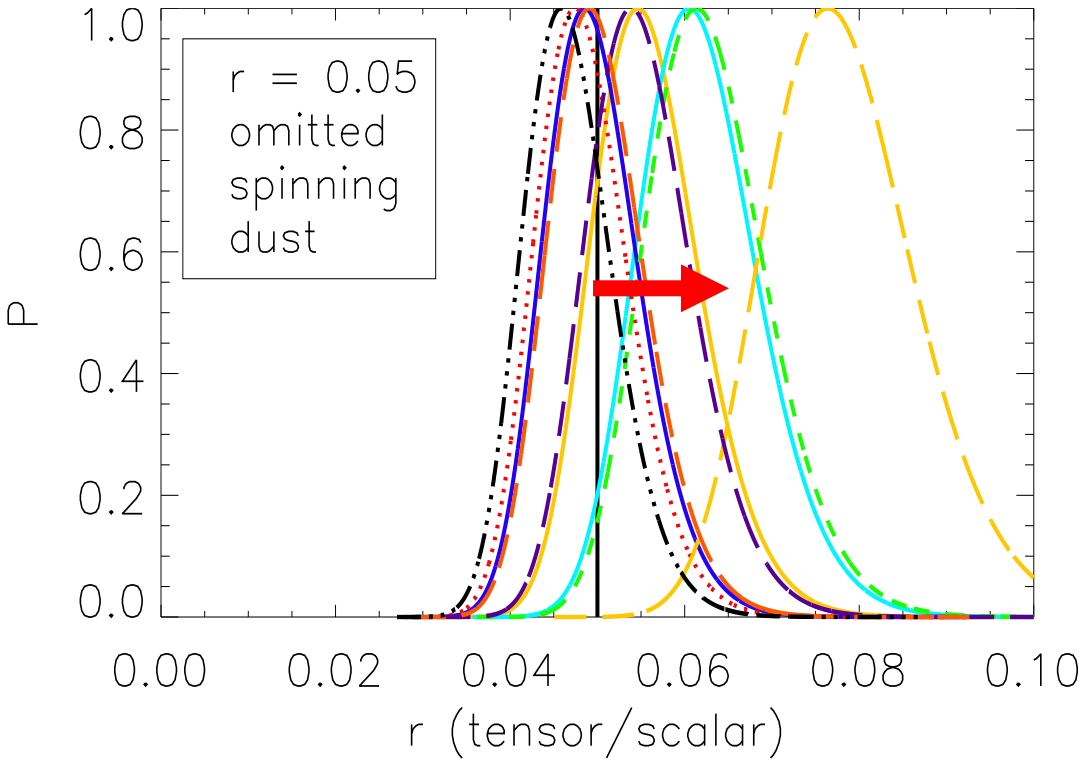

Remazeilles, Dickinson, Eriksen, Wehus, MNRAS (2016)

Impact on r of foreground mismodeling

Mismodeling two dust graybodies as a single graybody

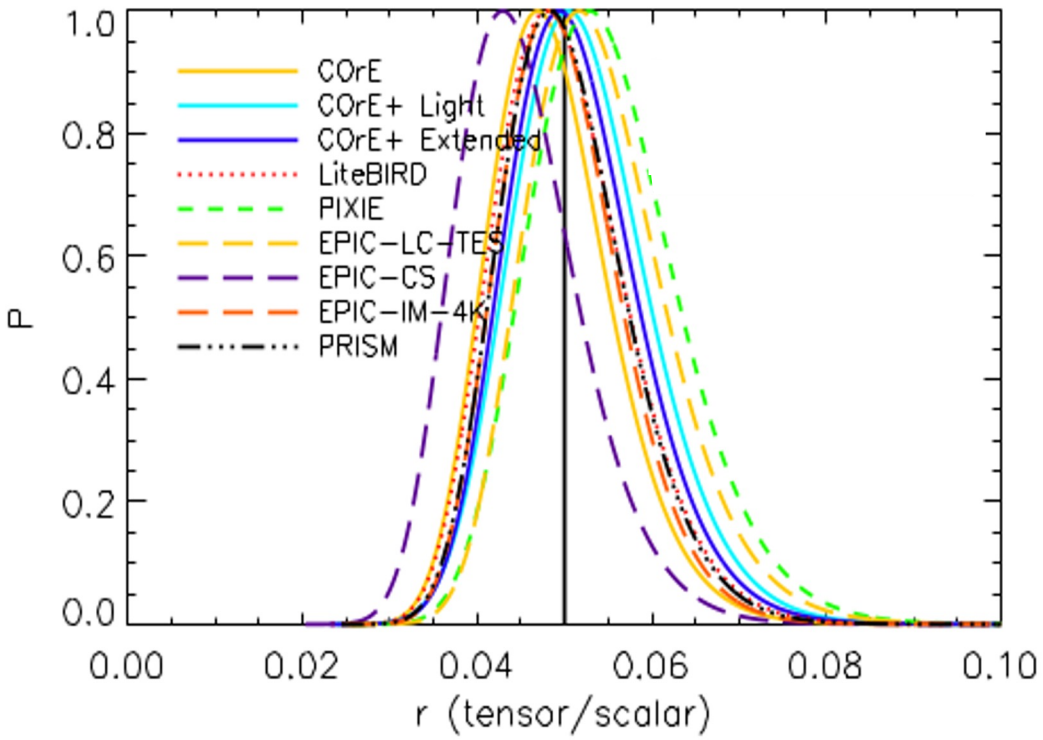

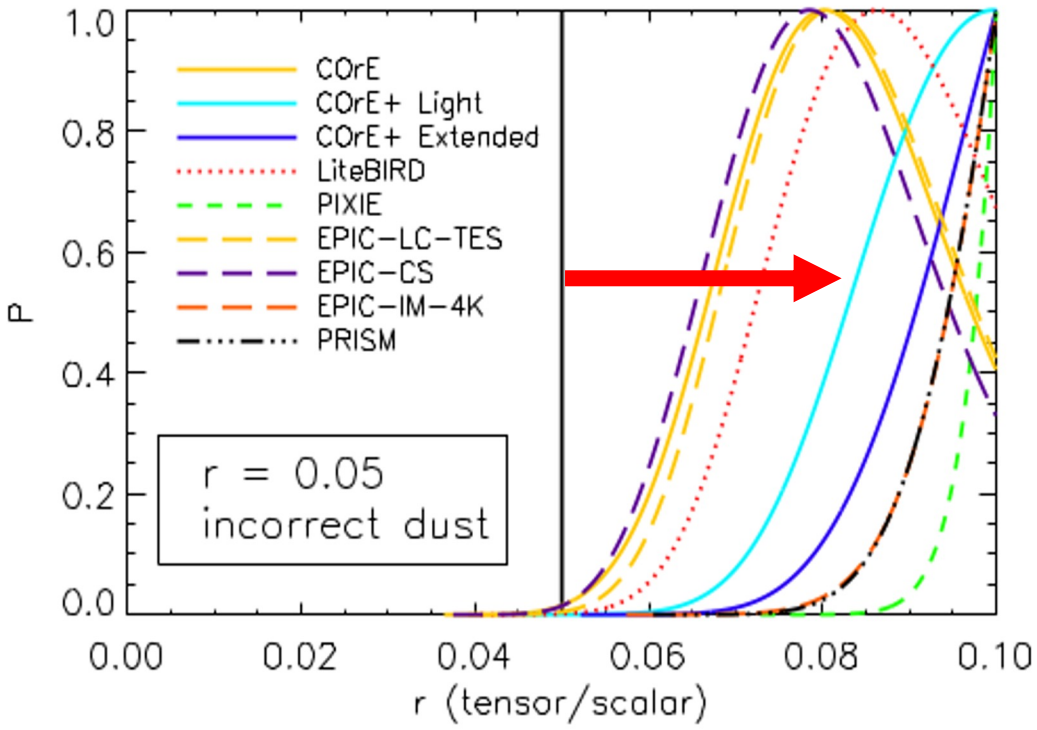

Remazeilles, Dickinson, Eriksen, Wehus, MNRAS (2016)

Getting evidence of foreground mismodeling?

CMB experiments with $\nu < 300$ GHz get $\chi^2 \simeq 1$ despite biased r

correct dust model

Mean $\chi^2/N_{\rm ch}$	Recovered r	Experiment
0.99	0.05271 ± 0.00595	*COrE*+ Light
0.99	0.05202 ± 0.00585	*COrE*+ Extended
0.98	0.05107 ± 0.00575	*COrE*
0.96	0.05132 ± 0.00578	*LiteBIRD*
0.99	0.05145 ± 0.00616	*PIXIE*
0.97	0.05074 ± 0.00572	*EPIC*-LC-TES
0.96	0.05086 ± 0.00583	*EPIC*-CS
0.97	0.05096 ± 0.00572	*EPIC*-IM-4K
0.99	0.05140 ± 0.00578	*PRISM*

incorrect dust model

Mean $\chi^2/N_{\rm ch}$	Recovered r	Experiment
1.07	0.08929 ± 0.00766	*COrE*+ Light
1.20	0.09218 ± 0.00624	*COrE*+ Extended
1.12	0.08023 ± 0.01045	*COrE*
1.10	0.08428 ± 0.00935	*LiteBIRD*
1.08	0.09711 ± 0.00265	*PIXIE*
1.32	0.08113 ± 0.00999	*EPIC*-LC-TES
1.08	0.07911 ± 0.01048	*EPIC*-CS
2.88	0.09434 ± 0.00485	*EPIC*-IM-4K
1.58	0.09446 ± 0.00467	*PRISM*

$$\chi^2(\hat{n}) = \sum_{\nu} \frac{\left(\mathrm{Data}(\nu,\hat{n}) - \mathrm{Model}(\nu,\hat{n})\right)^2}{\sigma^2_{\mathrm{noise}}(\nu,\hat{n})}$$

Remazeilles, Dickinson, Eriksen, Wehus, MNRAS (2016)

Getting evidence of foreground mismodeling?

CMB experiments with $\nu < 300\ \mathrm{GHz}$ get $\chi^2 \simeq 1$ despite biased r

How to fool yourself!

Good fit of total emission, not of individual components

Model degeneracies over narrow frequency ranges

Without high frequencies, no chi-square evidence for incorrect foreground modelling and biased detection of r

Remazeilles, Dickinson, Eriksen, Wehus, MNRAS (2016)

Spectral distortions of the foregrounds

Rethinking current foregrounds parameterizations

Baseline SEDs (spectral signatures)

power-law?

ν^{β}

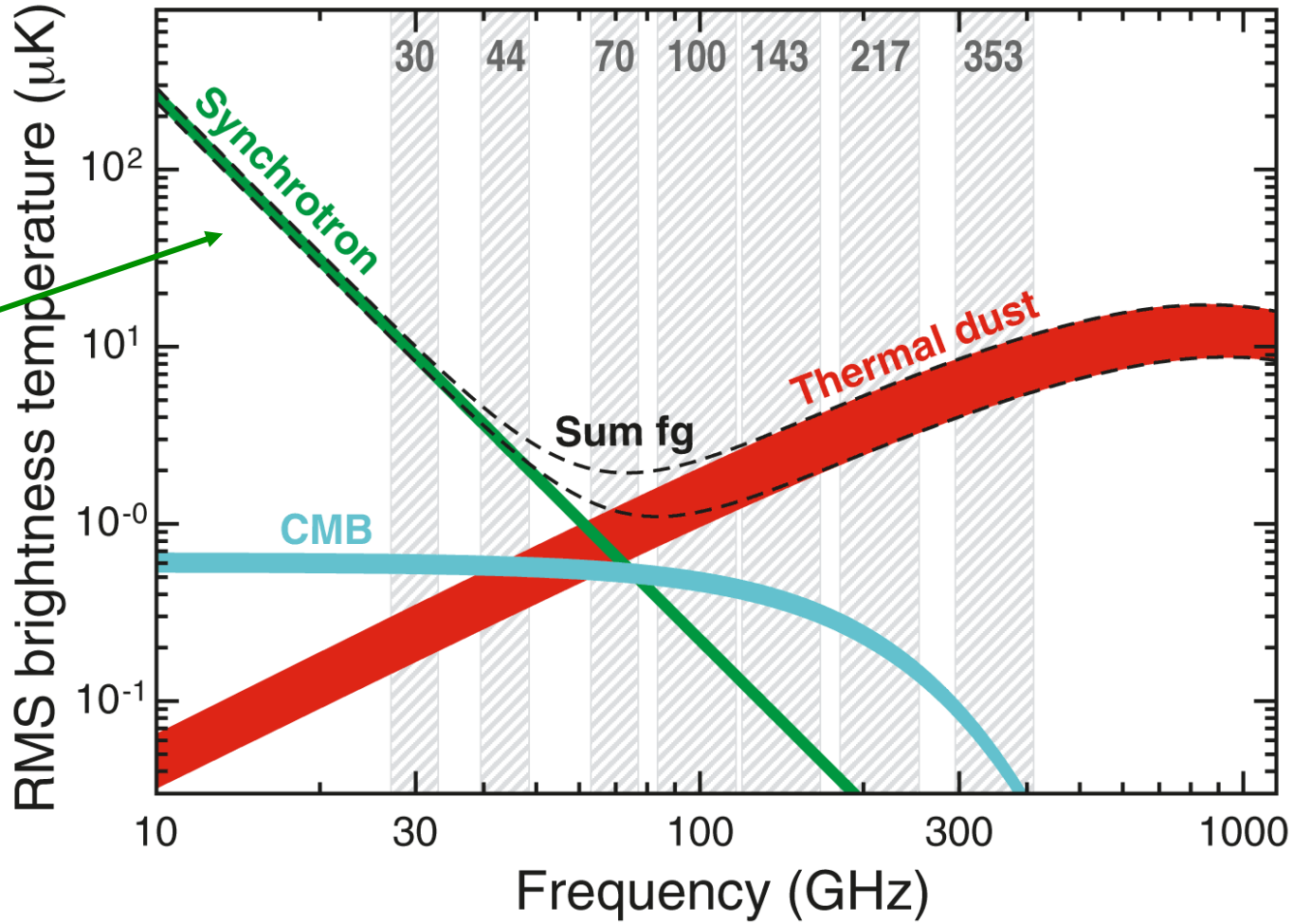

modified blackbody?

$\nu^{\beta} B_{\nu}(T)$

M. Remazeilles

Rethinking current foregrounds parameterizations

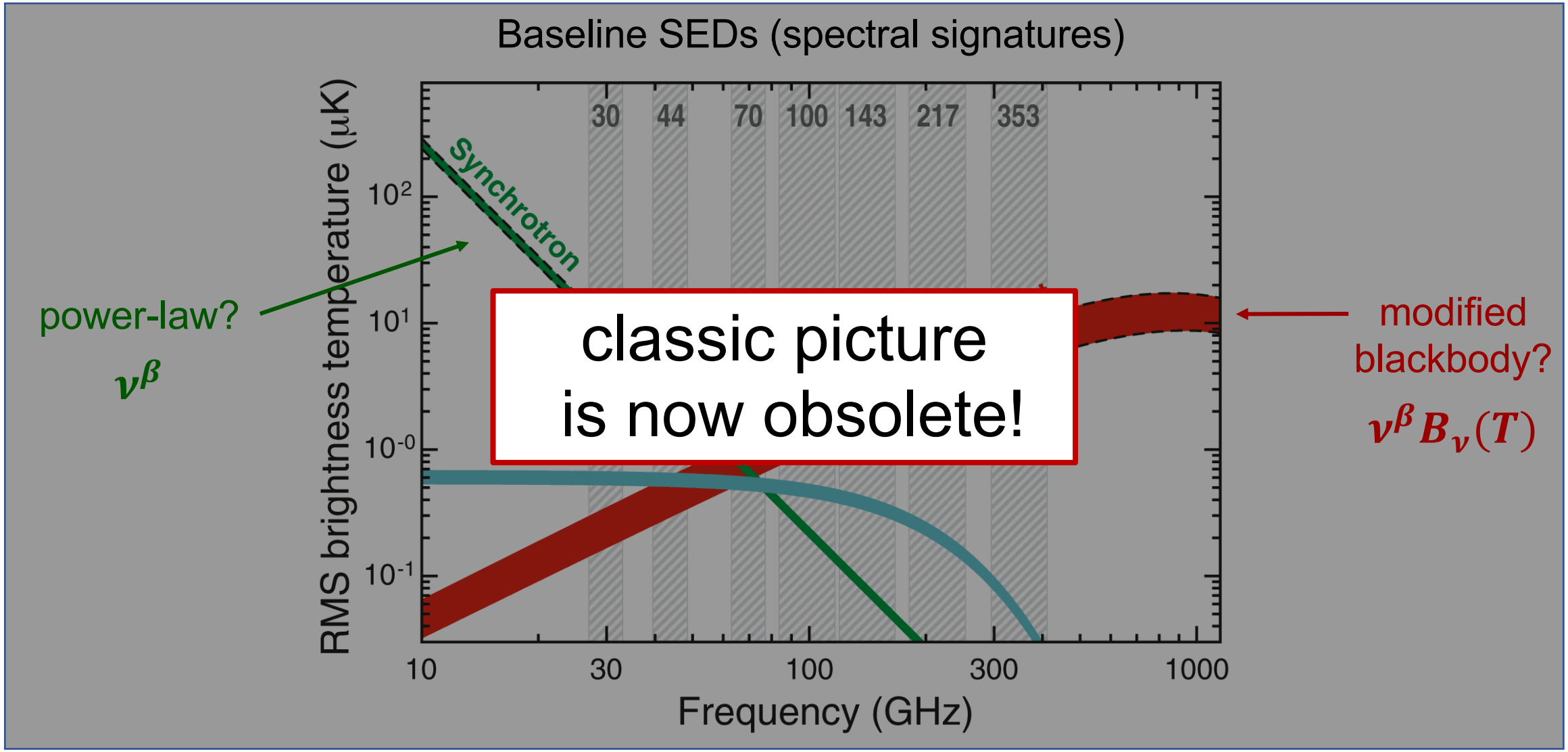

M. Remazeilles

Spectral distortions of the foreground SEDs

Line-of-sight integration of multiple contributions to thermal dust emission

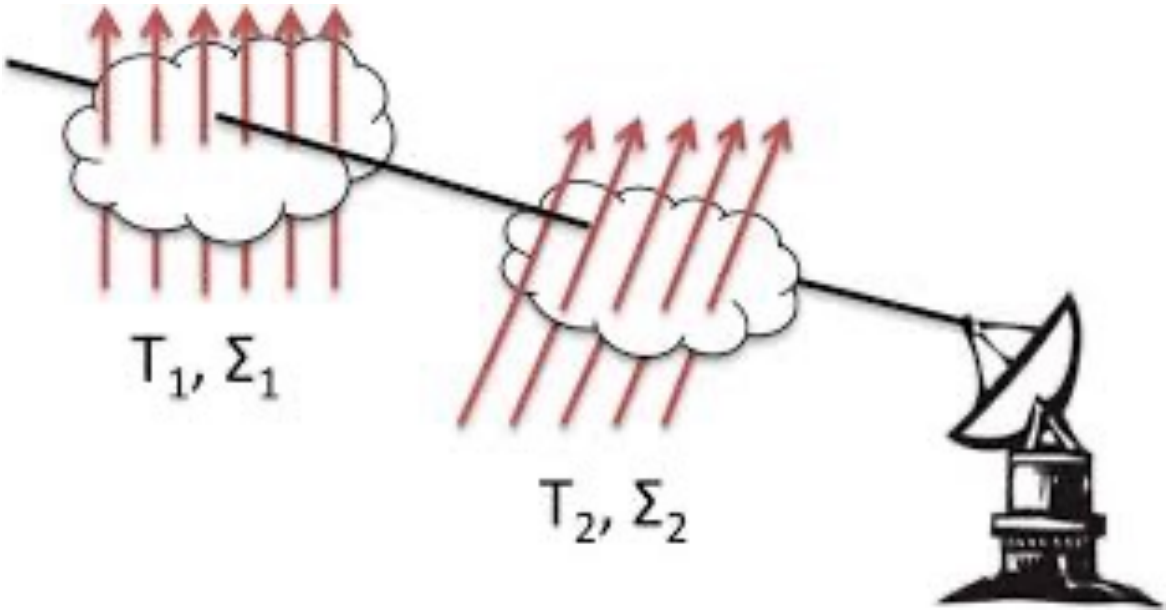

Tassis et al, MNRAS (2015)
Pelgrims et al, A&A (2021)

$$\nu^{\beta_1} B_\nu(T_1) + \nu^{\beta_2} B_\nu(T_2) \neq \nu^{\beta} B_\nu(T)$$

in each single pixel

M. Remazeilles

Spectral distortions of the foreground SEDs

Foreground emission integrated over larger beams at low frequencies

High-resolution high-frequency map

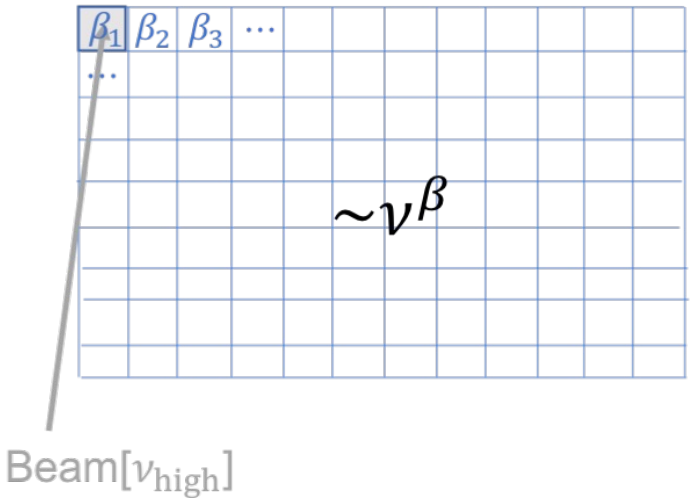

Low-resolution low-frequency map

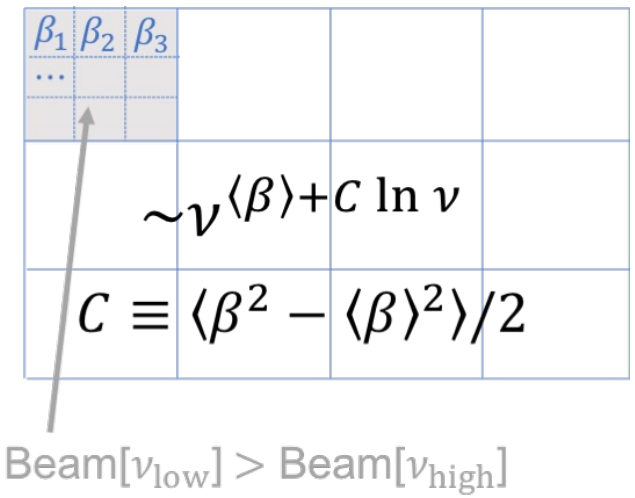

Remazeilles et al MNRAS (2021)

<u>Spectral distortion of the baseline foreground SED</u>

"power-law" at high frequency ⟷ "curved power-law" at low frequency

effective curvature = variance (2nd moment) of the spectral index in the beam

M. Remazeilles

Spectral distortions of the foreground SEDs

Foreground SED distortions

Averaging along the line of sight

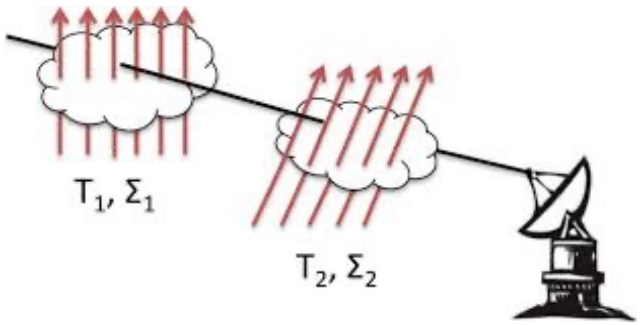

$$\nu^{\beta_1} B_\nu(T_1) + \nu^{\beta_2} B_\nu(T_2) \neq \nu^{\beta} B_\nu(T)$$

Averaging between lines of sight in the beam

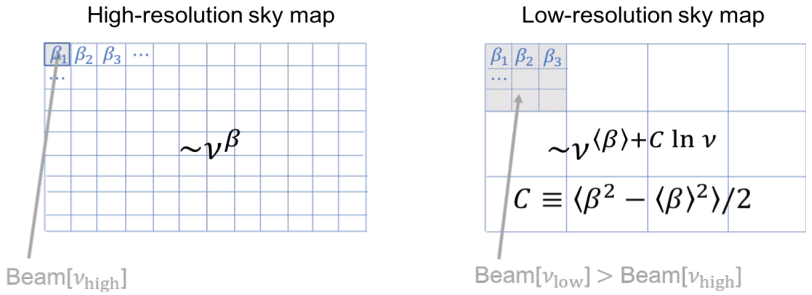

- Spectral distortions of the baseline foreground SEDs
- Decorrelation across frequencies
- Augmented list of expected foreground parameters

Chluba et al MNRAS (2017)
Remazeilles et al MNRAS (2021)
Vacher et al A&A (2022)

M. Remazeilles

Spectral distortions of the foreground SEDs

Foreground SED distortions

Averaging along the line of sight

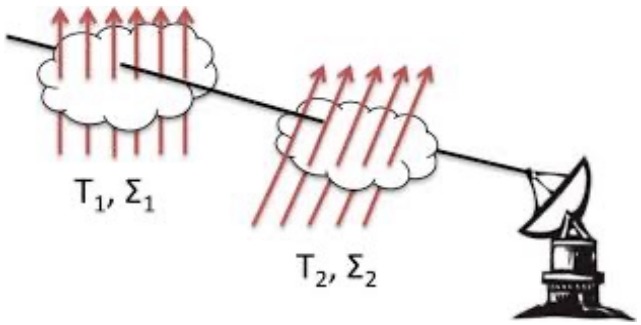

$$\nu^{\beta_1} B_\nu(T_1) + \nu^{\beta_2} B_\nu(T_2) \neq \nu^{\beta} B_\nu(T)$$

Averaging between lines of sight in the beam

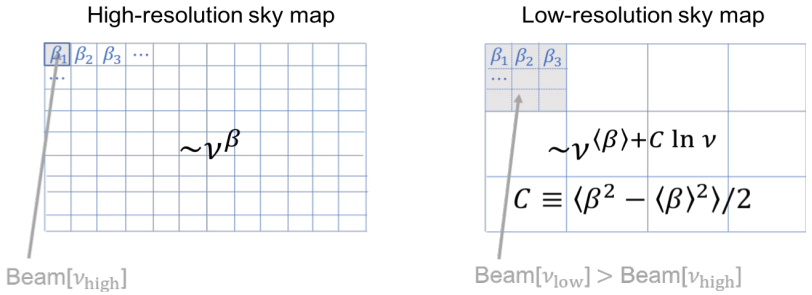

- Spectral distortions of the baseline foreground SEDs
- Decorrelation across frequencies
- Augmented list of expected foreground parameters

tiny corrections to foregrounds $\gg$ CMB B-mode !

Chluba et al MNRAS (2017)
Remazeilles et al MNRAS (2021)
Vacher et al A&A (2022)

M. Remazeilles

Extending current foreground parameterizations

Moment expansion of the foreground emission beyond leading-order SED

$$I_\nu(\hat{n}) = A(\hat{n}) f\left(\nu, \bar{\beta}\right) + A(\hat{n})\left(\beta(\hat{n}) - \bar{\beta}\right)\partial_\beta f\left(\nu, \bar{\beta}\right) + \frac{1}{2} A(\hat{n})\left(\beta(\hat{n}) - \bar{\beta}\right)^2 \partial_\beta^2 f\left(\nu, \bar{\beta}\right) + \cdots$$

$$\simeq \nu^\beta \qquad \simeq \frac{2h\nu^3}{c^2} \frac{\nu^\beta}{e^{\frac{h\nu}{kT}} - 1}$$

synchrotron thermal dust

(leading order)

Chluba, Hill, Abitbol, MNRAS (2017)
Remazeilles, Rotti, Chluba, MNRAS (2021)

Extending current foreground parameterizations

Moment expansion of the foreground emission beyond leading-order SED

$$I_\nu(\hat{n}) = A(\hat{n}) f(\nu, \bar{\beta}) + \underline{A(\hat{n})\left(\beta(\hat{n}) - \bar{\beta}\right)} \partial_\beta f(\nu, \bar{\beta}) + \underline{\frac{1}{2} A(\hat{n})\left(\beta(\hat{n}) - \bar{\beta}\right)^2} \partial_\beta^2 f(\nu, \bar{\beta}) + \cdots$$

$$\simeq \nu^\beta \qquad \simeq \frac{2h\nu^3}{c^2} \frac{\nu^\beta}{e^{\frac{h\nu}{kT}} - 1}$$

synchrotron thermal dust

(leading order)

Extra components (moments)

Chluba, Hill, Abitbol, MNRAS (2017)
Remazeilles, Rotti, Chluba, MNRAS (2021)

Extending current foreground parameterizations

Moment expansion of the foreground emission beyond leading-order SED

$$I_\nu(\hat{n}) = A(\hat{n}) f(\nu, \bar{\beta}) + \underline{A(\hat{n})(\beta(\hat{n}) - \bar{\beta})}\,\underline{\partial_\beta f(\nu, \bar{\beta})} + \underline{\frac{1}{2} A(\hat{n})(\beta(\hat{n}) - \bar{\beta})^2}\,\underline{\partial_\beta^2 f(\nu, \bar{\beta})} + \cdots$$

$$\simeq \nu^\beta \qquad \simeq \frac{2h\nu^3}{c^2} \frac{\nu^\beta}{e^{\frac{h\nu}{kT}} - 1}$$

synchrotron thermal dust

(leading order)

Extra components (moments)

New SEDs

Chluba, Hill, Abitbol, MNRAS (2017)
Remazeilles, Rotti, Chluba, MNRAS (2021)

Extending current foreground parameterizations

Moment expansion of the foreground emission beyond leading-order SED

$$I_\nu(\hat{n}) = A(\hat{n}) f(\nu, \bar{\beta}) + \underline{A(\hat{n})(\beta(\hat{n}) - \bar{\beta})}\,\underline{\partial_\beta f(\nu, \bar{\beta})} + \underline{\frac{1}{2} A(\hat{n})(\beta(\hat{n}) - \bar{\beta})^2}\,\underline{\partial_\beta^2 f(\nu, \bar{\beta})} + \cdots$$

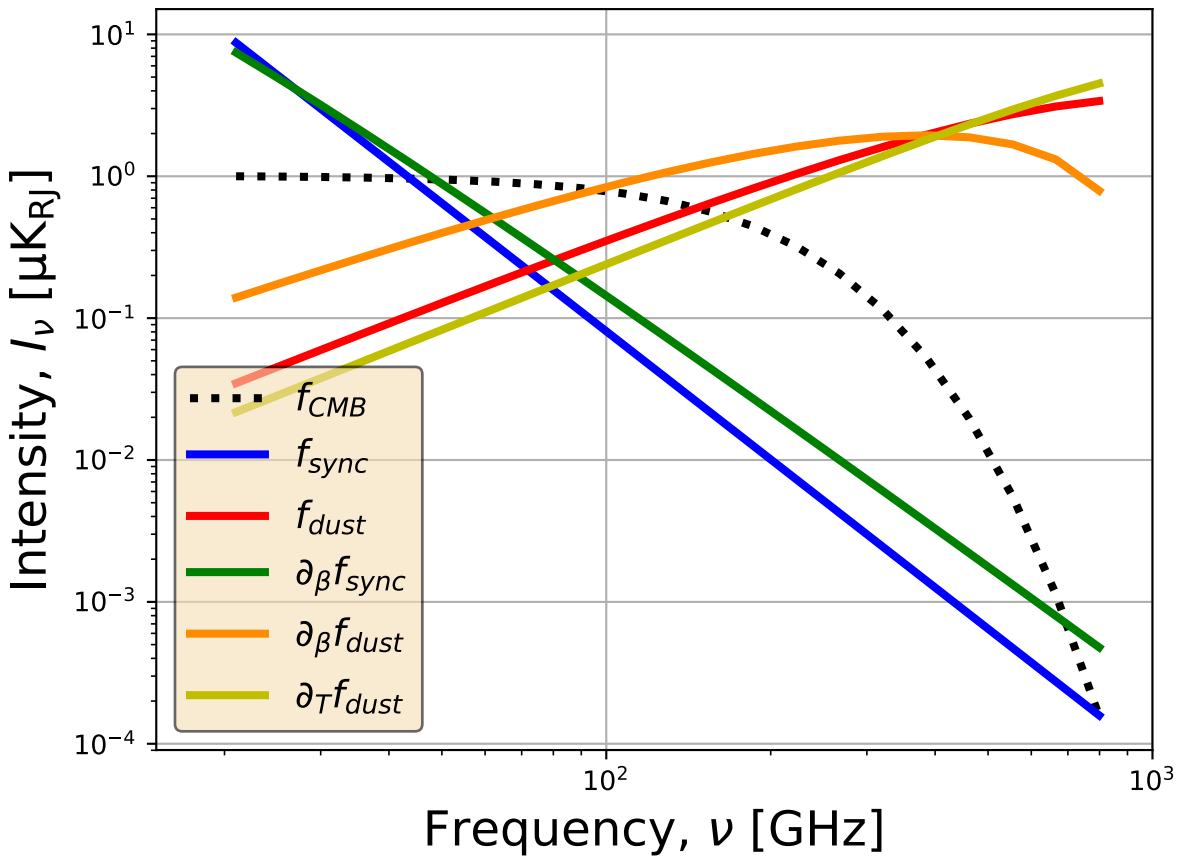

Extra components (moments)

New SEDs

Chluba, Hill, Abitbol, MNRAS (2017)
Remazeilles, Rotti, Chluba, MNRAS (2021)

M. Remazeilles

Deprojecting the foreground moments

Can we augment the routine NILC method for B-modes?

$$\hat{s}_{\mathrm{CMB}}(\vec{n}) = \sum_{\nu} w(\nu) \cdot d(\nu, \vec{n})$$

$$\sum_{\nu} w(\nu) \cdot f_{\mathrm{CMB}}(\nu) = 1$$

Residual foreground contamination to CMB B-modes

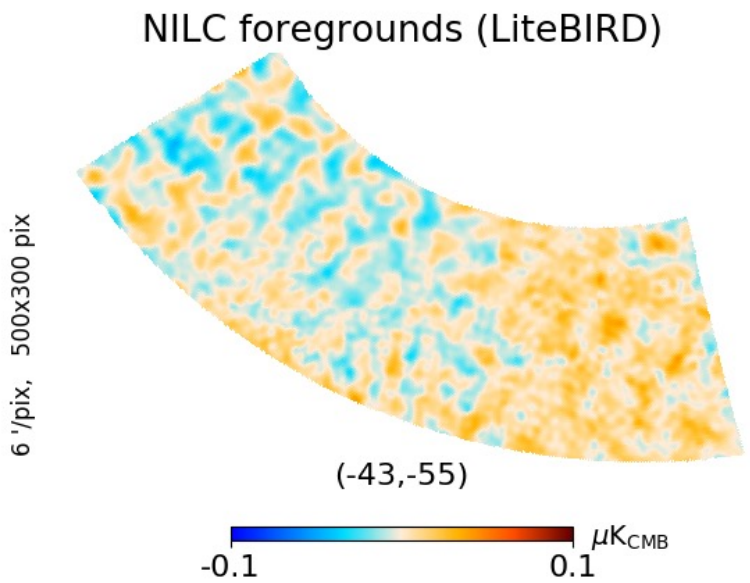

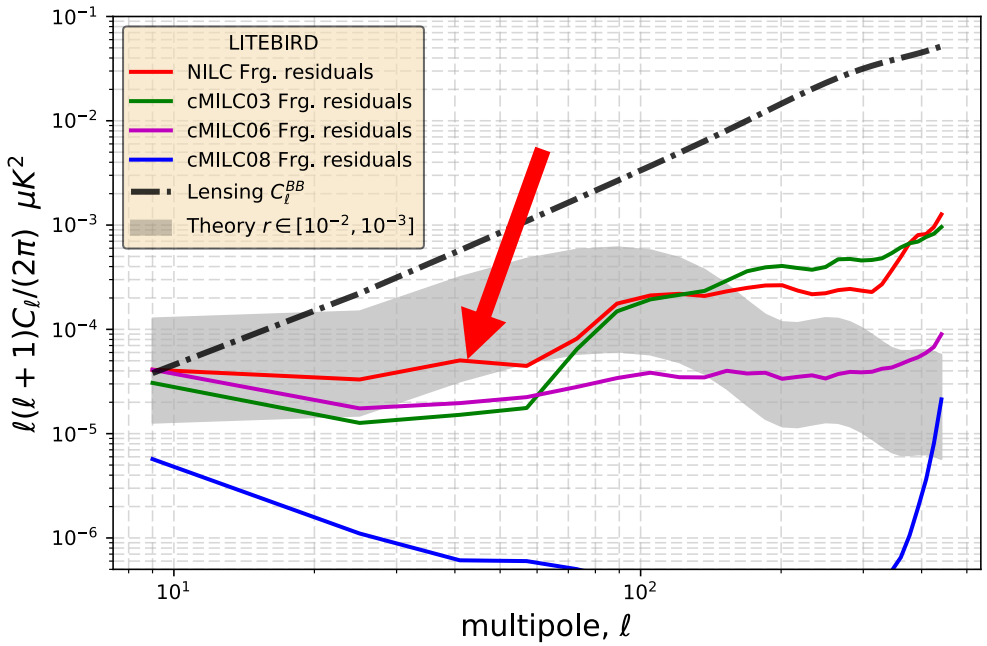

Remazeilles, Rotti, Chluba, MNRAS (2021)

M. Remazeilles

Deprojecting the foreground moments

cMILC: Constrained version of NILC to deproject the spectral moments of the foregrounds arising from line-of-sight averaging

$$\hat{s}_{\rm CMB}(\vec{n}) = \sum_{\nu} w(\nu) \cdot d(\nu, \vec{n})$$

$$\begin{cases} \sum_{\nu} w(\nu) \cdot f_{\rm CMB}(\nu) = 1 \\ \sum_{\nu} w(\nu) \cdot f_{\rm dust}(\nu) = 0 \\ \sum_{\nu} w(\nu) \cdot f_{\rm sync}(\nu) = 0 \end{cases}$$

Residual foreground contamination to CMB B-modes

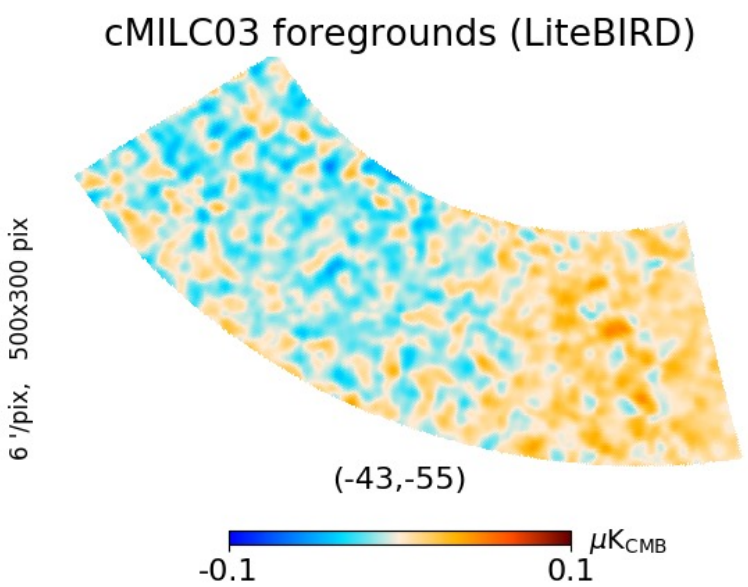

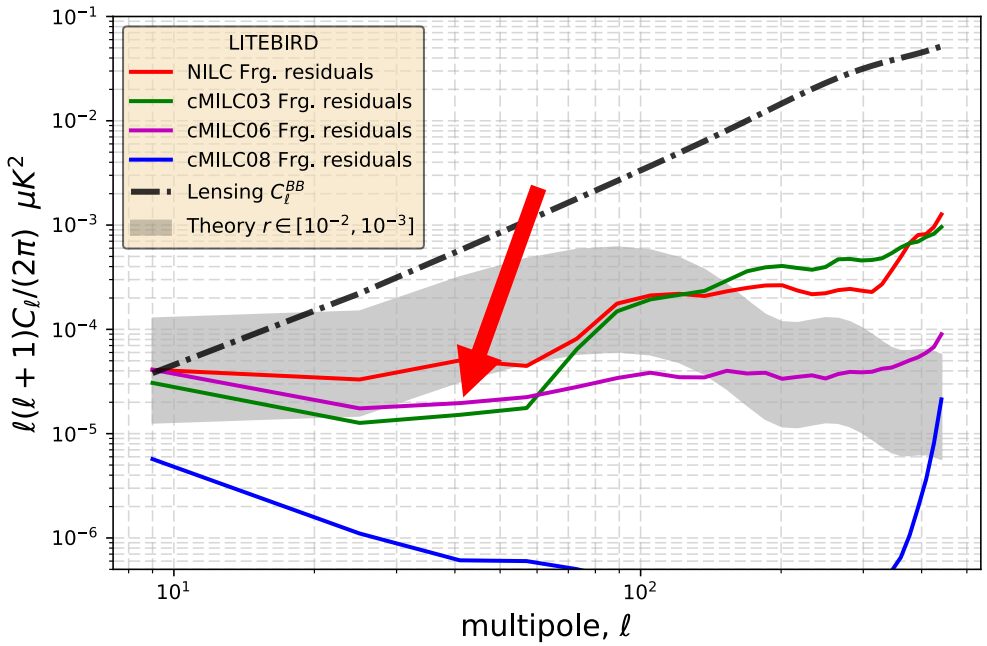

Remazeilles, Rotti, Chluba, MNRAS (2021)

M. Remazeilles

Deprojecting the foreground moments

cMILC: Constrained version of NILC to deproject the spectral moments of the foregrounds arising from line-of-sight averaging

$$\hat{s}_{\rm CMB}(\vec{n}) = \sum_{\nu} w(\nu) \cdot d(\nu, \vec{n})$$

$$\begin{cases} \sum_{\nu} w(\nu) \cdot f_{\rm CMB}(\nu) = 1 \\ \sum_{\nu} w(\nu) \cdot f_{\rm dust}(\nu) = 0 \\ \sum_{\nu} w(\nu) \cdot f_{\rm sync}(\nu) = 0 \\ \sum_{\nu} w(\nu) \cdot \frac{\partial f_{\rm dust}}{\partial \bar{\beta}_d}(\nu) = 0 \end{cases}$$

Residual foreground contamination to CMB B-modes

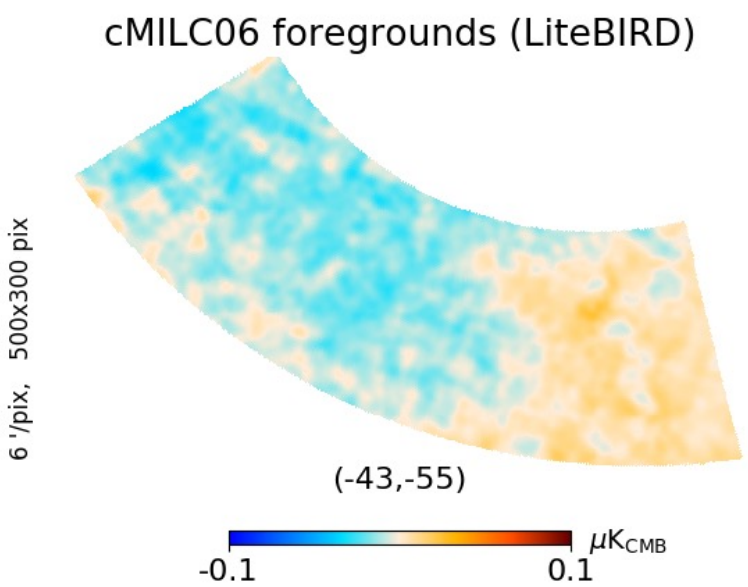

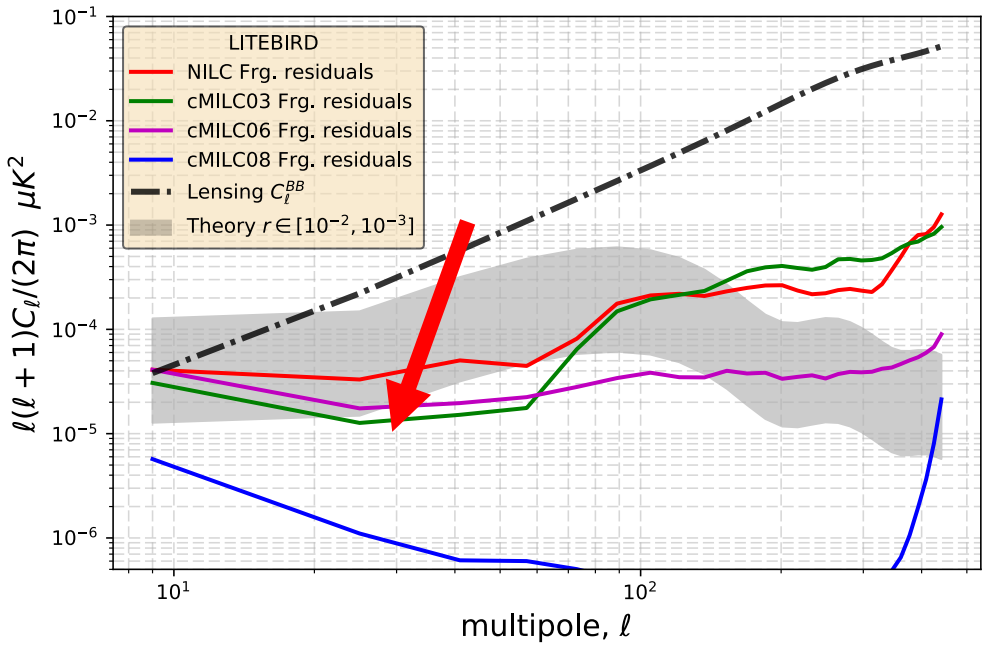

Remazeilles, Rotti, Chluba, MNRAS (2021)

M. Remazeilles

Deprojecting the foreground moments

cMILC: Constrained version of NILC to deproject the spectral moments of the foregrounds arising from line-of-sight averaging

$$\hat{s}_{\rm CMB}(\vec{n}) = \sum_\nu w(\nu)\cdot d(\nu,\vec{n})$$

$$\begin{cases} \sum_\nu w(\nu)\cdot f_{\rm CMB}(\nu) = 1 \\ \sum_\nu w(\nu)\cdot f_{\rm dust}(\nu) = 0 \\ \sum_\nu w(\nu)\cdot f_{\rm sync}(\nu) = 0 \\ \sum_\nu w(\nu)\cdot \frac{\partial f_{\rm dust}}{\partial \bar{\beta}_d}(\nu) = 0 \\ \sum_\nu w(\nu)\cdot \frac{\partial f_{\rm sync}}{\partial \bar{\beta}_s}(\nu) = 0 \\ \sum_\nu w(\nu)\cdot \frac{\partial f_{\rm dust}}{\partial \bar{T}_d}(\nu) = 0 \end{cases}$$

Residual foreground contamination to CMB B-modes

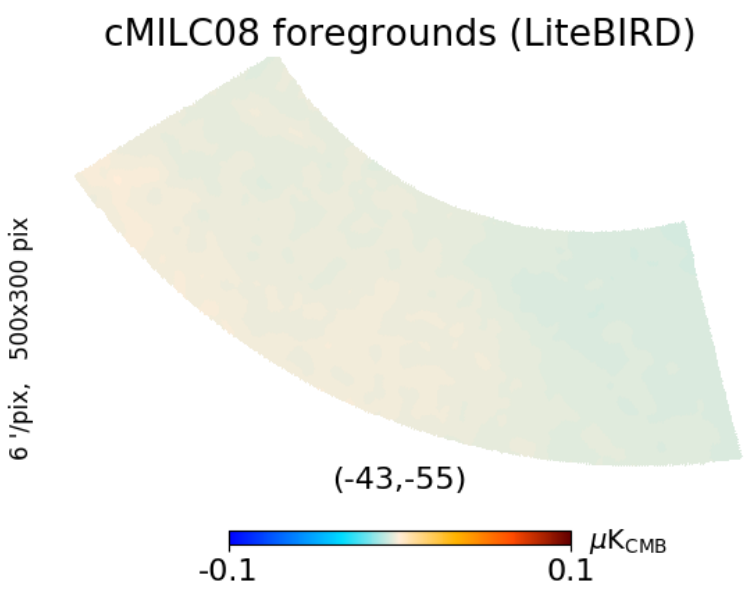

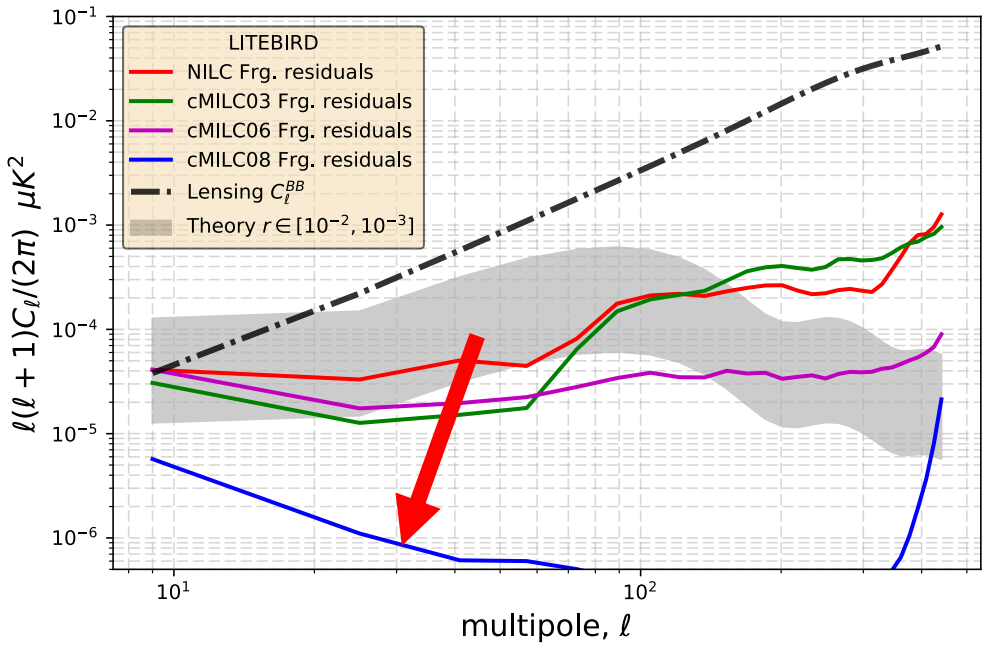

Remazeilles, Rotti, Chluba, MNRAS (2021)

M. Remazeilles

Deprojecting the foreground moments
(LiteBIRD simulation)

Foreground residuals

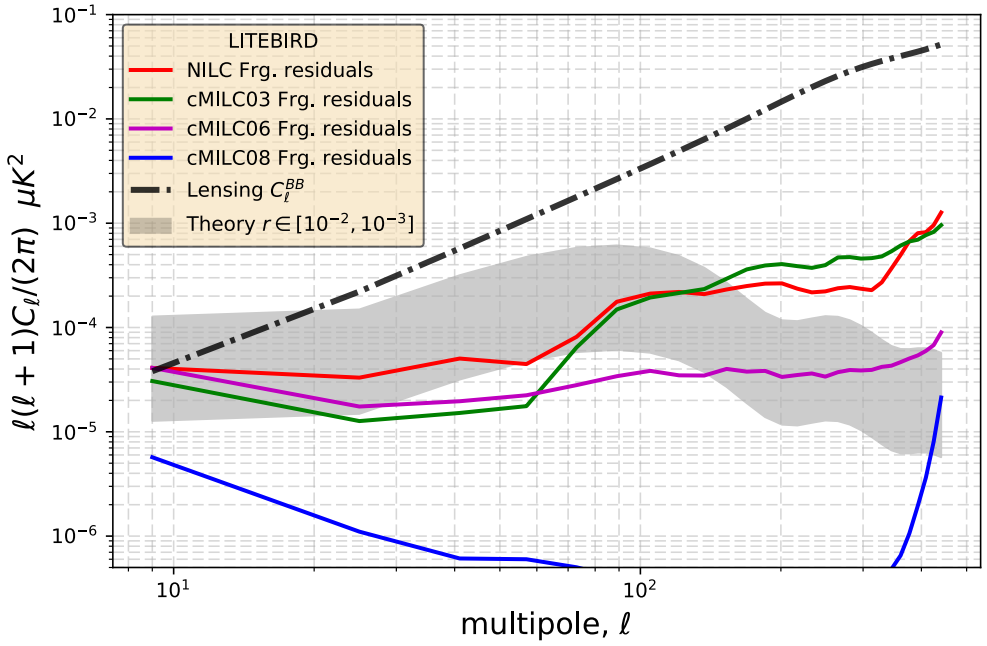

Significant reduction of residual foreground contamination with cMILC!

Noise

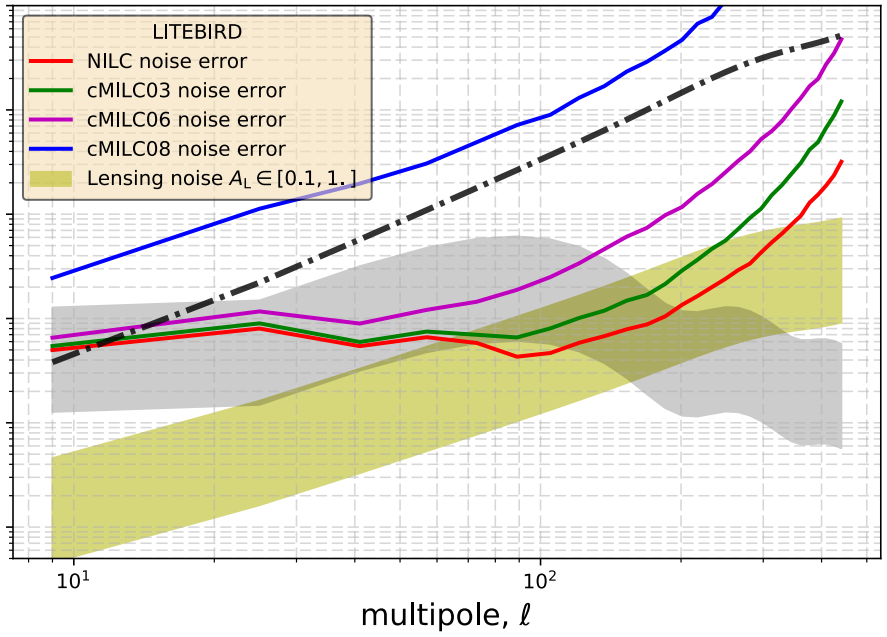

Increase of noise as a trade-off

Remazeilles, Rotti, Chluba, MNRAS (2021)

M. Remazeilles

Likelihood constraints on $r = 0$
(LiteBIRD simulation)

NILC

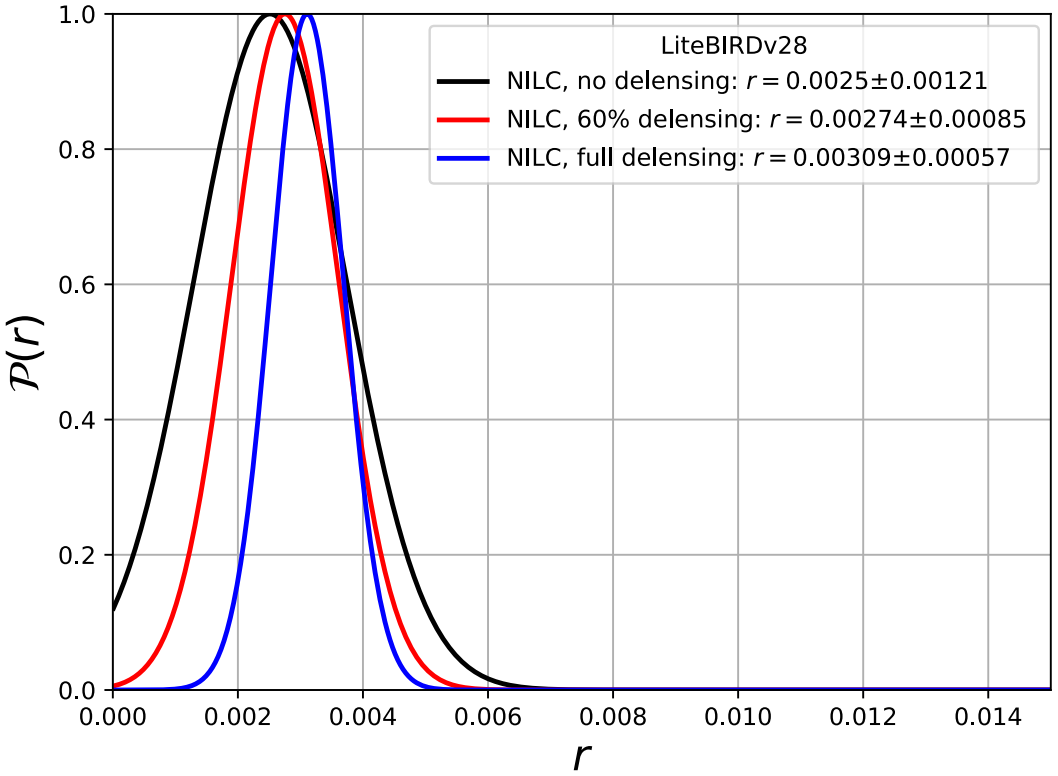

Biased detection $r \simeq 3\times10^{-3}$ due to residual foreground contamination

Remazeilles, Rotti, Chluba, MNRAS (2021)

Likelihood constraints on $r = 0$
(LiteBIRD simulation)

cMILC $(f_{\mathrm{sync}}, f_{\mathrm{dust}})$

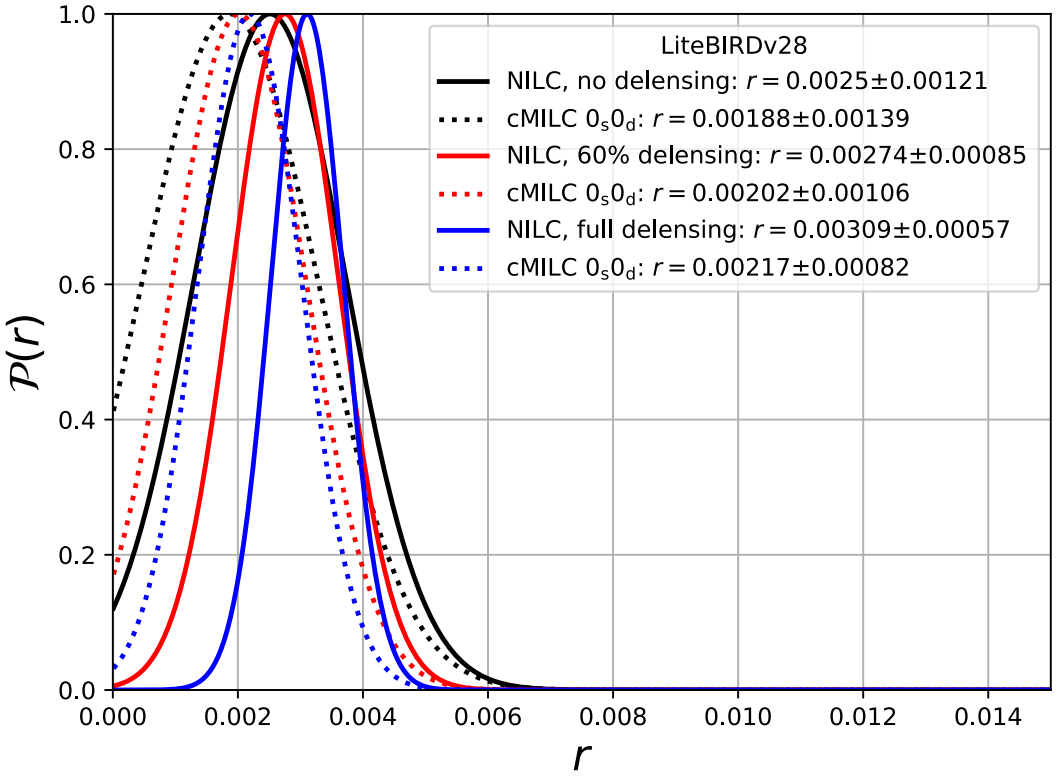

By deprojecting moments, cMILC progressively erases residual foreground biases

Remazeilles, Rotti, Chluba, MNRAS (2021)

Likelihood constraints on $r = 0$

(LiteBIRD simulation)

cMILC ($f_{\rm sync}$, $f_{\rm dust}$, $\partial_\beta f_{\rm dust}$)

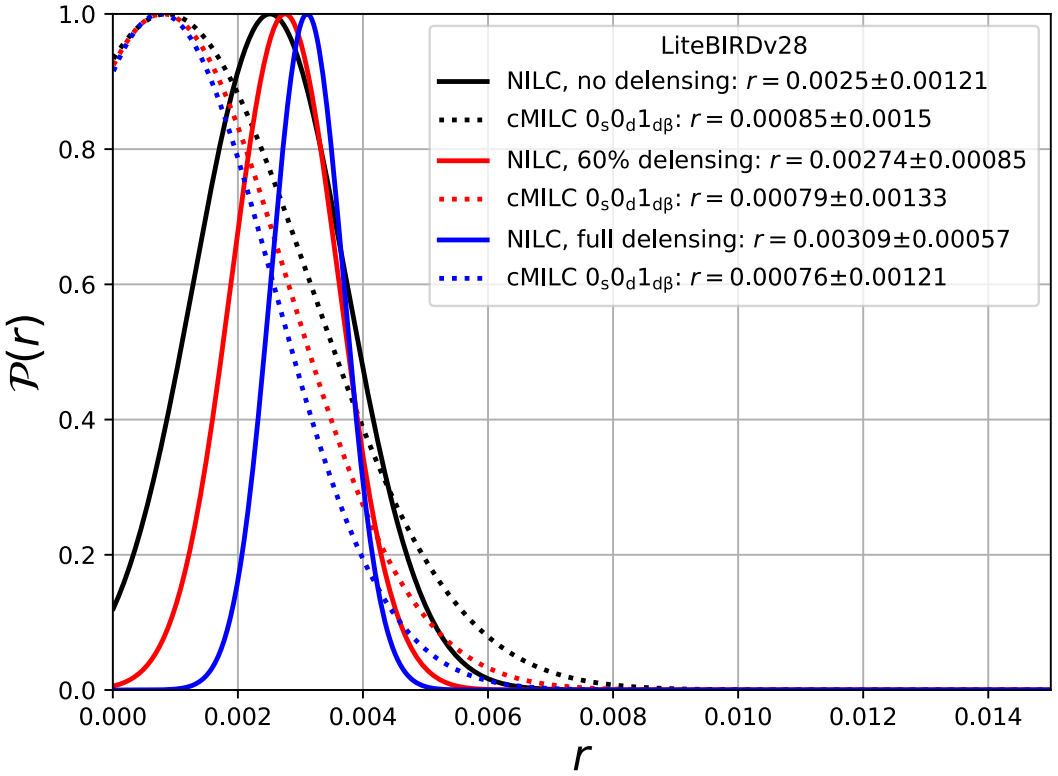

By deprojecting moments, cMILC progressively erases residual foreground biases

Remazeilles, Rotti, Chluba, MNRAS (2021)

Likelihood constraints on $r = 0$

(LiteBIRD simulation)

cMILC $(f_{\mathrm{sync}}, f_{\mathrm{dust}}, \partial_\beta f_{\mathrm{sync}}, \partial_\beta f_{\mathrm{dust}}, \partial_T f_{\mathrm{dust}})$

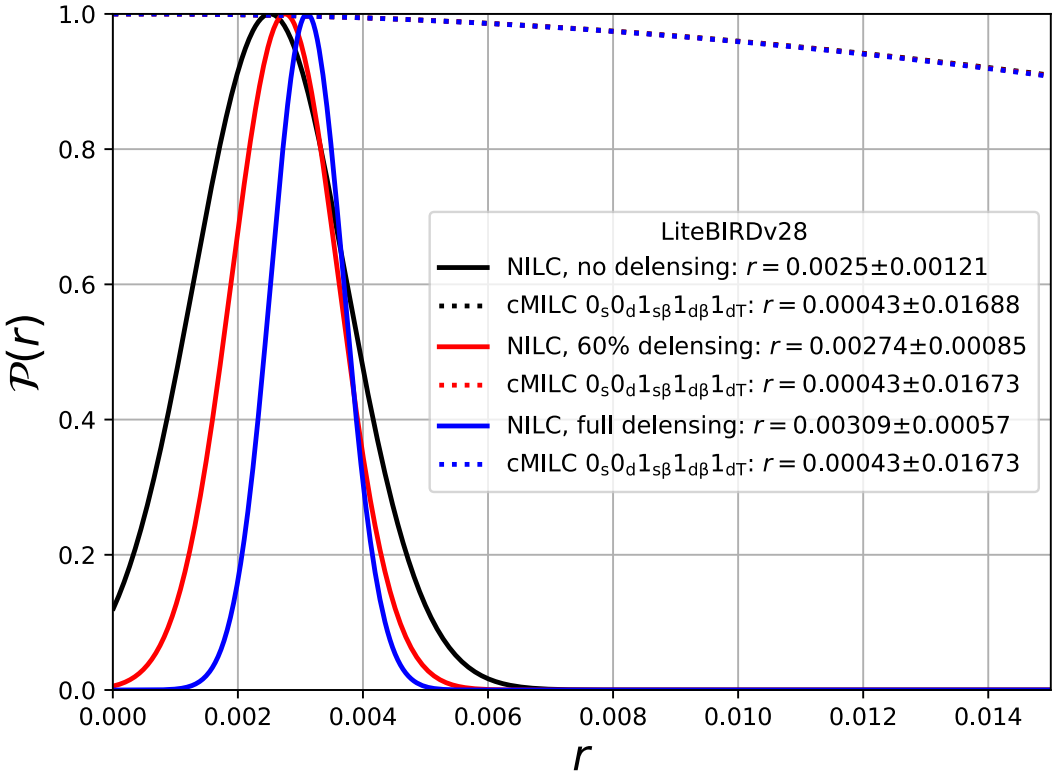

Deprojecting dust temperature moments results in large noise penalty

(LiteBIRD frequencies < 400 GHz)

Remazeilles, Rotti, Chluba, MNRAS (2021)

Likelihood constraints on $r = 0$

(LiteBIRD simulation)

cMILC ($f_{\rm sync}$, $f_{\rm dust}$, $\partial_\beta f_{\rm dust}$)

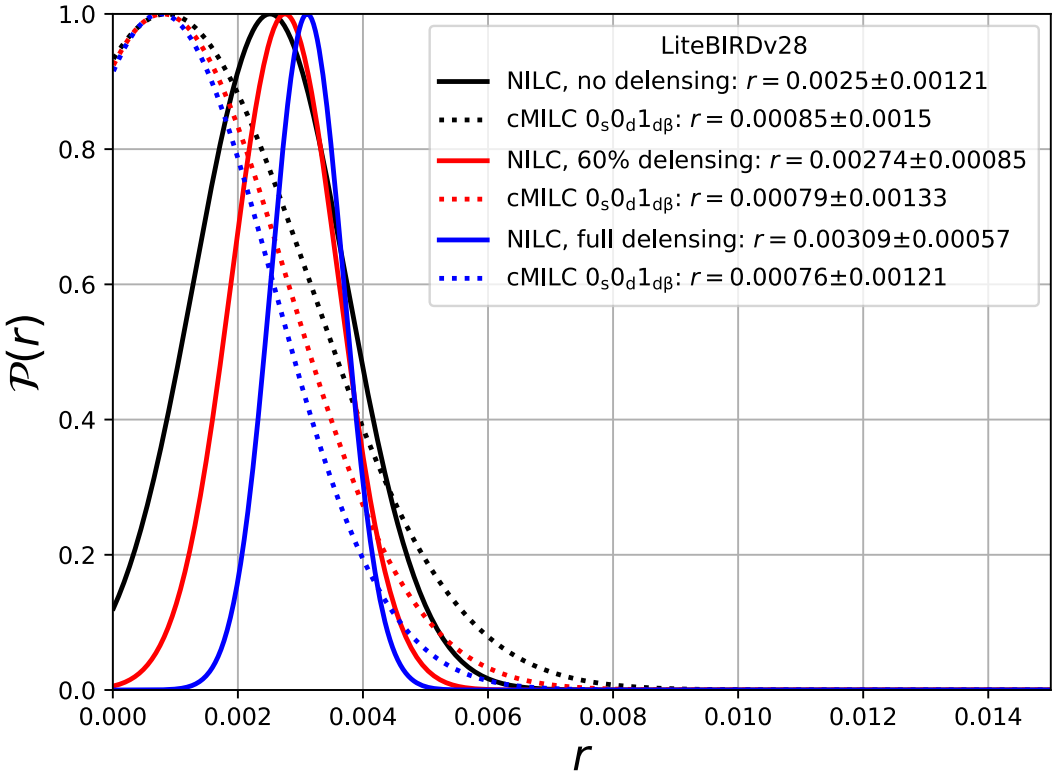

Sweet spot !

Foreground bias removed without paying much noise penalty

Remazeilles, Rotti, Chluba, MNRAS (2021)

Conclusions

- New faint signal regimes for component separation: B-mode, relativistic SZ, etc
- Poor knowledge of the spectral properties of foregrounds at the targeted sensitivities
- Extended frequency coverage is essential to get evidence of incorrect foreground modelling and biased signal detections
- Huge amplitude discrepancies between foregrounds and signals bring out new challenges:

  Tiny modelling errors on foregrounds = large errors/biases on cosmological signals

  Spectral distortions of the foregrounds complicate the picture
- “Thinking outside the box” for component separation is needed to overcome these challenges:

  Moment expansion of the foregrounds
  Foreground deprojection instead of global variance minimization
  Thinking beyond spectral modelling for component separation to tackle spectral degeneracies

M. Remazeilles